# Femoral and Tibial Diaphyseal Cross-Sectional Geometry in Pleistocene *Homo*

ERIK TRINKAUS
*Department of Anthropology, Washington University, Saint Louis, MO 63130, USA; trinkaus@artsci.wustl.edu*

CHRISTOPHER B. RUFF
*Center for Functional Anatomy and Evolution, John Hopkins University School of Medicine, 1830 East Monument Street, Baltimore, MD 21205, USA; cbruff@jhmi.edu*

**ABSTRACT**

Reassessment of Pleistocene *Homo* femoral and tibial diaphyseal cross-sectional properties indicates that there was a variably significant decrease in relative cortical area through the Pleistocene, especially in the middle portions of the femoral diaphysis and relative to Early Pleistocene humans in the tibia and Upper Paleolithic humans in the femur. Both bones show a reduction in relative mediolateral to anteroposterior diaphyseal strength though the midshaft, especially with respect to the femur and particularly between archaic and early modern humans. In the femur, where the diaphyseal strength can be scaled to estimated body mass and bone length, there was little or no change in anteroposterior reinforcement, the primary reflection of locomotor robustness, indicating little shift in locomotor ranging levels among these Pleistocene foraging populations. The changes in relative mediolateral strength may be related to variation in pelvic and body proportions, evident in associated pelves in the Late Pleistocene samples and more generally through Pleistocene *Homo*.

## INTRODUCTION

There has been concern with the relative reinforcement of the femoral and tibial diaphyses of Pleistocene human remains since the first systematic descriptions of Late Pleistocene fossils in the early 20th century (e.g., Boule 1911–13; Verneau 1906). Systematic assessments of such aspects continued through the mid-20th century as sample sizes increased (Matiegka 1938; McCown and Keith 1939; Twiesselmann 1961), and they continued as earlier, Middle, and then Early Pleistocene, *Homo* femora and tibiae became available (Day 1971; Leakey et al. 1978; Ruff et al. 1993; Trinkaus, 1976, 1984; Weidenreich 1941). During most of this time, the assessments were principally in terms of comparing some combination of linear dimensions of diaphyses (diameters or circumferences) to bone length, combined with assessments of the relative anteroposterior versus mediolateral distributions of cortical bone (e.g., Martin 1928). In these concerns of "robusticity," the assessments were principally in terms of populational variation and affinities, but with increasing recognition that the relative quantity and distribution of diaphyseal cortical bone reflected habitual loading patterns (Trinkaus 1976).

These comparative analyses were augmented in the 1970s by the addition of cross-sectional geometry, first applied to a Pleistocene human by Endo and Kimura (1970) using the midshaft fossilization break of the Amud 1 Neandertal tibia. This was followed by an analysis of the Amud 1 tibia and two additional Neandertal tibiae with fossilization breaks (La Chapelle-aux-Saints 1 and Shanidar 6) (Lovejoy and Trinkaus 1980), building on previous work on recent human tibiae (Lovejoy et al. 1976). These early works, in which the appropriate scaling of diaphyseal strength had not been resolved, were followed by the first cross-sectional analysis using reconstructed cross-sections of Pleistocene long bones without relying on fossilization breaks (Trinkaus and Ruff 1989).

It was in this context, building on these preliminary analyses and the earlier work of one of us (Ruff and Hayes 1983a), that we proposed and tested biomechanical models for the appropriate scaling of diaphyseal strength in Pleistocene *Homo*, using both an expanded sample of Late Pleistocene cross-sectional data and the few such data available for Early and Middle Pleistocene humans (Ruff et al. 1993). In this work, it was implicit that what was being assessed was the degree and pattern of diaphyseal cortical bone reinforcement in excess of what was needed for primary locomotor function and weight support, as a product of locomotor behavior and burden carrying. It was in the context of the then growing literature on diaphyseal bone remodeling in the context of differential biomechanical loading regimes (cf., Trinkaus et al. 1994 and references therein), and hence it was oriented towards elucidating differential levels and patterns of locomotor behavior through the Pleistocene and into the Holocene. That initial comprehensive analysis also documented that differential, ecogeographically patterned, body shapes of both recent and Pleistocene humans (Ruff 1994; Trinkaus 1981) accounted for much of the variation in femoral and tibial "robusticity" [as indicated by linear measure indices (Trinkaus 1976)], and therefore some method was necessary to factor in such corporeal variation.

*PaleoAnthropology* 2012: 13–62.  ISSN 1545-0031
doi:10.4207/PA.2012.ART69

It led to a re-evaluation of the Late Pleistocene "robusticity transition" (Trinkaus 1997, 2000), an idea that had been proposed based on earlier, linear assessments of Neandertal and early modern human appendicular "robusticity" (e.g., Trinkaus 1986).

In the subsequent two decades, there have been improvements in the scaling methods of lower limb weight-bearing diaphyses (cf., Trinkaus and Ruff 2000), in part related to the improvements in methods and reference data for estimating body mass from skeletal remains (Auerbach and Ruff 2004). It has become increasingly common to include cross-sectional geometry in the description of fossil human remains, as both new discoveries and reassessments of existing Pleistocene *Homo* postcrania have greatly expanded the available data base. It is now apparent that, although some aspects of diaphyseal cross-sectional shape are due to contrasting morphological patterns across Pleistocene human taxa (Trinkaus 2006a), at least some of the proportional differences in femoral bone distribution are related to differential hip proportions (Ruff 1995; Trinkaus, n.d.; see below). And these changes have occurred in the context of an explosion of (biomedical) research on the mechanical influences on diaphyseal cortical bone quantity and distribution (cf., Pearson and Lieberman 2004; Ruff et al. 2006; and references therein).

In this context, it is appropriate to collate the available femoral and tibial cross-sectional geometry data for Pleistocene *Homo*, from the earliest such remains securely attributed to the genus *Homo* (*sensu stricto*; see Wood 2010) near the Pliocene/Pleistocene boundary to the Late Pleistocene early modern humans at the time of the last glacial maximum. This analysis brings together both previously published data and new information, and it now comprises most of the known *Homo* non-pathological and mature femora and tibia with the potential to provide such data (Appendix). While new techniques for the quantification of the diaphyseal shape are emerging (e.g., Bondioli et al. 2010; Puymerail 2011), cross-sectional geometry permits both the biomechanical assessment of relevant cortical bone parameters and the incorporation of the maximum sample of (often fragmentary) Pleistocene human remains. These data are reassessed here to elucidate changing patterns of femoral and tibial diaphyseal robustness and shape, in the context of temporal, geographic, and taxonomic variation in body shape and locomotor behavior.

## MATERIALS AND METHODS

### SAMPLES

This analysis is concerned with the patterns of change, or stasis, in the cross-sectional geometric properties of femoral and tibial diaphyses in the genus *Homo* through the Pleistocene. More specifically, given the nature of the paleontological record and currently established trends, it is focused on remains from the initial Pleistocene to the last glacial maximum in the Late Pleistocene.

The earliest remains are those from eastern equatorial Africa which have been consistently attributed to the genus *Homo*, as opposed to *Australopithecus* (cf., McHenry 1994; Ruff 1995). This has been done in particular for femoral remains, which exhibit a suite of diaphyseal features that appear to be diagnostic of archaic *Homo* generally (Day 1971; Kennedy 1983; Ruff 1995; Trinkaus 1976, 1984), including the absence of a femoral pilaster despite variable development of the linea aspera and a frequently prominent medial buttress (cf., McCown and Keith 1939) which displaced the minimum shaft breadth distal of midshaft.

In the Late Pleistocene, recent analyses have documented significant changes within early modern humans related to mobility, geographical variation, and lower limb diaphyseal morphology after the last glacial maximum (Holt 2003; Shackelford 2007; see Holt and Formicola 2008). It is therefore appropriate to limit the current discussion to the temporally preceding remains.

Given the temporal distribution of archaic *Homo* remains, they are divided into three samples, an earlier Early Pleistocene one, a Middle Pleistocene one, and a Late Pleistocene sample. The first sample consists of remains from eastern Africa and neighboring western Asia which meet the above morphological criteria for assignment to the genus *Homo*. The second sample consists of remains from across the Old World. It includes ones from close to the Early/Middle Pleistocene boundary (Gesher-Benot-Ya'acov, Kresna, and Olduvai Hominid [OH] 28), from the late Middle Pleistocene (La Chaise-BD and Ehringsdorf), and variably scattered in between. Most of the other specimens are variably precisely dated within the Middle Pleistocene, but all appear to fall securely within that time span. A couple of these remains are essentially undated (Berg Aukas and Broken Hill [Kabwe]), and uncertainty surrounds the age of the Ngandong remains. Only femoral lengths, estimated femoral head diameters, some tibial diaphyseal diameters, and a few photographic observations are available for the large mid-Middle Pleistocene Atapuerca-SH sample (Arsuaga et al. 1991, 1999; Bonmatí et al. 2010; Ortega et al. 2009; cf., Ruff 2010).

The Berg Aukas femur has been attributed to the Middle Pleistocene based on its overall morphology (Grine et al. 1995), but it could derive from any period during the time span of archaic *Homo*, especially given its abnormal articular to diaphyseal proportions and exceptionally low neck-shaft angle (Grine et al. 1995; Trinkaus et al. 1999a). The Broken Hill remains are undated, but the Broken Hill E691 tibia was directly associated with the Broken Hill 1 cranium (Hrdlička 1930; Trinkaus 2009), which is normally morphologically attributed to the middle of the Middle Pleistocene (Bräuer 2008; Rightmire 2008). The Broken Hill femora derive from different, undetermined sinkhole(s) in the original formation (Hrdlička 1930); assuming that they were contemporaneous with each other and the associated ossa coxae, they should be Middle Pleistocene in age based on the archaic iliac pillar of the Broken Hill E719 os coxae (Stringer 1986). Moreover, the Broken Hill E690 femur has the diaphyseal morphology characteristic of Pleistocene archaic *Homo* femora (Trinkaus 1976, 1984), and the Broken Hill E793 midshaft section (Clark et al. 1968) fits within

the non-pilastric range of variation of Middle Pleistocene femora. The Ngandong remains have been variously dated to the later Middle and Late Pleistocene (Santa Luca 1980; Swischer et al. 1996), but recent geological assessments indicate that they could well derive from the second half of the Middle Pleistocene (Indriati et al. 2011); the two tibia from there are therefore included in the Middle Pleistocene sample.

The Late Pleistocene sample is subdivided, given the transition from late archaic to early modern humans during that time period. The late archaic humans consist entirely of western Eurasian Neandertals, from the MIS (marine isotope stage) 6/5 Krapina sample to the mid-MIS 3 Saint-Césaire 1 and Spy 2 remains. Most of them are Middle Paleolithic associated and derive from MIS 4 and 3. There are no Late Pleistocene archaic human femora or tibiae from eastern Asia or Africa. The early modern humans are divided into a MIS 5 southwest Asian (Middle Paleolithic modern human; MPMH) sample from the sites of Qafzeh and Skhul (McCown and Keith 1939; Vandermeersch 1981), and a MIS 3 earlier (Early and Mid) Upper Paleolithic (EUP/MUP) sample from across Eurasia. To the former sample can be added the MIS 6 fragmentary Omo-Kibish postcrania, currently providing only tibial shaft diameters (Pearson et al. 2008a, b). The latter sample is dominated by western Eurasian remains from the Mid Upper Paleolithic burials of southern, central, and eastern Europe, but it includes some European Early Upper Paleolithic femora plus earlier Upper Paleolithic femora and tibiae from southwest and east Asia. The Minatogawa sample and the Ohalo 2 remains modestly postdate the last glacial maximum (Baba and Endo 1982; Hershkovitz et al. 1995; Matsu'ura and Kondo 2011); they are nonetheless included to provide geographic and body size coverage for these earlier Upper Paleolithic humans.

Data are available for four pathological early modern human specimens, Brno 2 (Jelínek 1959), Dolní Věstonice 15 (Trinkaus et al. 2001), Nazlet Khater 2 (Crevecoeur 2008), and Tianyuan 1 (Shang and Trinkaus 2010). The femora of the first exhibit extensive periostosis and are markedly asymmetrical (Oliva 1996; Trinkaus personal observation). The femora of the second are abnormally short and irregularly bowed, but its tibiae are normal and are included (Trinkaus 2006b; Trinkaus et al. 2006a). The femora of the third are abnormally short (Crevecoeur 2008) and are not included. The Tianyuan 1 femora have an unusual mid and mid-distal femoral morphology, but the more proximal and distal diaphyses, as well as the tibial diaphysis, appear normal and are included (Shang and Trinkaus 2010).

To the extent that can be determined from specimens ranging from largely complete skeletons to isolated diaphyseal sections, almost all of the specimens are fully mature. Two mid-Upper Paleolithic specimens, Arene Candide IP and Dolní Věstonice 14, are late adolescent but should have been close to full maturity (Hillson et al. 2006; Sergi et al. 1974). One isolated Neandertal femoral diaphysis, Palomas 52, is morphologically mature but is unusually small for a Neandertal (but not for an early modern human) (Walker et al. 2011a). Femoral neck-shaft angles are included for the early adolescent KNM-WT 15000 and Sunghir 2; they are unlikely to have decreased further should the individuals have lived to maturity, given their already low values.

Only external diameters, and not cross-sectional data, are available for the Caviglione, Dmanisi, Kiik-Koba, Omo-Kibish, Pofi, Předmostí, Santa Croce, Stadelhöhle, and Zafarraya remains, as well as some of the Atapuerca-SH, Barma Grande, and Grotte-des-Enfants long bones (Table A13). The Liang Bua long bones (Brown et al. 2004; Morwood et al. 2005) also are omitted, given their uncertain phylogenetic and paleobiological status.

The individual specimens and available data are provided in the Appendix tables. Bone lengths, femoral head diameters, and estimated body mass are in Table A1. The cross-sectional geometric parameters are provided in Tables A2 to A11, external diaphyseal diameters are in Table A13, and femoral neck-shaft angles are listed in Table A15.

## CROSS-SECTIONAL PARAMETERS

The cross-sectional geometric parameters include total subperiosteal (TA) and cortical (CA) areas, the anteroposterior ($I_x$) and mediolateral ($I_y$) second moments of area, the maximum ($I_{max}$) and minimum ($I_{min}$; perpendicular to $I_{max}$) second moments of area, and the polar second moment of area (J [or $I_p$, the sum of either pair of perpendicular second moments of area]). The individual values for the fossil specimens are provided in Appendix Tables A2 to A11.

Cortical area provides a measure of resistance to axial loads (Ruff et al. 1993), and the combination of cortical and total area reflects the differential subperiosteal deposition and endosteal resorption of bone, principally during development (Ruff and Hayes 1983b; Ruff et al. 1994). As such, relative cortical area (percent CA, %CA) is as much, if not more, a measure of differential developmental and aging processes as it is of structural reinforcement of the diaphysis. The second moments of area ($I_i$) assess bending rigidity in the plane in question, and the polar second moment of area (J or $I_p$) provides both an indication of resistance to torsion and a general reflection of overall rigidity.

In addition to these parameters, section moduli ($Z_i$), which measure bending and torsional strength (rather than rigidity), were calculated for femoral and tibial midshafts (Appendix Table A12). $Z_x$ and $Z_y$ represent anteroposterior and mediolateral bending strengths, respectively, and $Z_p$ torsional (or twice average bending) strength. Section moduli also are useful for assessing relative strengths, since they can be related in a straightforward way to bending and torsional loadings (see below). Section moduli are calculated as second moments of area divided by the maximum distance to the outermost fiber of the section from the neutral axis or centroid of the section.

More recent image analysis programs include these parameters (e.g., "Momentmacro," www.hopkinsmedicine.org/fae/mmacro.htm; Sylvester et al. 2010). However, most of the present data were collected prior to the development of these programs, so an alternative method was used here. Taking half of the external bone diameter as an estimate of

the maximum distance to the outermost fiber has been used previously (e.g., Ruff 2002, 2008, 2009); however, this approach systematically over-estimates true section moduli (as noted therein). The recent availability of a very large (>1000 individuals) sample of recent human limb bones where section moduli had been determined directly, as well as from external bone diameters, allowed calculation of correction factors for femoral and tibial midshaft sections (Ruff et al., in prep.). Thus, in the present study, midshaft section moduli are calculated as second moments of area divided by half of the appropriate diameter (half of the average of anteroposterior and mediolateral diameters for the polar section modulus) and then adjusted using these correction factors (see formulae and resultant values in Appendix Table A12). Systematic and random errors using this technique are acceptably small (mean percent prediction errors of less than 0.5%; percent standard errors of estimate of 5–6%).

## MEASUREMENT GENERATION

The majority of the cross-sectional properties were computed from versions of SLICE (Nagurka and Hayes 1980), in which the parameters are computed from the digitized subperiosteal and endosteal contours. A subset of them were digitized from scaled photographs of fossilization (or excavation) breaks, ones that were close to perpendicular to the diaphyseal axis. These include sections of Berg Aukas 1, Ehringsdorf 5, Hoedjiespunt 1, Mammolo 1, Palomas 52, 92, and 96, La Quina 38, Shanidar 4 and 6, Cro-Magnon 4328, Dolní Věstonice 40 and 41, and Zhoukoudian-Upper Cave 67 and 68. The Castel del Guido 1, La Quina 5, and Zhoukoudian Locality 1 femoral cross-sections and the Sambungmacan 2 tibial cross-section were digitized from published cross-sectional drawings (Baba and Aziz 1992; Mallegni et al 1983; Martin 1923; Weidenreich 1941). The La Chaise-BD ones were digitized from published CT slices (Condemi 2001). The remainder of the cross-sections quantified using SLICE were reconstructed from subperiosteal contours derived either from sectioned casts (the KNM-ER specimens) or transferred using polysiloxane dental putty (Optosil, Bayer or Cuttersil, Heraeus Kulzer). Cortical thicknesses (minimally four) were determined from parallax-corrected radiographs, and the endosteal contours were interpolated within the constraints of the cortical thicknesses, following the subperiosteal contours. The resultant cross-sections were then projected enlarged and digitized. Average directional and random errors in calculating section properties using these techniques have been estimated at about 5% or less (O'Neill and Ruff 2004). The resultant data were generated by us, with the exception of the Arene Candide, Barma Grande, Grotte-des-Enfants, La Rochette, and Veneri values that are from Holt (1999).

A minority of the cross-sectional data derive from CT digital data from scans of the specimens. These include the 80% section of Berg Aukas 1, those of Boxgrove 1, the Kresna 11 values, and most of the ones from the Minatogawa sample (Grine et al. 1995; Kimura personal communication; Kimura and Takahashi 1992; Puymerail 2011; Trinkaus et al. 1999b).

When possible, the femora and tibiae were oriented, following Ruff and Hayes (1983a), using the coronal planes tangential to the posterior femoral condyles and through the anteroposterior middles of the tibial condyles to provide parasagittal and coronal planes. However, prior to the Late Pleistocene, only two femora (KNM-ER 1472 and 1481) and one tibia (Broken Hill E691) are sufficiently complete for us to have used these anatomically determined planes. Therefore, for the femora, the diaphyses were oriented such that a plane near midshaft through the linea aspera and the mediolateral middle of the diaphysis was in the parasagittal plane. For the tibiae, either the midshaft maximum dimension was placed in a parasagittal plane and/or the tangent to the mid-proximal anterolateral (from the interosseus line to the lateral side of the anterior crest) was made parasagittal. Experience has shown that these orientations closely approximate the anatomical orientations of the bones.

For complete or largely complete bones, the "biomechanical" length was first determined or estimated. For the femur, following Ruff and Hayes (1983a), it is the average of the distances parallel to the diaphyseal axis from the proximal extension of the diaphyseal axis on the superior neck, just medial of the greater trochanter, to each distal condyle. For the tibia, it is the average of the distances, parallel to the diaphyseal axis, from each mid-condyle to the mid-trochlear surface. The sections were then taken at 20%, 35%, 50%, 65%, and 80% of those lengths, measured from the distal end.

However, prior to the Late Pleistocene, and even within the Late Pleistocene, few specimens retain all of these landmarks without distortion. Therefore, diaphyseal landmarks, that experience has shown approximate the positions of these percentiles of length, were employed. For the femur, 80% was placed at the maximum extent of the gluteal buttress, and 65% was placed at the point where the proximal muscle insertion lines converge into the linea aspera proper. Midshaft (50%) was located at the maximum extent of the pilaster and the narrowest shaft breadth on early modern human femora. For archaic humans, with their subcircular diaphyses lacking pilasters and frequently prominent medial buttresses, midshaft is less clearly indicated morphologically. However, diaphyseal shape changes little for them along several centimeters of midshaft, and modest errors in the location of the 50% section should introduce little error into the values. The mid-distal (35%) and distal (20%) sections are harder to morphologically locate, and they were rarely taken when length could not be at least approximated.

On the tibial diaphysis, the midshaft (50%) is normally located where the soleal line meets the posteromedial corner of the diaphysis. The mid-proximal section (65%) is close to the position of the nutrient foramen, and especially on the tibial pilaster if one is present. The mid-distal (35%) cross-section approximates the distal minimum circumference and can be located as such. The proximal (80%) and distal (20%) ones are more difficult to locate and were taken primarily on tibiae which also provide lengths.

A number of these values have been published previously. These include specimens from Amud, Arago, Boxgrove, Broken Hill E691, Dolní Věstonice, Krapina, Fond-de-Forêt, Kresna, Mladeč, Oliveira, Paviland, Pavlov, Qafzeh, Saint-Césaire 1, Shanidar, Skhul, Spy, Tabun, and Tianyuan (Lovejoy 1982; Puymerail 2011; Shang and Trinkaus 2010; Sládek et al. 2000; Trinkaus and Ruff 1989, 1999a,b; Trinkaus 2000, 2003, 2009; Trinkaus et al. 1999b 1999c, 2006b, 2007). Selected sections (principally 50% and 80%) have been provided for many of the Upper Paleolithic specimens by Holt (1999) and Shackelford (2005). However, individual data for many of the specimens have been unavailable, and some of the previously published values have been modestly revised.

## CROSS-SECTIONAL DIAPHYSEAL SHAPE

The distributions of cortical bone in the diaphyseal cross-sections were compared using cortical area versus total area and using relative perpendicular second moments of area.

For the femoral diaphysis from the mid-proximal (65%) section distally, the anteroposterior versus mediolateral bone distribution was assessed using the anatomically oriented second moments of area ($I_x$ versus $I_y$). This was done since the archaic *Homo* femora through the middle half of the shaft have contours which vary around circularity, and using $I_{max}$ versus $I_{min}$ would compare different aspects of the diaphyses depending on the orientation of $I_{max}$.

In the proximal femur, given the frequently marked anteversion of Pleistocene femora (Day et al. 1975; Sládek et al. 2000; Twiesselmann 1961), the biomechanically relevant subtrochanteric planes are rarely the mid-diaphyseal or condylar anatomical ones. This is reflected, in part, in the posterolateral, rather than strictly lateral, positioning of the gluteal buttress in these anteverted femora. Therefore, the femoral 80% relative rigidities were compared using two sets of perpendicular second moments of area. In order to best approximate the anteversion (and gluteal buttress) plane, $I_{min}$ versus $I_{max}$ was employed, even though a couple of the specimens are largely circular in this region (La Chapelle-aux-Saints 1 and Spy 2) or have a largely anteroposterior orientation to $I_{max}$ (Skhul 5). At the same time, to be sure to assess the degree of relative mediolateral rigidity, the 80% cross-sectional proportions also were assessed using $I_x$ and $I_y$, even though $I_y$ does not always correspond to the maximum internal-external rigidity of the subtrochanteric diaphysis.

The tibial second moment of area comparisons through the middle of the diaphysis (35% to 65%) employ $I_{max}$ versus $I_{min}$, since $I_{max}$ is always close to anteroposterior and thereby approximations in orientation become less relevant. Tibial midshaft $I_x$ and $I_y$ were nonetheless employed in the calculation of tibia 50% $Z_x$ and $Z_y$ (see Appendix Table A12).

In addition to these cross-sectional parameters, comparisons are made using standard osteometric diameters (Bräuer 1988) at the femoral (pilastric) and tibial midshafts, the femoral subtrochanteric (meric) level, and the tibial mid-proximal (cnemic) level (see Appendix Table A13). These dimensions have lower morphological resolution than full cross-sectional measures, but they are available for larger samples of Pleistocene *Homo* femora and tibiae and permit the inclusion of data from lost or otherwise unavailable remains. The data derive from primary published descriptions of the fossils and personal measurement of the original specimens (in some cases modestly refining the published values).

Since the subtrochanteric femoral proportions may be affected by femoral neck orientation, as well as by pelvic proportions, comparisons also are included for neck-shaft angles, taken in the anteversion plane of the proximal femur.

## RELATIVE DIAPHYSEAL STRENGTH

The strengths of femoral and tibial diaphyses should be assessed relative to the baseline loads placed upon them, which consist in these diaphyses of body mass times the beam length around which it operates (Ruff et al. 1993). To do otherwise (e.g., Lovejoy and Trinkaus 1980) provides an inaccurate impression of the relative strengths of the diaphyses.

Beam length for these bones is approximated by their biomechanical lengths. In the past, several approaches have been employed to incorporate the effects of body mass (Trinkaus and Ruff 2000). Initially, we (Ruff et al. 1993) calculated the allometric scaling coefficient between body mass and femoral length for recent humans (length$^{5.33}$) and used it, along with percentage adjustments for the broader Neandertal bodies, to scale femoral diaphyses (see also Trinkaus 1997). With the determination of formulae for estimating body mass from stature and bi-iliac breadth (Ruff 1994; see also Ruff 2000, Ruff et al. 2005) and from femoral head diameter (Grine et al. 1995; McHenry 1994; Ruff et al. 1991; see Auerbach and Ruff 2004; Ruff et al. 1997), body mass was estimated for Pleistocene *Homo* specimens and used to scale lower limb (weight-bearing) diaphyses (e.g., Shang and Trinkaus 2010; Trinkaus 2006b; Trinkaus and Ruff 1999a, b; Trinkaus et al. 1999b, c).

However, it has become increasingly apparent that the body proportions of archaic *Homo*, although generally following the ecogeographical patterns evident among recent humans, if with steeper slopes (cf., Trinkaus 1981; Ruff 1994; Holliday 1997; Trinkaus et al. 1999b), may not conform as tightly to them as previously expected. Wide pelves seem to be characteristic of archaic *Homo* generally (Bonmatí et al. 2010; Ponce de León et al. 2008; Rak 1991; Rosenberg et al. 2006; Ruff 2010; Trinkaus 2011a; Walker et al. 2011b). Crural indices, while "tropical" in at least one early *Homo* specimen (Walker and Leakey 1993), are low in both cold and temperate late archaic humans. One East Asian early modern human has a crural index suggesting warm climate body proportions, but its lower limb relative articular dimensions imply elevated body mass (Shang and Trinkaus 2010). And the only sufficiently complete archaic *Homo* equatorial tibia (Broken Hill E691) has diaphyseal proportions suggesting linear body shape but relatively large articulations (Trinkaus 2009).

These considerations are combined with the dearth of reliable femoral and especially tibial lengths available for Early and Middle Pleistocene *Homo*. The bone lengths provided in Appendix Table A1 are those for which either a direct measurement or a reasonably reliable estimate can be made, at most estimating the length from a largely complete diaphysis. However, of them 42% (N=84) required estimation, and among pre-Upper Paleolithic specimens 51% (N=41) needed estimation. Among Early and Middle Pleistocene specimens (N=14), only two femora and two tibiae provide direct length measures.

Yet, given the necessity to scale diaphyseal strength to a measure that takes into account the ecogeographical and individual variation in body size and shape, it is necessary to have a reliable bone length and body mass for each one. The bone lengths employed are those which can be measured or reliably estimated from the bone itself; none of the previously employed estimates from assumed body proportions are included. Body mass (see Appendix Table A1) is estimated solely from femoral head diameter, or femoral head diameter estimated from associated lower limb weight-bearing articulations (acetabular height or lateral femoral condyle depth).

Following Ruff (2010; see also Auerbach and Ruff 2004), it has become apparent that the three available sets of formulae for body mass estimation (all from recent humans) are differentially appropriate for individuals of contrasting body sizes. Given this, the formula of McHenry (1994) is used for small individuals (femoral head diameter <38mm), an average of the estimates from the McHenry (1994), Ruff et al. (1991), and Grine et al. (1995) is employed for middle sized individuals (femoral head diameter 38 to 47mm), and an average of the Ruff et al. (1991) and Grine et al. (1995) results is used for large specimens (femoral head diameter >47mm). The McHenry (1994) and Grine et al. (1995) formulae are for pooled-sex samples. The Ruff et al. (1991) ones include formulae for males and females; the sex specific formulae were used when sex can be reliably assessed pelvically, and for the other specimens the male and female estimates were averaged prior to averaging them with the results of the other formulae.

At least among recent humans, these femoral head derived body mass estimates generally correspond to those derived from bi-iliac breadth and estimated stature (Auerbach and Ruff 2004). It is nonetheless recognized that femoral head size reflects not body mass, but joint reaction forces at the hip. The latter is principally a factor of body mass, but it is also affected by the moment arm lengths for body mass and the gluteal abductor muscles around the hip, and by locomotor activity levels during development, all of which varied in Pleistocene *Homo*. With these caveats in mind, it is nonetheless the most reliable measurement available for most pre-Upper Paleolithic *Homo* that provides reasonable estimates of body mass. Moreover, this approach permits the biomechanical evaluation of relative diaphyseal hypertrophy in addition to that induced by differential body mass and proportions, something which linear "robusticity indices" do not permit.

## COMPARISONS

The comparisons are done principally graphically, in particular for the biomechanically more relevant 50% to 80% femoral sections and the 50% and 65% tibial ones. The proximal (80%) and distal (20%) tibial ones, plus the distal (20%) femoral one, are rarely preserved, difficult to locate on incomplete diaphyses, and appear to be influenced by relative epiphyseal dimensions. Their values, as available, are provided in the Appendix, but they are minimally employed in the comparisons. Given that it and the 20% section reflect the weakest region of the tibial diaphysis, especially in torsion (Lovejoy et al. 1976; Ruff and Hayes 1983a), more limited comparisons are made with tibial 35% section.

Right and left values, as available for bilaterally preserved specimens, are provided in the Appendix tables. In the comparisons, however, right and left values were averaged prior to the calculation of sample statistics or the generation of graphs.

Degrees of difference across the samples are assessed using raw residuals from the Upper Paleolithic reduced major axis (RMA) regression lines (see Appendix Table A14). The resultant residuals for all four samples, given small sample sizes and the non-normal distributions of 29% (N=21) of the comparisons, are principally compared using Kruskal-Wallis non-parametric tests; ANOVA P-values are provided with the Kruskal-Wallis ones in Appendix Table A14. The assessments of P-values employ sequentially reductive multiple comparison corrections within sets of comparisons (Proschan and Waclawiw 2000; Rice 1989).

# DIAPHYSEAL REINFORCEMENT

## RELATIVE CORTICAL AREA

An elevated relative cross-sectional cortical area, or a high percent of the total subperiosteal area made up by the cortical bone, has been considered a reflection of the hypertrophy of Pleistocene human diaphyses and of their femora in particular (e.g., Ben-Itzhak et al. 1988; Day 1971; Kennedy 1985; Weidenreich 1941). This has been expressed as "medullary stenosis" (Kennedy 1983), percent cortical area (%CA or pctCA) (e.g., Ben-Itzhak et al. 1988; Ruff et al. 1993; Shang and Trinkaus 2010), or the distribution of cortical area values relative to total area (e.g., Trinkaus 1997, 2006b). It is a combination of the latter two approaches that is used here. Because the relative size of the medullary canal is a reflection of the differential endosteal resorption and subperiosteal deposition during development and to some extent through adulthood (Ruff and Hayes 1983b; Ruff et al. 1994), it is inappropriate to refer to the resultant small medullary canals in some fossil diaphyses as "medullary stenosis."

Plots of the mean %CA values for the femoral and tibial sections are shown in Figure 1. In general, especially in the middle diaphyseal sections, Early and Middle Pleistocene specimens have the highest %CA and later specimens (MPMH and EUP/MUP) have the lowest %CA, but there is some variability. In the femoral sections, the EUP/MUP sample consistently has the lowest average %CA, and the

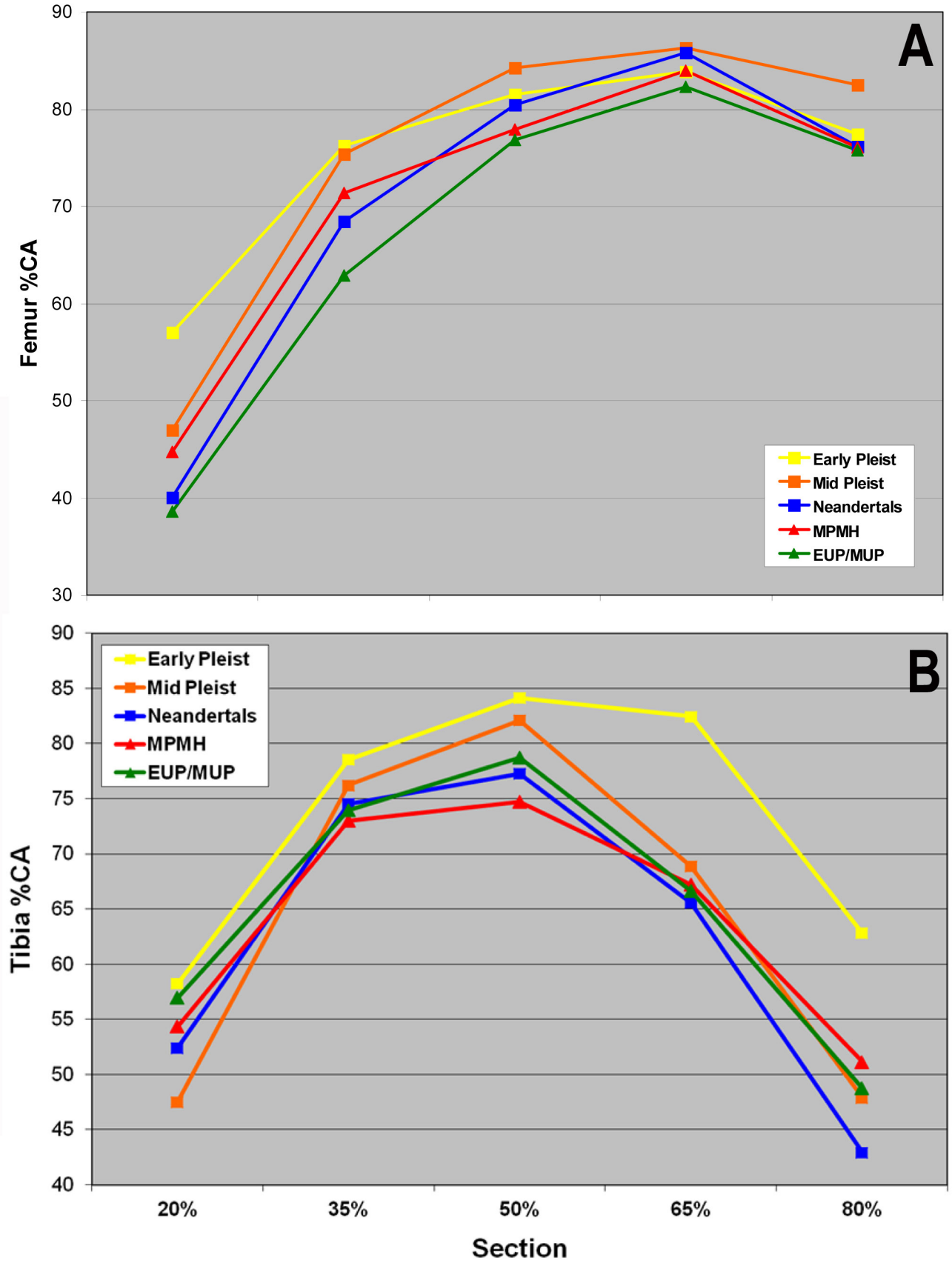


*Figure 1. Mean percent cortical (%CA) for five diaphyseal sections of the femur (A) and tibia (B) for Pleistocene* Homo.

Early and/or Middle Pleistocene samples have generally higher %CA. However, at the 65% section, the Neandertals approach the high value for the Middle Pleistocene sample, and at the 80% section, only the Middle Pleistocene sample stands out from the other four samples.

Early Pleistocene tibiae have higher %CA along the entire shaft, and the Middle Pleistocene specimens are high in the middle three sections. Early modern human samples are lower in the middle sections but less so in the proximal and distal ones, while Neandertals are generally low throughout. All of the femoral mean values are above those for a pooled recent human sample (Ruff et al. 1993), especially for 50% to 80%.

These comparisons, however, only address mean values. The distributions of cortical versus total subperiosteal area for those sections providing adequate sample sizes (femur 35% to 80% and tibia 50% and 65) provide considerably more scatter (Figures 2 and 3). Of these, only the 35% and 50% femoral distributions provide significant differences across the five samples. In the former, it is primarily the lower values for the earlier Upper Paleolithic sample that creates the significant difference; across the four pre-Upper Paleolithic samples, the Kruskal-Wallis P-value is 0.144. The pre-EUP/MUP sample Kruskal-Wallis P-value for the 50% section is 0.049, driven mostly by the high values for several of the Middle Pleistocene specimens. In the tibial 50% and 65% comparisons, there is only a modest difference across the four samples, which does not reach significance despite the high values for the two Early Pleistocene specimens at each of these sections.

Therefore, to the extent that relative cortical area reflects diaphyseal hypertrophy, there is a reduction on average through the Pleistocene in the mid and mid-distal femur, but less consistent directional change otherwise. Elevated %CA appears to be generally characteristic of Pleistocene *Homo* femora and tibiae, although its direct mechanical relevance is limited (Ruff 1992).

## DIAPHYSEAL HYPERTROPHY

The relative overall hypertrophy, or "robusticity," of the femoral diaphysis can be assessed, as detailed above, by comparing the femoral midshaft polar section modulus to its external baseline bending/torsional load, estimated as body mass times femur length. In the resultant assessment (Figure 4), the comparisons are dominated by the Late Pleistocene samples. There are only two Early Pleistocene femora with the three requisite femoral variables (length, head diameter, and midshaft cross-sectional parameters), KNM-ER 1472 and 1481. For the Middle Pleistocene, data are available only for OH-28, and two of the variables are estimated (femur length from the largely complete diaphysis and head diameter from acetabular height).

Given these limitations, the distributions of the samples are very uniform (see Figure 4). There is some scatter among the larger of the Late Pleistocene specimens, with extensive overlap across those three samples. OH-28 falls well within that scatter, if modestly low. The two Early Pleistocene femora bracket a small Neandertal (Palomas 96) and are similar to small EUP/MUP specimens. Overall the differences across the samples are not statistically significant. Within the Late Pleistocene, the EUP/MUP sample is on average less robust than the Neandertal and the MPMH samples, but the difference does not reach significance given the considerable overlap of the samples (Kruskal-Wallis P: 0.342; ANOVA P: 0.148)(see Figure 4). These results follow previous assessments of Late Pleistocene human femora (Trinkaus 1997, 2006b), and conform to a prior assessment of archaic *Homo* femora (Ruff et al. 1993) in which midshaft overall rigidity was scaled using different techniques.

For the tibia, there are no sufficiently complete Early and Middle Pleistocene tibiae for a similar assessment. Previous analyses of Late Pleistocene tibiae have not found any significant differences between samples in diaphyseal robustness (e.g., Shang and Trinkaus 2010; Trinkaus 2006b). The three Middle Pleistocene tibiae that provide length or a reasonable length estimate, Boxgrove 1, Broken Hill E691, and Ngandong 14 (Trinkaus 2009; Trinkaus et al. 1999b), provide values similar to Late Pleistocene tibiae, the actual positions depending upon what body proportions and hence body mass estimates are assumed for the individuals

## DIAPHYSEAL CROSS-SECTIONAL SHAPE

In addition to differential diaphyseal hypertrophy across these Pleistocene samples, there are differences in the cross-sectional, and especially subperiosteal, shapes of the diaphyses. Some of these contrasts are morphological, in terms of the subperiosteal contour, whereas others are more biomechanical and reflect the distribution of bone relative to anatomical axes of the diaphyses.

In the femur, the principal morphological difference is the development of a midshaft (or mid-proximal to mid-distal shaft) pilaster in most of the early modern human femora, a pattern that is unknown in archaic *Homo* femoral diaphyses (excluding the questionably Pleistocene Trinil femora). Early to Late Pleistocene archaic human femora have variable development of the linea aspera, but when there is an increase in the anteroposterior midshaft dimension, it is created either by an anteroposterior elongation of an ovoid subperiosteal contour with a prominent linea aspera (e.g., Atapuerca-SH femur 12, Castel del Guido 1, Feldhofer 1, Mammolo 1, Rochers-de-Villeneuve 1) or a posterior expansion of the medial buttress near midshaft (e.g., Berg Aukas 1, Saint-Césaire 1). At the same time, as noted above, archaic *Homo* femora usually have a prominent development of a medial buttress, a swelling of bone that begins proximally in the subtrochanteric region and extends beyond midshaft, slowly rotating posteromedially on the diaphysis. It is this subperiosteal thickening of the proximal and mid-medial diaphysis that displaces the minimum shaft breadth distally of midshaft. In addition, early modern human femora frequently have a prominent gluteal buttress, a rounded swelling of bone on the lateral (or posterolateral) subtrochanteric diaphysis, usually delineated by a longitudinal sulcus posteriorly and sometimes anteriorly. Such a feature is present in a minority of archaic

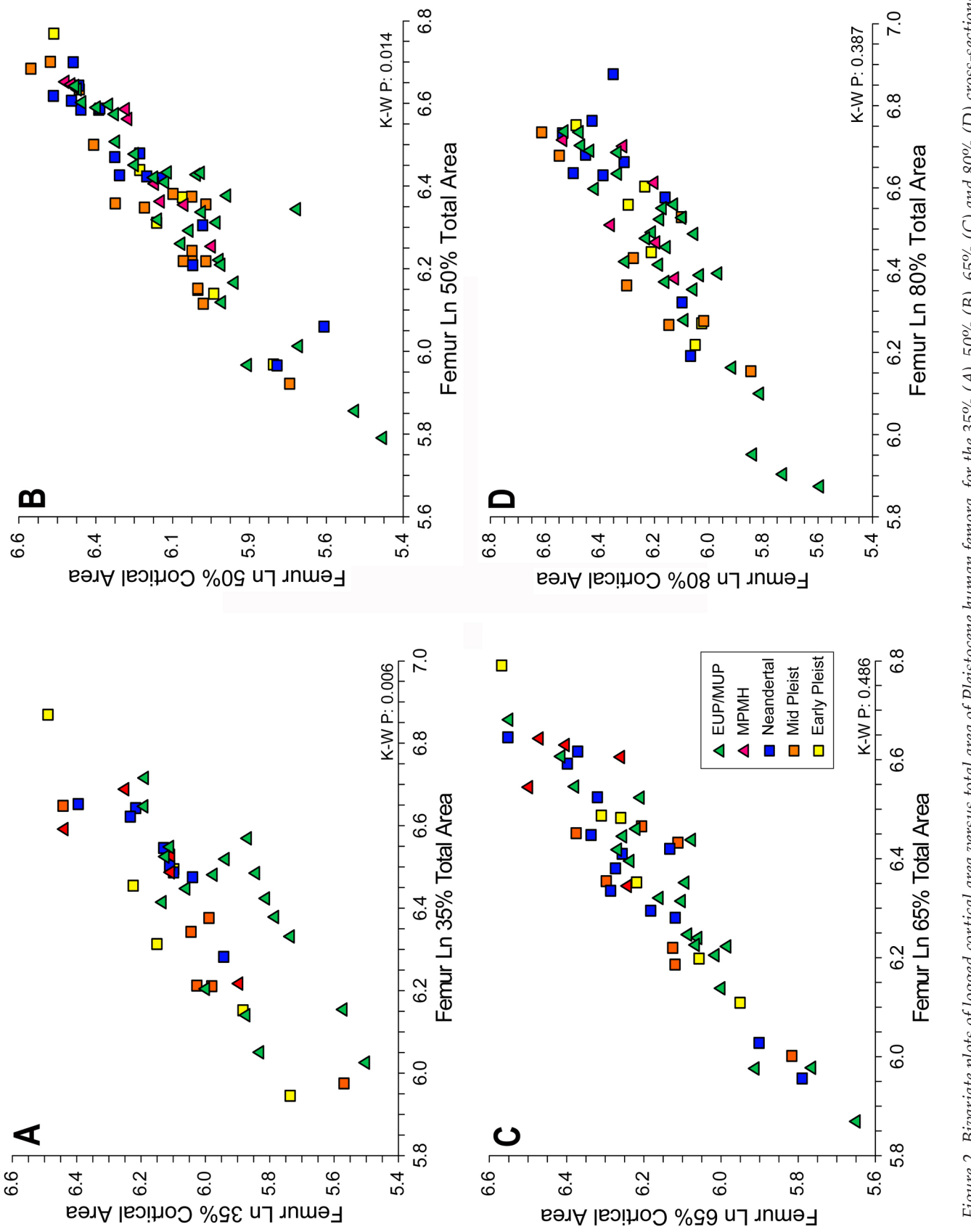


*Figure 2. Bivariate plots of logged cortical area versus total area of Pleistocene human femora, for the 35% (A), 50% (B), 65% (C) and 80% (D) cross-sections.*

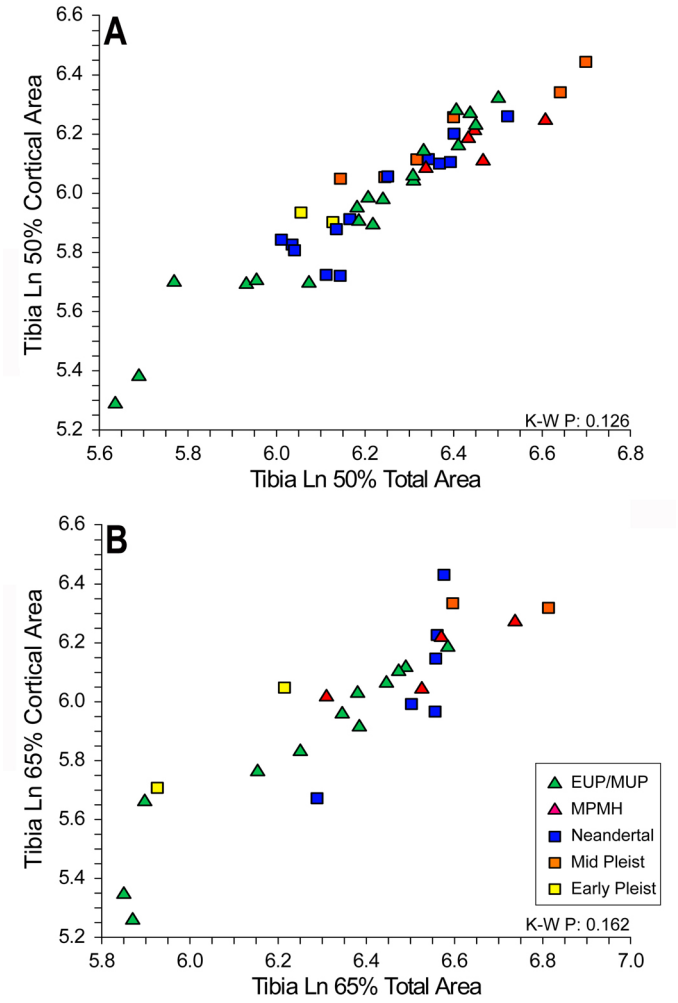


*Figure 3. Bivariate plots of logged cortical area versus total area of Pleistocene human tibiae for the 50% (A) and 65% (B) cross-sections.*

*Homo* femora, but it is rarely prominent.

In the tibial diaphysis, the strictly morphological differences between archaic and early modern humans are primarily in terms of the development of longitudinal sulci between the different crests. Although sometimes present, especially in the mid-proximal region, these "sulci" are usually shallow if present in archaic human tibiae, and they are characteristically absent near midshaft, producing convex or flat cross-sectional contours of the diaphysis.

Despite these morphological differences, which may serve a taxonomic purpose for distinguishing between late archaic and early modern human femora and tibiae, it is unclear what are the biomechanically relevant similarities or differences. These distributions of bone can be assessed through the relative perpendicular second moments of area. As noted above, the anteroposterior ($I_x$) and mediolateral ($I_y$) ones are used for the mid-proximal to distal femur, but both $I_x$ versus $I_y$ and the maximum ($I_{max}$) versus its perpendicular ($I_{min}$) are employed for the proximal femur, and $I_{max}$ versus $I_{min}$ is used for the tibia. These distributions of bone also can be assessed, with less precision but larger samples, through external diaphyseal diameters.

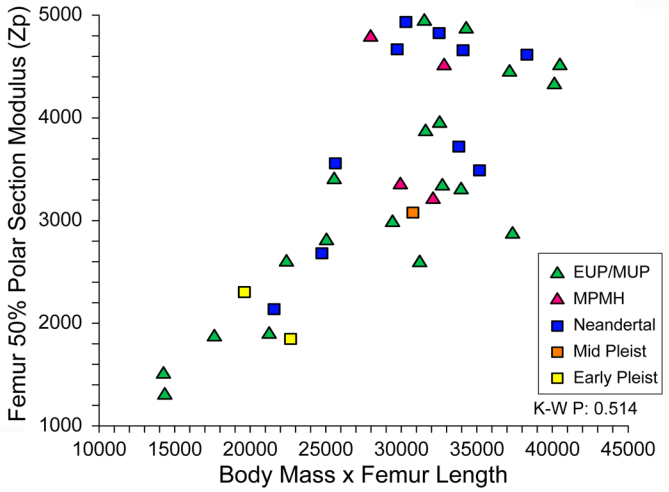


*Figure 4. Bivariate plot of femoral midshaft (50%) polar section modulus versus body mass times femur length.*

## TIBIAL DIAPHYSEAL SHAPE

In the comparisons of the mean $I_{max}$ to $I_{min}$ ratios for the tibiae, most of the samples follow similar patterns from distal to proximal, with the variation primarily proximal (Figure 5). However, it needs to kept in mind that the Early Pleistocene N=1 for the two distal sections and N=2 for the three more proximal ones. In the Middle Pleistocene N=2 for all but the 50% section. The 80% samples remain small for both Middle Paleolithic groups (N=3 each), and only reach a substantial size (N=9) for the Upper Paleolithic sample.

Despite these limitations for the earlier samples and the proximal section, it is apparent that the earlier Upper Paleolithic sample stands out from the other samples in its average diaphyseal proportions in all but the 20% section. It is joined by the Middle Paleolithic modern human sample in the mid-proximal section and to a lesser extent in the 80% section. At the other extreme, the Early Pleistocene sample is below the others (less anteroposteriorly expanded) through the middle three sections of the diaphysis.

The differences between the Upper Paleolithic, Early Pleistocene and temporally intermediate samples are evident in the distributions of their 35% to 65% perpendicular second moments of area, plus the anteroposterior versus mediolateral diaphyseal diameters for the midshaft and mid-proximal shaft (Figures 6 and 7). There is considerable scatter in the distributions, but all of the comparisons provide significant differences across the samples. Given tibial sample size limitations for scaling to bone length and body mass, it remains unclear whether it is differential anteroposterior and/or mediolateral hypertrophy which is producing these differences in tibial diaphyseal proportions across the Pleistocene *Homo* samples.

## FEMORAL DIAPHYSEAL SHAPE

Using the mean ratios of the femoral anteroposterior versus mediolateral second moments of area (Figure 8) provides a substantial contrast between the archaic *Homo* and the early modern human femora. In this, the Early Pleistocene

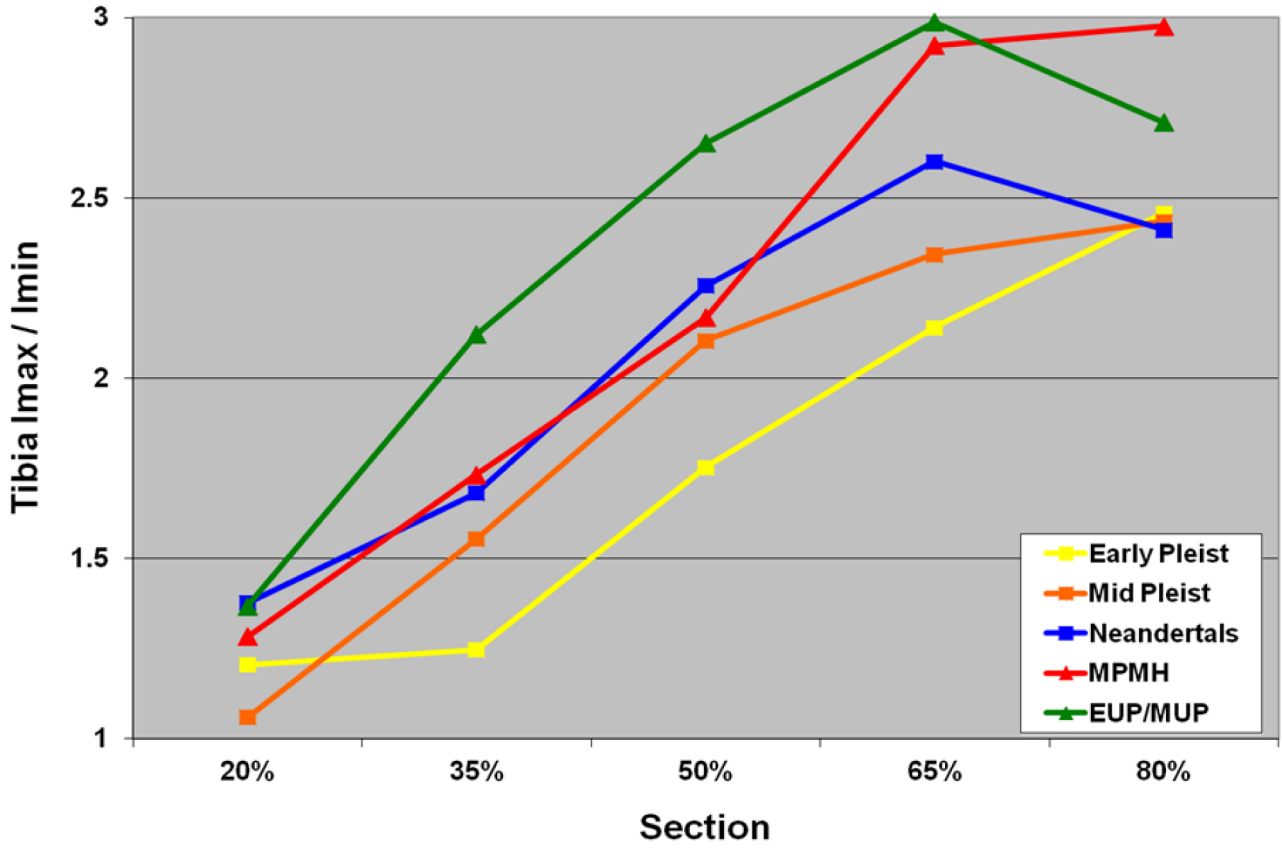


*Figure 5. Mean maximum versus minimum second moments of area ($I_{max}/I_{min}$) for Pleistocene* Homo *tibiae.*

sample consistently has the lowest ratios, the Middle Pleistocene and Neandertal samples are similar, and the two early modern human samples have markedly higher ratios, especially from 35% to 65%. There is little difference in the pattern of the ratios from distal to proximal across the three archaic human samples. The same similarity of pattern applies to the two early modern human samples. There is little separation distally. In the subtrochanteric region, which reflects in part pelvic and proximal femoral proportions, there is little separation of the Middle and Late Pleistocene mean values, but the Early Pleistocene sample has lower ratios.

## Midshaft Considerations

When the mid-distal to mid-proximal proportions are compared using individual values (Figure 9), whether with second moments of area or the larger sample size available for midshaft external diameters, significant differences remain across the samples (highly significant for the two midshaft and the mid-proximal comparisons). There is modest overlap across the samples, especially for the smaller individuals (the reduced major axis slopes between the anteroposterior and mediolateral variables are all >1.0, indicating some size scaling for the proportions). Yet, most of individuals in the two early modern human samples remain consistently above the archaic human distributions. The Early Pleistocene sample does remain the lowest in the distributions (the one high value in midshaft diameters is Dmanisi D4167), but there is considerable overall scatter among the Middle and Late Pleistocene archaic human femora. The three archaic *Homo* samples nonetheless remain insignificantly different from each other (Kruskal-Wallis P: 35%: 0.464; 50%: 0.183; 65%: 0.314). It is the high values for the MPMH and EUP/MUP samples through the midshaft that drive the highly significant differences across these samples.

Given sample sizes for femora with midshaft cross-sectional properties plus length and femoral head values, it is possible to compare 50% $Z_x$ (A-P) and $Z_y$ (M-L) separately to body mass times bone length. When this is done (Figure 10), there is little difference across the samples in scaled anteroposterior rigidity, although KNM-ER 1481 and OH-28 fall among the lower of the specimens. In the scaled mediolateral comparison, there is more separation of the samples, and the comparison reaches significance (especially if the ANOVA P-value (0.016) is considered). If the late archaic humans are compared to a pooled early modern human one, the Neandertals are significantly higher (Wilcoxon P=0.002). Adding the three earlier archaic specimens to an archaic versus modern comparison retains the significant difference (Wilcoxon P=0.003). It therefore appears that the differences between archaic and early modern human femoral midshafts in anteroposterior versus mediolateral proportions are not driven by differences in anteroposterior rigidity, but by a relatively lower mediolateral hypertrophy in the latter sample.

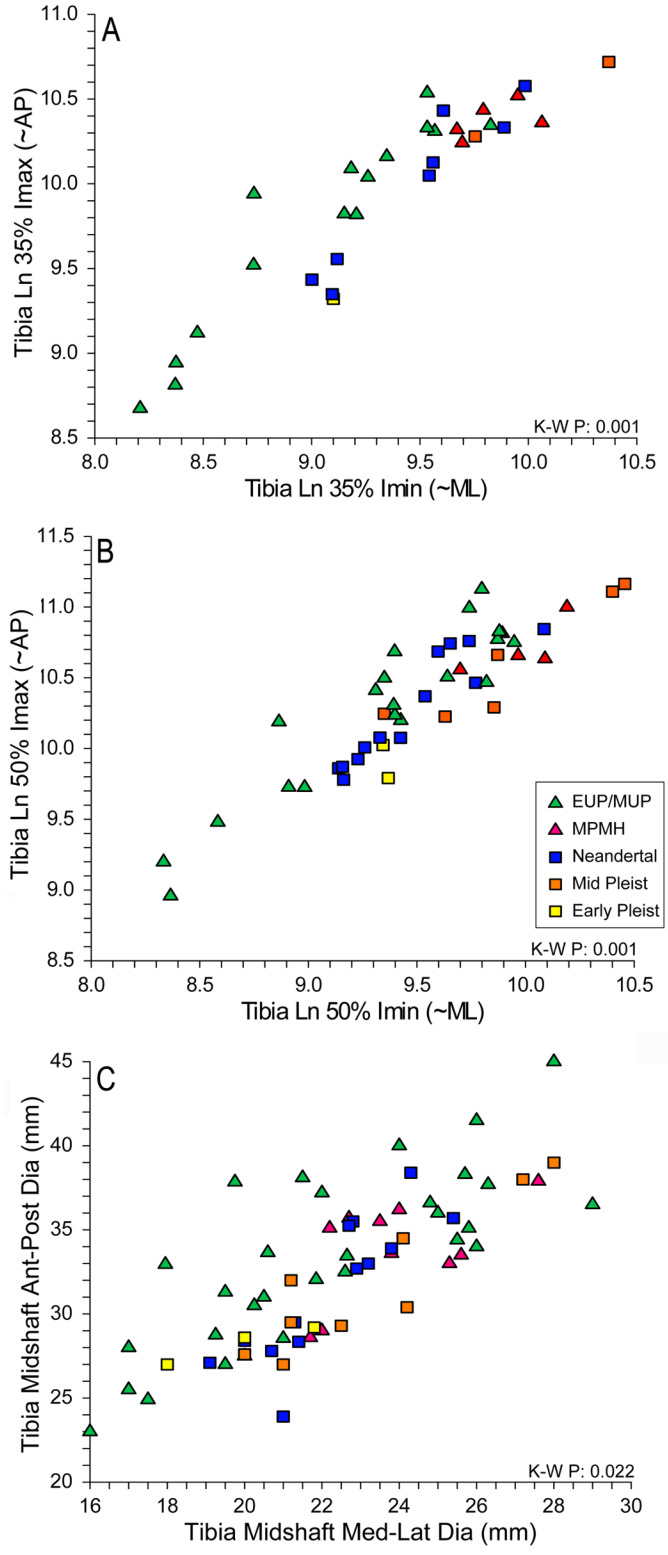


*Figure 6. Bivariate plots of logged maximum ($I_{max}$) versus minimum ($I_{min}$) second moments of area of Pleistocene human tibiae for the 35% (A) and 50% (B) cross-sections, plus of the midshaft anteroposterior versus mediolateral external diameters (C).*

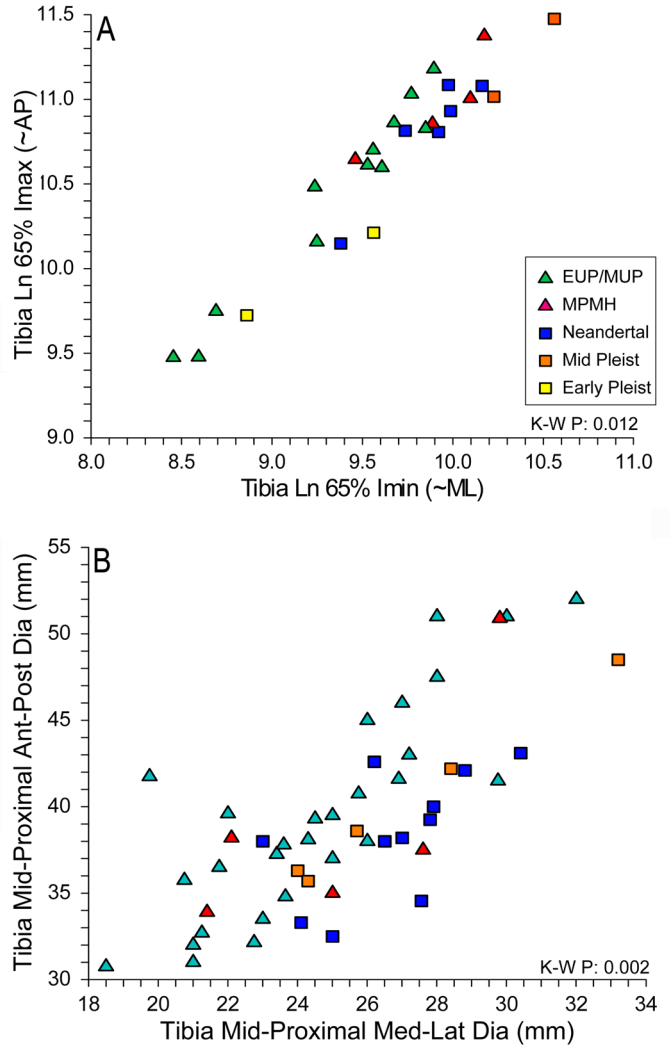


*Figure 7. Bivariate plots of logged maximum ($I_{max}$) versus minimum ($I_{min}$) second moments of area of Pleistocene human tibiae for the mid-proximal (65%) cross-section (A), plus of the proximal anteroposterior versus mediolateral external diameters (B).*

## Subtrochanteric Considerations

Paralleling results for mean ratio comparisons (see Figure 8), when individual values for anteroposterior ($I_x$) and mediolateral ($I_y$) bending rigidities of the subtrochanteric section are compared (Figure 11), Early Pleistocene specimens all fall near the lower edge of the distribution, whereas the specimens from the other groups are more variable and overlapping. Within the Middle Pleistocene sample, the early OH-28 and Kresna 11, along with the undated Broken Hill E690, have the lowest values, one early specimen (Gesher-Benot-Ya'acov 1) is in the middle of the overall distribution with Berg Aukas 1 and Tabun E1, and the three high (rounder) specimens are the Broken Hill E689 and E709 femora and the late La Chaise-BD 5 femur. In comparisons of 80% $I_{min}$ versus $I_{max}$ (measures closer to the anteroposterior versus mediolateral second moments of area in the plane of the head and neck for most of these specimens) (see Figure 11C), there is a tighter distribution of the

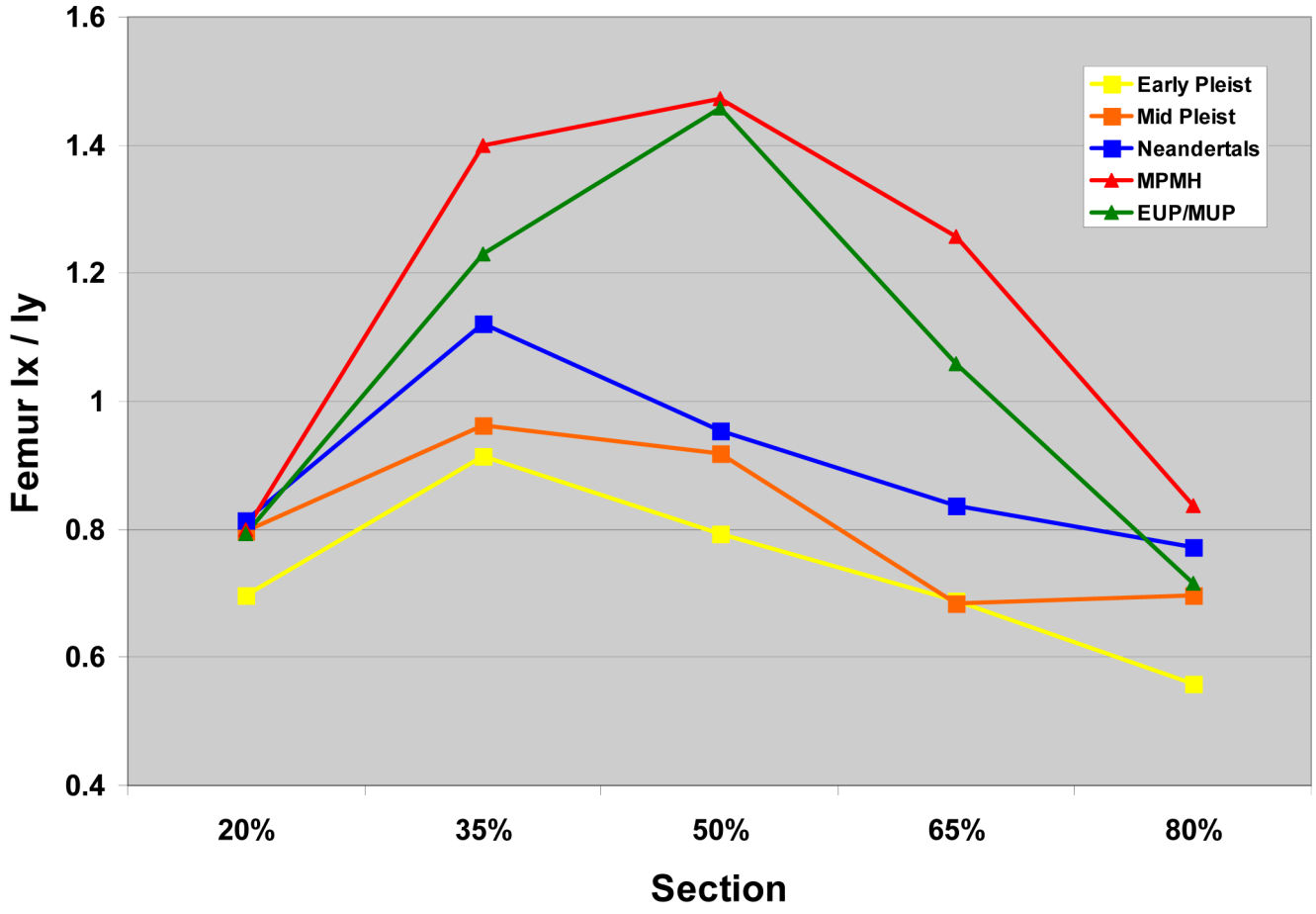


*Figure 8. Mean anteroposterior versus mediolateral second moments of area ($I_x/I_y$) for Pleistocene* Homo *femora.*

values and a slightly greater difference across the samples. The high (round) value in external diameter comparisons is Skhul 5; in the second moment of area comparisons, the MPMH specimens largely bracket the rest of the distributions.

Following Ruff (1995), in which the relative mediolateral reinforcement of the subtrochanteric diaphysis is an indirect, biomechanical effect of pelvic and proximal femoral proportions, it would appear appropriate that there is a shift among archaic *Homo* proximal femora that generally follows, given dating issues and individual variation with small sample sizes, the increased encephalization during this time period (Ruff et al. 1997) combined with a rounding out of the pelvis. It is less clear why most of the Middle Paleolithic modern human sample should fall along the higher (rounder) margin of the earlier Upper Paleolithic sample.

One of the variables in the hip region that might influence subtrochanteric bending moments is femoral neck orientation, as quantified by the neck-shaft angle. There is little difference in neck-shaft angles across the archaic human and Upper Paleolithic samples (P=0.750), despite increased variation in the last sample (see Appendix Table A15; Figure 12). However, the Middle Paleolithic modern human sample has high neck-shaft angles, at the top of the Upper Paleolithic range of variation and separate from all of the archaic humans. Adding in the Middle Paleolithic modern humans produces a P=0.034 across the five samples. Assuming similar neck lengths across these samples, the more vertical orientation of the Middle Paleolithic modern human femoral necks should reduce the bending moments on the proximal diaphysis. This might explain, in part, the difference in proximal femoral proportions between the two early modern human samples, given their similar pelvic configurations, but it would be only one aspect of pelvic and hip morphology to consider in comparisons of the Middle Paleolithic modern human versus the archaic human samples.

## DISCUSSION

Despite a significant change in femoral and tibial diaphyseal discrete morphology between archaic and early modern humans and several shifts in diaphyseal linear and especially cross-sectional geometric parameters, there appears to have been little change in the overall hypertrophy, or robustness, of at least Pleistocene *Homo* femora. The one assessment for which there are minimally adequate remains (given the dearth of sufficiently complete Early and Middle Pleistocene specimens), femoral midshaft overall rigidity scaled to femur length and estimated body mass, does not show a significant trend from the Early to the Late Pleistocene, although there is a suggestion of a slight reduction

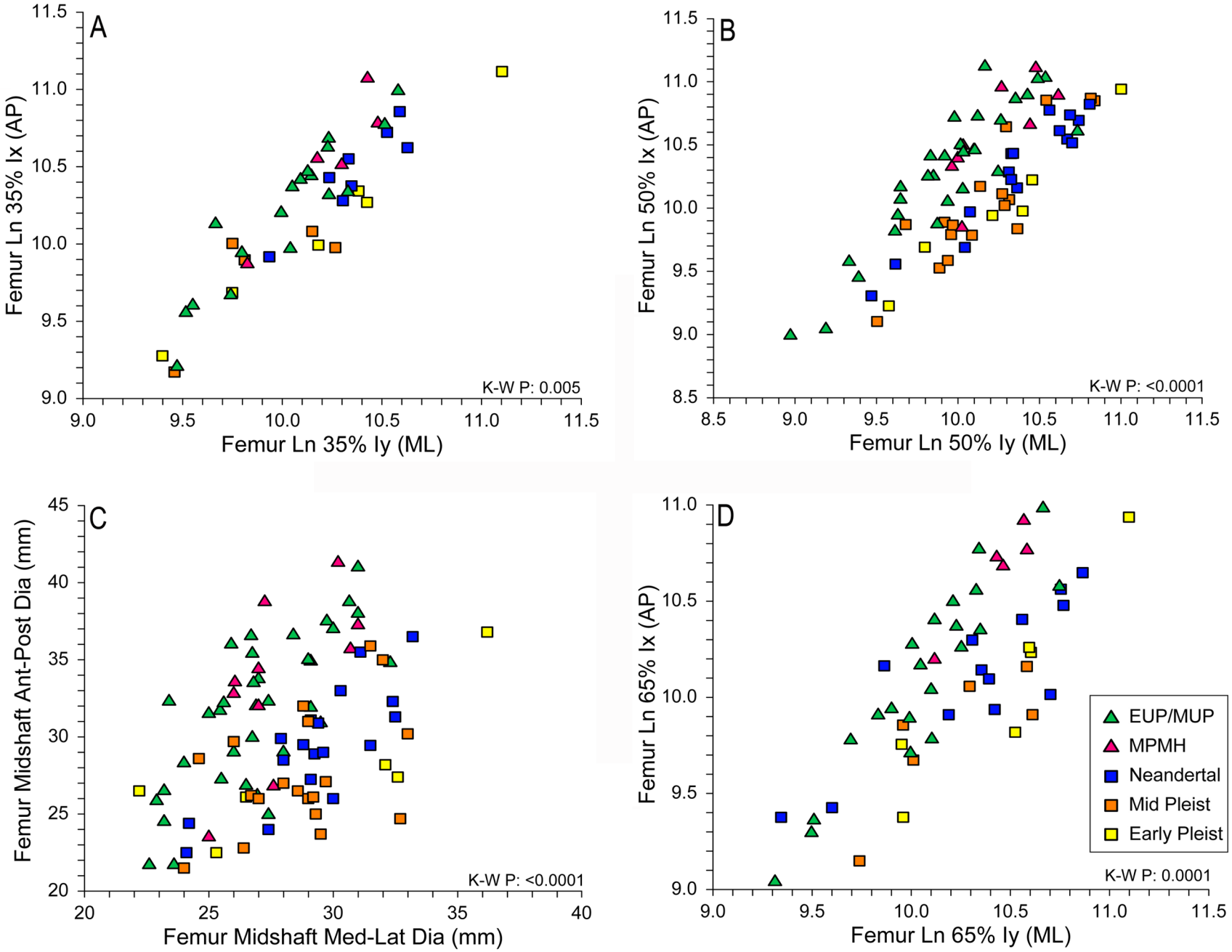


*Figure 9. Bivariate plots of logged anteroposterior ($I_x$) versus mediolateral ($I_y$) second moments of area of Pleistocene human femora for the 35% (A), 50% (B) and 65% (D) cross-sections, plus of the midshaft anteroposterior versus mediolateral external diameters (C).*

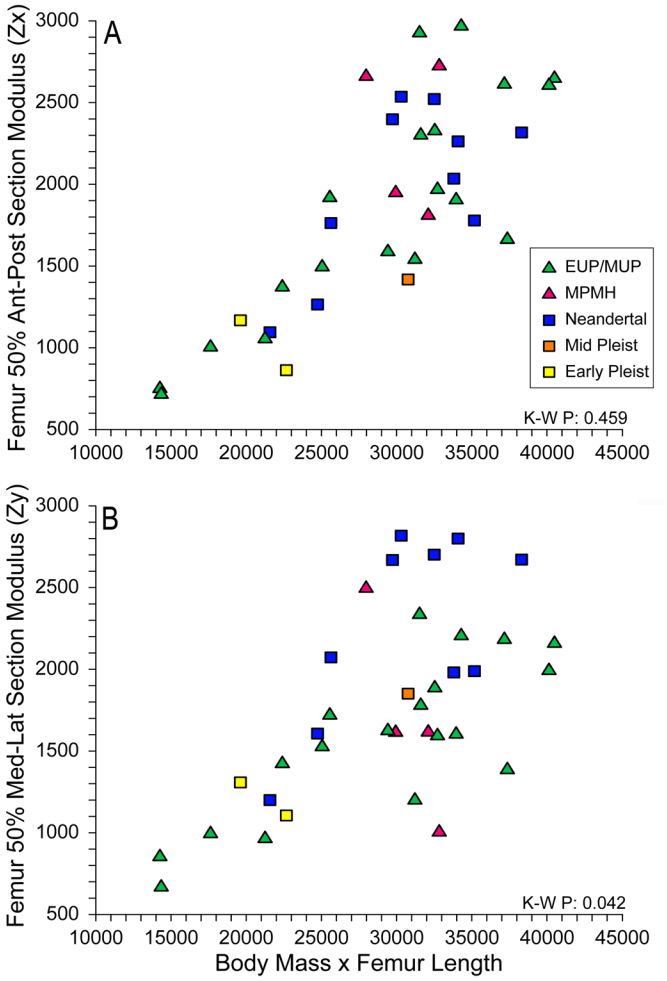


*Figure 10. Bivariate plots of midshaft (50%) anteroposterior ($Z_x$) (A) and mediolateral ($Z_y$) (B) section moduli versus body mass x length.*

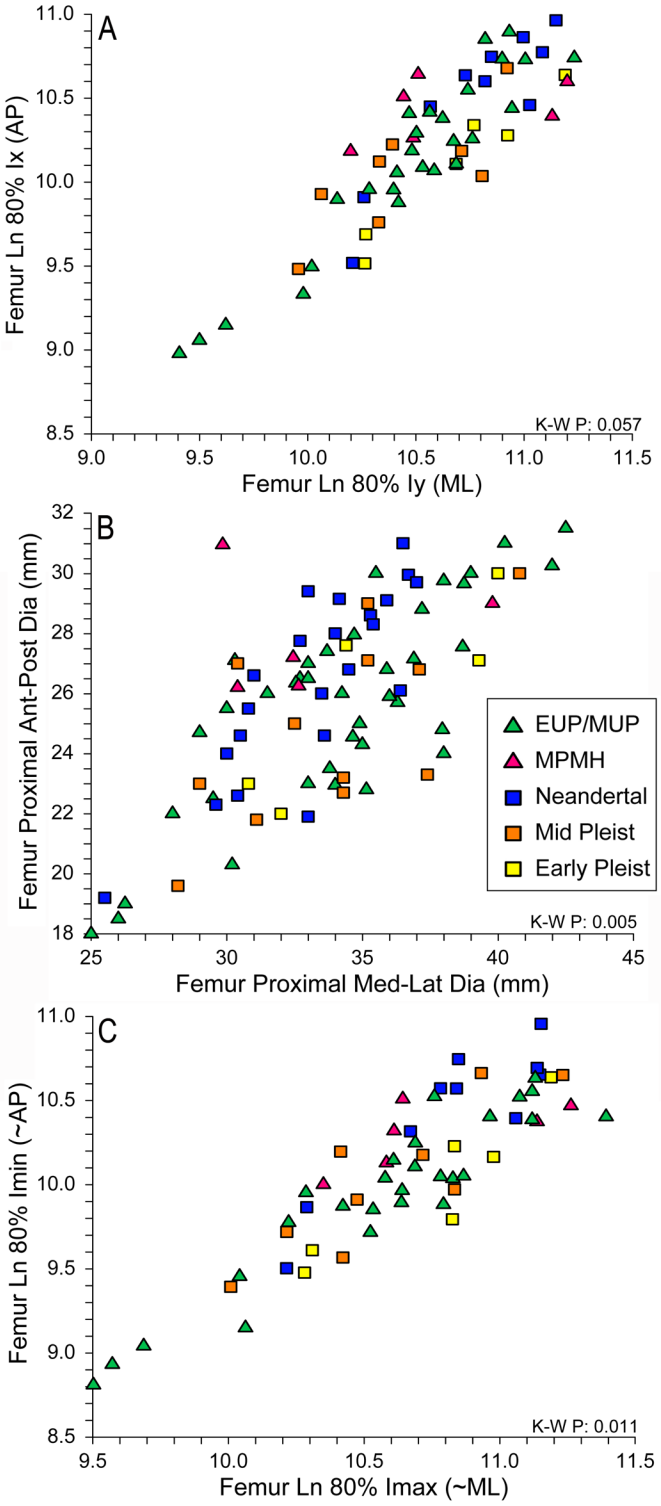


*Figure 11. Bivariate plots of the logged anteroposterior ($I_x$) versus mediolateral ($I_y$) second moments of area (A), anteroposterior versus mediolateral external diameters (B), and logged minimum ($I_{min}$) versus maximum ($I_{max}$) second moments of area (C) for Pleistocene human femora at the subtrochanteric (80%) level.*

with the earlier Upper Paleolithic. To the extent that it reflects diaphyseal hypertrophy, there is a modest decrease in relative cortical area from the Early to the Late Pleistocene in the mid and distal femur. However, it is not present in the more proximal femoral data. There appears to be a reduction in tibial relative cortical area, especially between the Early Pleistocene and later samples, but sample sizes are insufficient for it to reach statistical significance.

It is possible that there were subtle trends in reducing femoral (and tibial) robustness through the Pleistocene, as has been previously suggested (Ruff 2006; Ruff et al. 1993). However, those assessments were in part dependent on assumed linear body proportions for the earlier Pleistocene specimens, all of which come from low latitude sites and hence warm climates. If those specimens are given relatively broad pelves, as more recent data on fossil pelvic remains and relative articular dimensions suggest despite the high crural index of at least one early individual (KNM-WT 15000 [Ruff and Walker 1993]), they may well have had higher body masses relative to bone length that the modern human equatorial models imply. This change in assessing their body masses would reduce their previously inferred

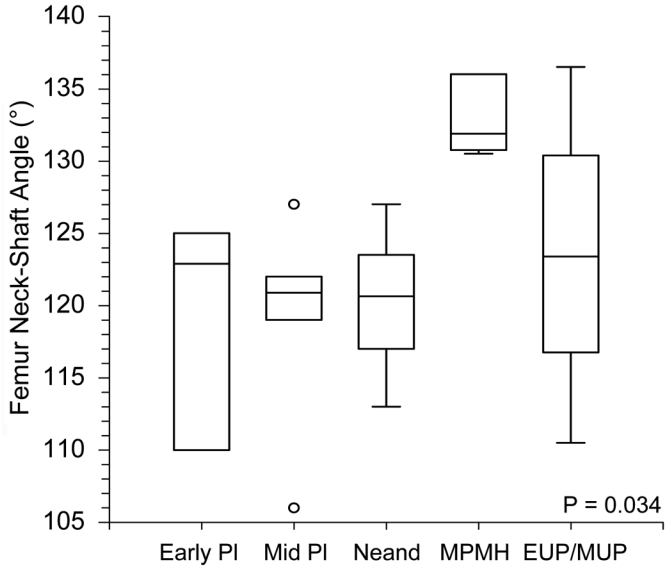


*Figure 12. Boxplots of femoral neck-shaft angles for Pleistocene humans.*

femoral robustness and make them more similar to later Pleistocene human femora. This is what using only their femoral head diameters to estimate body mass does (see Figure 4).

It is nonetheless recognized that using femoral heads alone to estimate body mass may be obscuring biomechanically relevant variation. As noted above, femoral head size reflects hip joint reaction force during development, of which body mass is only one source, if the primary one. Largely complete associated pelvic and proximal femoral remains would be necessary to test whether these body masses are sufficiently accurate for the purposes here; currently only Upper Paleolithic modern humans, one Middle Paleolithic modern human, and possibly two Neandertals may provide such data (Trinkaus 2011a; Walker et al. 2011b).

A shift in tibial diaphyseal cross-sectional shape is present through the mid-diaphysis from the Early Pleistocene to later samples, and then again with the Upper Paleolithic. These changes are sufficient to provide significant contrasts across these samples from the 35% to the 65% sections. It is not known whether these tibial differences derive from increased anteroposterior or reduced mediolateral rigidity.

In the femur, there is a pronounced contrast in cross-sectional proportions from mid-distal to mid-proximal diaphysis, however quantified. In this case, however, scaling to length and body mass indicates that the majority of the variation comes from differences in mediolateral reinforcement of the diaphysis rather than any substantial change in anteroposterior strengthening. It may well be that the frequent presence of a medial buttress on the archaic *Homo* femora is contributing to this difference. Given the apparently broad pelves of most archaic humans, from the Early to the Late Pleistocene (Bonmatí et al. 2010; Rak 1991; Rosenberg et al. 2006; Ruff 1995, 2010), and the reduced pelvic breadths in early modern humans (Holliday 1995; Trinkaus 2011a), this variation in femoral diaphyseal breadth may be an indirect effect of pelvic and crural body proportions, and hence have little to do with locomotor loading patterns *per se*.

Interestingly, the associated absence of significant cross-sample variation in scaled anteroposterior strength occurs despite the pronounced pilasters of many of the early modern human femora. Contra Trinkaus et al. (1998) and Beauval et al. (2005), the anteroposterior variation is unlikely to indicate differences in the degree of longer distance locomotion. As such, it conforms to the paleopathological (Berger and Trinkaus 1995) and paleodemographic (Trinkaus 2011b) reflections of the importance of mobility among all of these Pleistocene foragers (cf., Trinkaus n.d.). The nature of that mobility (logistical versus residential [Kelly, 1983]) cannot be assessed from these femoral comparisons, and it may well have contrasted in pattern, rather than level, among these Pleistocene foraging populations (cf., Féblot-Augustins 1997; Holt and Formicola 2008). It remains possible that relative anteroposterior versus mediolateral diaphyseal reinforcement reflects differential ranging among later Upper Paleolithic and Holocene groups (e.g., Holt 2003; Holt and Formicola 2008; Ogilvie 2004; Ruff 1999), but it does not appear to do so across these Pleistocene samples.

The relatively broad subtrochanteric femoral diaphyses of Early Pleistocene and especially earlier Middle Pleistocene humans are likely to be a similar product of differential pelvic and hip proportions (Ruff 1995). What remains unclear is why, with reduced pelvic breadths, the earlier Upper Paleolithic humans are not more different from earlier groups, albeit that their subtrochanteric shape is influenced by a distinct gluteal buttress (at times with anterior and posterior sulci along it) rather than by a general mediolateral expansion of the proximal diaphysis. It is also unclear why most (all but Qafzeh 8) of the Middle Paleolithic modern humans lack a prominent gluteal buttress.

## CONCLUSION

This reassessment of femoral and tibial cross-sectional diaphyseal properties through Pleistocene *Homo* reinforces some of the trends that had been previously identified and modestly modifies some of the others. In the tibial diaphysis, there are decreases in relative cortical area, especially between the Early Pleistocene and later human groups, and there is a reduction in mediolateral to anteroposterior rigidity, between the Early Pleistocene and subsequent samples and then with the earlier Upper Paleolithic. Femoral relative cortical area changed less, with little change proximally and reductions in the middle and mid-distal shaft. Femoral cross-sectional shape, however, exhibits marked changes, principally through the middle portions of the diaphysis and mostly contrasting archaic versus early modern humans. There is nonetheless some reduction in anteroposterior to mediolateral proportions between the Early Pleistocene sample and later archaic human samples.

Through the Pleistocene, and especially between later

archaic and early modern humans, these changes in relative mid-femoral diaphyseal reinforcement appear to be driven principally by reductions in mediolateral reinforcement. Appropriately scaled anteroposterior reinforcement changes little, indicating little or no shift in loading from locomotor ranging behaviors. It is hypothesized that the mid-femoral mediolateral reduction, probably in combination with less chronologically patterned proximal femoral proportional changes, derives from shifts in pelvic and proximal femoral proportions through the Pleistocene.

## ACKNOWLEDEGMENTS

The acquisition and compilation of these femoral and tibial cross-sectional data has been possible through the assistance of many individuals since the 1970s. Curators and colleagues who have provided access to original specimens for measurement, molding, photography, and/or radiography include T. Akazawa, B. Arensburg, T.S. Balueva, A. Bietti, S. Condemi, M. Dočkalova, Y. Coppens, D. George, I. Hershkovitz, H. Joachim, W.J. Kennedy, A. Leguebe, H. de Lumley, M. Oliva, R. Orban, H.P. Powell, J. Radovčić, F. Rashid, M. Sakka, A. Segre, H. Shang, J. Svoboda, C. Stringer, M. Teschler-Nicola, B. Vandermeersch, M.J. Walker, J. Zias, and J. Zilhão. A.P. Buzhilova, M. Chech, G.C. Conroy, D. Geraads, J.J. Hublin, B. Maureille, M.B. Mednikova, and E. Tchernov have provided casts and/or radiographs of specimens. A. Walker provided the corrected cast of KNM-ER 1808mn and assistance with measuring other specimens at the Kenya National Museums. The Government of Kenya, the Governors of the National Museums of Kenya, and the Government of Tanzania allowed access to Kenyan and Tanzanian fossils in the Kenya National Museums. B. Holt, R. Hennessy, L. Puymerail, and T. Kimura provided original cross-sectional data. A. Nelson furnished cross-sectional thicknesses for the Ngandong tibiae. S.E. Churchill provided a scaled photograph of the Hoedjiespunt tibia. This work has been funded over the years by NSF grants BNS76-14344, BNS-8004578, BNS-8519749, BNS-8919155, and SBR-9318702, Wenner-Gren Foundation grants 2979 and ICRG-14, the Leakey Foundation, the Centre National de la Recherche Scientifique, the Japan Society for the Promotion of Science, the Chinese Academy of Science, and our respective institutions. To all we are grateful.

## REFERENCES

Arensburg. B. 1977. New Upper Paleolithic human remains from Israel. *Eretz Israel* 13, pp. 208–215.

Arsuaga, J. L., Carretero, J. M., Martínez, I., and Gracia, A. 1991. Cranial remains and long bones from Atapuerca/Ibeas, Spain. *Journal of Human Evolution* 20, 191–230.

Arsuaga, J.L., Lorenzo, C., Carretero, J.M., Gracia, A., Martínez, I., García, N., Bermúdez de Castro, J.M., and Carbonell, E. 1999. A complete human pelvis from the Middle Pleistocene of Spain. *Nature* 399, 255–258.

Auerbach, B.M. and Ruff, C.B. 2004. Human body mass estimation: a comparison of "morphometric" and "mechanical" methods. *American Journal of Physical Anthropology* 125, 331–342.

Baba, H. and Aziz, F. 1992. Human tibial fragment from Sambungmacan, Java. In: Akazawa, T., Aoki, K., Kimura, T. (eds.), *The Evolution and Dispersal of Modern Humans in Asia*. Hokusen-sha, Tokyo, pp. 349–361.

Baba, H. and Endo, B. 1982. Postcranial skeleton of the Minatogawa man. In: Suzuki, H., Hanihara, K. (eds.), *The Minatogawa Man. The Upper Pleistocene Man from the Island of Okinawa*. Bulletin of the University Museum, University of Tokyo 19, pp. 61–195.

Beauval, C., Maureille, B., Lacrampe-Cuyaubère, F., Serre, D., Peressinotto, D., Bordes, J.G., Cochard, D., Couchoud, I., Dubrasquet, D., Laroulandie, V., Lenoble, A., Mallye, J.B., Pasty, S., Primault, J., Rohland, N., Pääbo, S., and Trinkaus, E. 2005. A late Neandertal femur from Les Rochers-de-Villeneuve, France. *Proceedings of the National Academy of Sciences USA* 102, 7085–7090.

Ben-Itzhak, S., Smith, P., and Bloom, R.A. 1988. Radiographic study of the humerus in Neandertals and *Homo sapiens sapiens*. *American Journal of Physical Anthropology* 77, 231–242.

Berger, T.D. and Trinkaus, E. 1995. Patterns of trauma among the Neandertals. *Journal of Archaeological Science* 22, 841–852.

Biddittu. I., Mallegni. F., and Segre, A.G. 1987. Riss age human remains, recovered from Pleistocene deposits in Ponte Mammolo (Rome-Italy). *Zeitschrift für Morphologie und Anthropologie* 77, 181–191.

Bondioli, L., Bayle, P., Dean, C., Mazurier, A., Puymerail, L., Ruff, C., Stock, J.T., Volpato, V., Zanolli, C., and Macchiarelli, R. 2010. Technical note: Morphometric maps of long bone shafts and dental roots for imaging topographic thickness variation. *American Journal of Physical Anthropology* 142, 328–334.

Bonmatí, A., Gómez-Olivenda, A., Arsuaga, J.L., Carretero, J.M., Gracia, A., Martínez, I., Lorenzo, C., Bérmudez de Castro, J.M., and Carbonell, E. 2010. Middle Pleistocene lower back and pelvis from an aged human individual from the Sima de los Huesos site, Spain. *Proceedings of the National Academy of Sciences USA* 107, 18386–18391.

Boule, M. 1911-13. L'homme fossile de La Chapelle-aux-Saints. *Annales de Paléontologie* 6, 111–172; 7, 21–56, 85–192; 8, 1–70.

Bräuer, G. 1988. Osteometrie. In: Knussman, R. (ed.), *Anthropologie I*. Fischer Verlag, Stuttgart. pp. 160–232.

Bräuer, G. 2008. The origin of modern anatomy: By speciation or intraspecific evolution? *Evolutionary Anthropology* 17, 22–37.

Brown, P., Sutikna, T., Morwood, M.J., Soejono, R.P., Jatmiko, Saptomo, E.W., and Due, R.A. 2004. A new small-bodied hominin from the Late Pleistocene of Flores, Indonesia. *Nature* 431, 1055–1061.

Cardini, L. 1955. Giacimento musteriano della Grotta Santa Croce in Bisceglie e scoperta di un femora unamo neandertaliano. *Quaternaria* 2, 312.

Churchill, S.E., Berger, L.R., and Parkington, J.E. 2000. A Middle Pleistocene human tibia from Hoedjiespunt, Western Cape, South Africa. *South African Journal of Science* 96, 367–368.

Clark, J.D., Brothwell, D.R., Powers, R., and Oakley, K.P. 1968. Rhodesian man: notes on a new femur fragment. *Man* 3,105–111.

Condemi, S. 2001. *Les Néandertaliens de La Chaise*. Comité des Travaux Historiques et Scientifiques, Paris.

Crevecoeur, I. 2008. *Étude Anthropologique du Squelette du Paléolithique Supérieur de Nazlet Khater 2 (Égypte)*. Leuven University Press, Leuven.

Day, M.H. 1971. Postcranial remains of *Homo erectus* from Bed IV, Olduvai Gorge, Tanzania. *Nature* 232, 383–387.

Day, M.H., Leakey, R.E.F., Walker, A.C., and Wood, B.A. 1975. New hominids from East Rudolf, Kenya, I. *American Journal of Physical Anthropology* 42, 461–475.

Endo, B. and Kimura, T. 1970. Postcranial skeleton of the Amud man. In: Suzuki, H. and Takai, F. (eds.), *The Amud Man and his Cave Site*. Academic Press of Japan, Tokyo. pp. 231–406.

Féblot-Augustins, J. 1997. Middle and Upper Paleolithic raw material transfers in western and central Europe: assessing the pace of change. *Journal of Middle Atlantic Archaeology* 13, 57–90.

Formicola, V. 1990. The triplex burial of Barma Grande (Grimaldi, Italy). *Homo* 39, 130–143.

García Sánchez, M. 1986. Estudio preliminar de los restos Neandertalenses del Boquete de Zafarraya (Alcaucin, Malaga). ). In: *Homenaje a Luis Siret*. Consejeria de Cultura de la Junta de Andalucia, Malaga. pp. 49–56.

Geraads, D. and Tchernov, E. 1983. Fémurs humains du pléistocène moyen de Gesher Benot Ya'acov (Israël). *L'Anthropologie* 87, 138–141.

Grimaud-Hervé, D., Valentin, F., Sémah, F., Sémah, A.M., Djubiantono, T., and Widianto, H. 1994. Le fémur humain Kresna 11 comparé à ceux de Trinil. *Comptes Rendus de l'Academie des Sciences*, Série II, 318, 1139–1144.

Grine, F., Jungers, W.L., Tobias, P.V., and Pearson, O.M. 1995. Fossil *Homo* femur from Berg Aukas, northern Namibia. *American Journal of Physical Anthropology* 97, 151–185.

Heim, J.L. 1982. Les hommes fossiles de La Ferrassie II: Les squelettes adultes (squelettes des membres). *Archives de l'Institut de Paléontologie Humaine* 38, pp. 1–272.

Hershkovitz, I., Speirs, M.S., Frayer, D., Nadel, D., Wish-Baratz, S., and Arensburg, B. 1995. Ohalo II H2: A 19,000-year-old skeleton from a water-logged site at the Sea of Galilee, Israel. *American Journal of Physical Anthropology* 96, 215–234.

Hillson, S.W., Franciscus, R.G., Holliday, T.W., and Trinkaus, E. 2006. The ages-at-death. In: Trinkaus, E. and Svoboda, J.A. (eds), *Early Modern Human Evolution in Central Europe: The People of Dolní Věstonice and Pavlov*. Oxford University Press, New York. pp. 31–45.

Holliday, T.W. 1995. *Body Size and Proportions in the Late Pleistocene Western Old World and the Origins of Modern Humans*. PhD Thesis, University of New Mexico.

Holliday, T.W. 1997. Body proportions in Late Pleistocene Europe and modern human origins. *Journal of Human Evolution* 32, 423–447.

Holt, B., 1999. *Biomechanical Evidence for Decreased Mobility in Upper Paleolithic and Mesolithic Europe*. PhD Thesis, University of Missouri-Columbia.

Holt, B.M. 2003. Mobility in Upper Paleolithic and Mesolithic Europe: evidence from the lower limb. *American Journal of Physical Anthropology* 122, 200–215.

Holt, B.M. and Formicola, V. 2008. Hunters of the Ice Age: The biology of Upper Paleolithic people. *Yearbook of Physical Anthropology* 51, 70–99.

Hublin, J.J. 1992. Le fémur humain pléistocène moyen de l'Aïn Maarouf (El Hajeb, Maroc). *Comptes Rendus de l'Academie des Sciences*, Série II, 314, 975–980.

Hrdlička, A. 1930. The skeletal remains of early man. *Smithsonian Miscellaneous Collections* 83, 1–379.

Indriati, E., Swisher, C.C. III, Lepre, C., Quinn, R.L., Suriyanto, R.A., Hascaryo, A.T., Grün, R., Feibel, C.S., Pobiner, B.L., Aubert, M., Lees, W., and Antón, S.C. 2011. The age of the 20 meter Solo River terrace, Java, Indonesia and the survival of *Homo erectus* in Asia. *PLoS One* E6(6), e21562.

Jelínek, J. 1959. Der fossile Mensch Brno II. *Anthropos* 9, 17–22.

Kelly, R.L. 1983. Hunter-gatherer mobility strategies. *Journal of Anthropological Research* 39, 277–306.

Kennedy, G.E. 1983. A morphometric and taxonomic assessment of a hominine femur from the lower member, Koobi Fora, Lake Turkana. *American Journal of Physical Anthropology* 61, 429–436.

Kennedy, G.E. 1985. Bone thickness in *Homo erectus. Journal of Human Evolution* 14, 699–708.

Kimura, T. and Takahashi, H. 1992. Cross sectional geometry of the Minatogawa limb bones. In: Akazawa, T., Aoki, K., and Kimura, T. (eds.), *The Evolution and Dispersal of Modern Humans in Asia*. Hokusen-Sha, Tokyo. pp. 305–320.

Klaatsch, H. and Lustig, W. 1914. Morphologie der paläolithische Skelettreste des mittleren Aurignacien der Grotte von La Rochette, Dep. Dordogne. *Archiv für Anthropologie* 41, 81–126.

Kunter, M. and Wahl, J. 1992. Das Femurfragment eines Neandertalers aus der Stadelhöhle des Hohlensteins im Lonetal. *Fundberichte Baden-Württemberg* 17, 111–124.

Leakey, R.E., Leakey, M.G., and Behrensmeyer, A.K. 1978. The hominid catalogue. In: Leakey, M.G. and Leakey, R.E. (eds.), *Koobi Fora Research Project 1. The fossil hominids and an introduction to their context, 1968-1974*. Oxford University Press, Oxford. pp. 86–182.

Lordkipanidze, D., Jashashvili, T., Vekua, A., Ponce de León, M., Zollikofer, C.P.E., Rightmire, G.P., Pontzer, H., Ferring, R., Oms, O., Tappen, M., Bukhsianidze, M., Agusti, J., Kahlke, R., Kiladze, G., Martinez-Navarro, B., Mouskhelishvili, A., Nioradze, M., and Rook, L. 2007. Postcranial evidence from early *Homo* from Dmanisi, Georgia. *Nature* 449, 305–310.

Lovejoy, C.O. 1982. Diaphyseal biomechanics of the locomotor skeleton of Tautavel man with comments on the evolution of skeletal changes in Late Pleistocene man. In: Lumley, H. de (ed.), *L'Homo erectus et la Place de l'Homme de Tautavel parmi les Hominidés Fossiles*. CNRS,

Paris. pp. 447–470.
Lovejoy, C.O. and Trinkaus, E. 1980. Strength and robusticity in the Neandertal tibia. *American Journal of Physical Anthropology* 53, 465–470.
Lovejoy, C.O., Burstein, A.H., Heiple, K.G., 1976. The biomechanical analysis of bone strength: A method and its application to platycnemia. *American Journal of Physical Anthropology* 44, 489–505.
Mallegni, F., 1986. Les restes humains du gisement de Sedia del Diavolo (Rome) remontant au Riss final. *L'Anthropologie* 90, 539–553.
Mallegni, F., Mariani-Costantini, R., Fornaciari, G., Longo, E.T., Giacobini, G., and Radmilli, A.M. 1983. New European fossil hominid material from an Acheulian site near Rome (Castel del Guido). *American Journal of Physical Anthropology* 62, 263–274.
Mallegni, F., Bertoldi, F., and Manolis, S.K. 1999. The Gravettian female human skeleton from Grotta Paglicci, south Italy. *Homo* 50, 127–148.
Mallegni, F., Bertoldi, F., and Manolis, S.K. 2000. Paleobiology of two Gravettian skeletons from Veneri cave (Parabita, Puglia, Italy). *Homo* 51, 235–257.
Martin, H. 1923. *L'Homme Fossile de La Quina*. Librairie Octave Doin, Paris.
Martin, R. 1928. *Lehrbuch der Anthropologie*, 2nd ed. Fischer Verlag, Jena.
Massari, C. 1958. Alcuni rilievi sul quinto scheletro della Barma Grande. *Rivista Scienze Preistoriche* 13, 47–53.
Matiegka, J. 1938. *Homo předmostensis. Fosilní člověk z Předmostí na Moravě II. Ostatní Části Kostrové*. Česká Akademie Věd a Umění, Prague.
Matsu'ura, S. and Kondo, M. 2011. Relative choronology of the Minatogawa and the Upper Minatogawa series of human remains from Okinawa Island, Japan. *Journal of Anthropological Sciences* 119, 173–182.
McCown, T.D. and Keith, A. 1939. *The Stone Age of Mount Carmel II: The Fossil Human Remains from the Levalloiso-Mousterian*. Clarendon Press, Oxford.
McHenry, H.M. 1994. Early hominid postcrania. Phylogeny and function. In: Corruccini, R.S. and Ciochon, R.L. (eds.), *Integrative Paths to the Past* (Advances in Human Evolution Series, Vol 2). Prentice Hall, Englewood Cliffs. pp. 168–251.
Mednikova, M. and Trinkaus, E. 2001. Femoral midshaft diaphyseal cross-sectional geometry of the Sunghir 1 and 4 Gravettian human remains. *Anthropologie (Brno)* 39, 135–141.
Morwood, M.J., Brown, P., Jatmiko, Saptomo, E.W., Westaway, K.E., Due, R.A., Roberts, R.G., Maeda, T., Wasisto, S., and Djubiantono, T. 2005. Further evidence for small-bodied hominins from the Late Pleistocene of Flores, Indonesia. *Nature* 437, 1012–1017.
Nagurka, M.L. and Hayes, W.C. 1980. An interactive graphics package for calculating cross-sectional properties of complex shapes. *Journal of Biomechanics* 13, 59–64.
Nelson, A.J. 1995. *Cortical Bone Thickness in the Primate and Hominid Postcranium – Taxonomy and Allometry*. PhD Thesis, University of California, Los Angeles.
Ogilvie, M.D. 2004. Mobility and the locomotor skeleton at the foraging to farming transition. In: Meldrum, D.J. and Hilton, C.E. (eds.), *From Biped to Strider*. Kluwer Academic, New York. pp. 183–201.
Oliva, M. 1996. Mladopaleolitický hrob Brno II jako příspěvek k počátkům šamanismu. *Archeologické rozhledy* 48, 353–383, 537–542.
O'Neill, M.C. and Ruff, C.B. 2004. Estimating human long bone cross-sectional geometric properties: a comparison of noninvasive methods. *Journal of Human Evolution* 47, 221–235.
Ortega, M.C., Gracia, A., Carretero, J.M., Martínez, I., Quam, R., and Arsuaga, J.L. 2009. Restauration d'un fémur fossile humain du site de la Sima de los Huesos (Atapuerca, Espagne). *L'Anthropologie* 113, 233–244.
Passarello, P. and Palmieri, A. 1968. Studio sui resti umani di tibia e di ulna provenienti da strata pleistocenici della cava Pompi de Pofi (Frosinone). *Rivista di antropologia* 55, 139–162.
Pearson, O.M. and Lieberman, D.E. 2004. The aging of Wolff's "law": ontogeny and responses to mechanical loading in cortical bone. *Yearbook of Physical Anthropology* 47, 63–99.
Pearson, O.M., Royer, D.F., Grine, F.E., and Fleagle, J.G. 2008a. A description of the Omo 1 postcranial skeleton, including newly discovered fossils. *Journal of Human Evolution* 55, 421–437.
Pearson, O.M., Fleagle, J.G., Grine, F.E., and Royer, D.F. 2008b. Further new hominin fossils from the Kibish Formation, southwestern Ethiopia. *Journal of Human Evolution* 55, 444–447.
Ponce de León, M., Golovanova, L., Doronichev, V., Romanova, G., Akazawa, T., Kondo, O., Ishida, H., and Zollikofer, C.P.E., 2008. Neanderthal brain size at birth provides insights into the evolution of human life history. *Proceedings of the National Academy of Sciences USA* 105, 13764–13768.
Proschan, M.A. and Waclawiw, M.A. 2000. Practical guidelines for multiplicity adjustment in clinical trials. *Controlled Clinical Trials* 21, 527–539.
Puymerail, L. 2011. *Caracterisation de l'Endostructure et des Propriétés Biomécaniques de la Diaphyse Fémorale: La Signature de la Bipédie et la Réconstruction des Paléo-Répertoires Posturaux et Locomoteurs des Homininés*. Thèse de Doctorat, Muséum National d'Histoire Naturelle.
Rak, Y. 1991. The pelvis. In: Bar Yosef, O. and Vandermeersch, B. (eds.), *Le Squelette Moustérien de Kébara 2*. Editions du C.N.R.S., Paris. pp. 147–156.
Rice, W.R. 1989. Analyzing tables of statistical tests. *Evolution* 43, 223–225.
Rightmire, G.P. 2008. *Homo* in the Middle Pleistocene: Hypodigms, variation, and species recognition. *Evolutionary Anthropology* 17, 8–21.
Rosenberg, K.R., Lü Z., and Ruff, C.B. 2006. Body size, body proportions, and encephalization in a Middle Pleistocene archaic human from northern China. *Proceedings of the National Academy of Sciences USA* 103, 3552–3556.
Ruff, C.B. 1992. Biomechanical analyses of archaeological

human material. In: Saunders, S.R. and Katzenburg, A. (eds.), *The Skeletal Biology of Past Peoples*. Alan R. Liss, New York. pp. 41–62

Ruff, C.B. 1994. Morphological adaptation to climate in modern and fossil hominids. *Yearbook of Physical Anthropology* 37, 65–107.

Ruff, C.B. 1995. Biomechanics of the hip and birth in early *Homo*. *American Journal of Physical Anthropology* 98, 527–574.

Ruff, C.B. 1999. Skeletal structure and behavioral patterns of prehistoric Great Basin populations. In: Hemphill, B.E. and Larsen, C.S. (eds.), *Prehistoric Lifeways in the Great Basin Wetlands: Bioarchaeological Reconstruction and Interpretation*. University of Utah Press, Salt Lake City. pp. 290–320.

Ruff, C.B. 2000. Body mass prediction from skeletal frame size in elite athletes. *American Journal of Physical Anthropology* 113, 507–517.

Ruff, C.B. 2002. Long bone articular and diaphyseal structure in Old World monkeys and apes, I: Locomotor effects. *American Journal of Physical Anthropology* 119, 305–342.

Ruff, C.B. 2006. Gracilization of the modern human skeleton. *American Scientist* 94, 508–514.

Ruff, C.B. 2008. Femoral/humeral strength in early African *Homo erectus*. *Journal of Human Evolution* 54, 383–390.

Ruff, C.B. 2009. Relative limb strength and locomotion in *Homo habilis*. *American Journal of Physical Anthropology* 138, 90–100.

Ruff, C.B. 2010. Body size and body shape in early hominins – implications of the Gona Pelvis. *Journal of Human Evolution* 58, 166–178.

Ruff, C.B. and Hayes, W.C. 1983a. Cross-sectional geometry of Pecos Pueblo femora and tibiae – a biomechanical investigation: I. Method and general patterns of variation. *American Journal of Physical Anthropology* 60, 259–381.

Ruff, C.B. and Hayes, W.C. 1983b. Cross-sectional geometry of Pecos Pueblo femora and tibiae – a biomechanical investigation: II. Sex, age, and side differences. *American Journal of Physical Anthropology* 60, 383–400.

Ruff, C.B. and Walker, A. 1993. Body size and body shape. In: Walker A. and Leakey, R (eds.), *The Nariokotome Homo erectus Skeleton*. Cambridge MA: Harvard University Press. pp. 234–265.

Ruff, C.B., Scott, W.W., and Liu, A.Y.C. 1991. Articular and diaphyseal remodeling of the proximal femur with changes in body mass in adults. *American Journal of Physical Anthropology* 86, 397–413.

Ruff, C.B., Trinkaus, E., Walker, A., and Larsen, C.S. 1993. Postcranial robusticity in *Homo*, I: Temporal trends and mechanical interpretations. *American Journal of Physical Anthropology* 91, 21–53.

Ruff, C.B., Walker, A., and Trinkaus, E. 1994. Postcranial robusticity in *Homo*, III: Ontogeny. *American Journal of Physical Anthropology* 93, 35–54.

Ruff, C.B., Trinkaus, E., and Holliday, T.W. 1997. Body mass and encephalization in Pleistocene *Homo*. *Nature* 387, 173–176.

Ruff, C.B., Niskanen, M., Junno, J.A., and Jamison, P. 2005. Body mass prediction from stature and bi-iliac breadth in two high latitude populations, with application to earlier higher latitude humans. *Journal of Human Evolution* 48, 381–392.

Ruff, C.B., Holt, B., and Trinkaus, E. 2006. Who's afraid of the big bad Wolff? "Wolff's Law" and bone functional adaptation. *American Journal of Physical Anthropology* 129, 484–498.

Santa Luca, A.P. 1980. The Ngandong Fossil Hominids. *Yale University Publications in Anthropology* 78, 1–175.

Sergi, S., Parenti, R., and Paoli, G. 1974. Il giovane paleolitico della Caverna delle Arene Candide. *Studi Paletnologia, Paleoantropologia, Paleontologia e Geologia Quaternario* 2, 13–38.

Shackelford, L.L. 2005. *Patterns of Geographic Variation in the Postcranial Robusticity of Late Upper Paleolithic Humans*. Ph.D. Thesis, Washington University.

Shackelford, L.L. 2007. Regional variation in the postcranial robusticity of Late Upper Paleolithic humans. *American Journal of Physical Anthropology* 133, 655–668.

Shang, H. and Trinkaus, E. 2010. *The Early Modern Human from Tianyuan Cave, China*. Texas A&M University Press, College Station TX.

Sigmon, B. 1982. Comparative morphology of the locomotor skeleton of *Homo erectus* and the other fossil hominids, with special reference to the Tautavel innominate and femora. In: Lumley, H. de (ed.), *L'Homo erectus et la Place de l'Homme de Tautavel parmi les Hominidés Fossiles*. CNRS, Paris. pp. 422–446.

Sládek, V., Trinkaus, E., Hillson, S.W., and Holliday, T.W. 2000. *The People of the Pavlovian: Skeletal Catalogue and Osteometrics of the Gravettian Fossil Hominids from Dolní Věstonice and Pavlov*, Dolní Věstonice Studies 5. Archeologický ústav AV ČR, Brno.

Stringer, C.B. 1986. An archaic character in the Broken Hill innominate E.719. *American Journal of Physical Anthropology* 71, 115–120.

Stringer, C.B., Trinkaus, E., Roberts, M.B., Parfitt, S.A., and Macphail, R.I. 1998. The Middle Pleistocene human tibia from Boxgrove. *Journal of Human Evolution* 34, 509–547.

Swischer, C.C. III, Rink, W.J., Antón, S.C., Schwarcz, H.P., Curtis, G.H., Suprijo, and Widiasmoro. 1996. Latest *Homo erectus* of Java: Potential contemporaneity with *Homo sapiens* in southeast Asia. *Science* 274, 1870–1874.

Sylvester, A.D., Garofalo, E., and Ruff, C.B. 2010. An R program for automating bone cross section reconstruction. *American Journal of Physical Anthropology* 142, 665–669.

Trinkaus, E. 1976. The evolution of the hominid femoral diaphysis during the Upper Pleistocene in Europe and the Near East. *Zeitschrift für Morphologie und Anthropologie* 67, 291–319.

Trinkaus, E. 1981. Neanderthal limb proportions and cold adaptation. In: Stringer, C.B. (ed.), *Aspects of Human Evolution*. Taylor & Francis, London. pp. 187–224.

Trinkaus, E. 1983. *The Shanidar Neandertals*. Academic Press,

New York.
Trinkaus, E. 1984. Does KNM-ER 1481A establish *Homo erectus* at 2.0 myr BP? *American Journal of Physical Anthropology* 64, 137–139.
Trinkaus, E. 1986. The Neandertals and modern human origins. *Annual Review of Anthropology* 15, 193–218.
Trinkaus, E. 1997. Appendicular robusticity and the paleobiology of modern human emergence. *Proceedings of the National Academy of Sciences USA* 94, 13367–13373.
Trinkaus, E. 2000a. The "Robusticity Transition" revisited. In: Stringer, C., Barton, R.N.E., and Finlayson, C. (eds.), *Neanderthals on the Edge*. Oxford: Oxbow Books, pp. 227–236.
Trinkaus, E. 2000b. The human remains from Paviland Cave: Late Pleistocene and Holocene human remains from Paviland Cave. In: Aldhouse-Green, S.H.R. (ed.), *Paviland Cave and the 'Red Lady': A Definitive Report*. Western Academic and Specialist Press Ltd, Bristol. pp. 141–199.
Trinkaus, E. 2003. Biomechanical analysis of the Krapina archaic *Homo* humeral, femoral and tibial diaphyses. In: Fiedler, L., Heinrich, W.D., Justus,A., and Brühl, E. (eds.), *Erkenntnisjäger. Kultur und Umwelt des frühen Menschen (Festschrift für Dietrich Mania)*. Veröffentlichungen des Landesamtes für Archäologie Sachsen-Anhalt – Landesmuseum für Vorgeschichte 57, 607–614.
Trinkaus, E. 2006a. Modern human versus Neandertal evolutionary distinctiveness. *Current Anthropology* 47, 597–620.
Trinkaus, E. 2006b. The lower limb remains. In: Trinkaus, E. and Svoboda, J.A. (eds.), *Early Modern Human Evolution in Central Europe: The People of Dolní Věstonice and Pavlov*. Oxford University Press, New York, pp. 380–418.
Trinkaus, E. 2009. The human tibia from Broken Hill, Kabwe, Zambia. *PaleoAnthropology* 2009, 145–165.
Trinkaus, E. 2011a. The postcranial dimensions of the La Chapelle-aux-Saints 1 Neandertal. *American Journal of Physical Anthropology* 145, 461–468.
Trinkaus, E. 2011b. Late Pleistocene adult mortality patterns and modern human establishment. *Proceedings of the National Academy of Sciences USA* 108, 1267–1271.
Trinkaus, E. n.d. The paleobiology of modern human emergence. In: Smith, F.H., and Ahern, J.C.M. (eds.), *Origin of Modern Humans*, 2nd edition. Wiley-Blackwell, New York (in press).
Trinkaus, E. and Ruff, C.B. 1989. Diaphyseal cross-sectional geometry and biomechanics of the Fond-de-Forêt 1 femur and the Spy 2 femur and tibia. *Bulletin de la Societé Royale Belge d'Anthropologie et de Préhistoire* 100, 33–42.
Trinkaus, E. and Ruff, C.B. 1999a. Diaphyseal cross-sectional geometry of Near Eastern Middle Paleolithic humans: The femur. *Journal of Archaeological Science* 26, 409–424.
Trinkaus, E. and Ruff, C.B. 1999b. Diaphyseal cross-sectional geometry of Near Eastern Middle Paleolithic humans: The tibia. *Journal of Archaeological Science* 26, 1289–1300.
Trinkaus, E. and Ruff, C.B. 2000. Comment on: O.M. Pearson, "Activity, climate, and postcranial robusticity. Implications for modern human origins and scenarios of adaptive change." *Current Anthropology* 41, 598.
Trinkaus, E., Churchill, S.E., and Ruff, C.B. 1994. Postcranial robusticity in *Homo*, II: Humeral bilateral asymmetry and bone plasticity. *American Journal of Physical Anthropology* 93, 1–34.
Trinkaus, E., Ruff, C.B., Churchill, S.E., and Vandermeersch, B. 1998. Locomotion and body proportions of the Saint-Césaire 1 Châtelperronian Neandertal. *Proceedings of the National Academy of Sciences USA* 95, 5836–5840.
Trinkaus, E., Ruff, C.B., and Conroy, G.C. 1999a. The anomalous archaic *Homo* femur from Berg Aukas, Namibia: A biomechanical assessment. *American Journal of Physical Anthropology* 110, 379–391.
Trinkaus, E., Stringer, C.B., Ruff, C.B., Hennessy, R.J., Roberts, M.B., and Parfitt, S.A. 1999b. Diaphyseal cross-sectional geometry of the Boxgrove 1 Middle Pleistocene human tibia. *Journal of Human Evolution* 37, 1–25.
Trinkaus, E., Churchill, S.E., Ruff, C.B., and Vandermeersch, B. 1999c. Long bone shaft robusticity and body proportions of the Saint-Césaire 1 Châtelperronian Neandertal. *Journal of Archaeological Science* 26, 753–773.
Trinkaus, E., Formicola, V., Svoboda, J., Hillson, S.W., and Holliday, T.W. 2001. Dolní Věstonice 15: Pathology and persistence in the Pavlovian. *Journal of Archaeological Science* 28, 1291–1308.
Trinkaus, E., Hillson, S.W., Franciscus, R.G., and Holliday, T.W. 2006a. Skeletal and dental paleopathology. In: Trinkaus, E. and Svoboda, J.A. (eds.), *Early Modern Human Evolution in Central Europe: The People of Dolní Věstonice and Pavlov*. Oxford University Press, New York. pp. 419–458.
Trinkaus, E., Smith, F.H., Stockton, T.C., and Shackelford, L.L. 2006b. The human postcranial remains from Mladeč. In: Teschler-Nicola, M. (ed.), *Early Modern Humans at the Moravian Gate: The Mladeč Caves and their Remains*. Springer Verlag, Vienna. pp. 385–445.
Trinkaus, E., Maki, J., and Zilhão, J. 2007. Middle Paleolithic human remains from the Gruta da Oliveira (Torres Novas), Portugal. *American Journal of Physical Anthropology* 134, 263–273.
Twiesselmann, F. 1961. Le fémur Néanderthalien de Fond-de-Forêt (Province de Liège). *Mémoire de l'Institut Royal des Sciences Naturelles de Belgique* 148, 1–164.
Vandermeersch, B. 1981. *Les Hommes Fossiles de Qafzeh (Israël)*. Paris: C.N.R.S.
Verneau, R. 1906. *Les Grottes de Grimaldi (Baoussé-Roussé), Tome II – Fascicule I. Anthropologie*. Imprimérie de Monaco, Monaco.
Walker, A. and Leakey, R. 1993. The postcranial bones. In: Walker, A. and Leakey, R. (eds.), *The Nariokotome Homo erectus Skeleton*. Harvard University Press, Cambridge MA. pp. 95–160.
Walker, A., Zimmerman, M.R., and Leakey, R.E.F. 1982. A possible case of hypervitaminosis A in *Homo erectus*. *Nature* 296, 248–250.
Walker, M.J., Ortega, J., López, M.V., Parmová, K., and

Trinkaus, E. 2011a. Neandertal postcranial remains from the Sima de las Palomas del Cabezo Gordo, Murcia, southeastern Spain. *American Journal of Physical Anthropology* 144, 505–515.

Walker, M.J., Ortega, J., Parmová, K., López, M.V., and Trinkaus, E. 2011b. Morphology, body proportions and postcranial hypertrophy of a female Neandertal from the Sima de las Palomas, southeastern Spain. *Proceedings of the National Academy of Sciences USA* 108, 10087–10091.

Weidenreich, F. 1941. The extremity bones of *Sinanthropus pekinensis*. *Palaeontologia Sinica* 5D, 1–82.

Wood, B.A. 2010. Reconstructing human evolution: Achievements, challenges, and opportunities. *Proceedings of the National Academy of Sciences USA* 107, 8902–8909.

Wu, X.Z. and Poirier, F.E. 1995. *Human Evolution in China. A Metric Description of the Fossils and a Review of the Sites*. Oxford University Press, Oxford.

# Appendix

The following tables provide the original cross-sectional diaphyseal measurements available for Pleistocene *Homo* femora and tibiae up to approximately the time of the Late Pleistocene last glacial maximum. The cross-sectional measurements consist of: total area (TA) and cortical area (CA) in $mm^2$; and the anteroposterior ($I_x$), mediolateral ($I_y$), maximum ($I_{max}$), minimum ($I_{min}$) second moments of area in $mm^4$; the polar moment of area (J, in $mm^4$) is the sum of any two perpendicular second moments of area (Tables A2 to A11). To these are added standard external osteometric linear diameters of the midshafts and proximal diaphyses (Table A13). From the second moments of area and diaphyseal diameters, section moduli ($Z_x$, $Z_y$ and $Z_p$, in $mm^3$) were computed based on a pooled recent human sample (see text and Table A12). These diaphyseal measurements are preceded by available directly measureable or estimated femoral and tibial lengths and femoral head diameters, plus body mass estimated from the femoral head diameters (Table A1). Estimated lengths and articular measurements are in parentheses.

Relatively few of the specimens provide sufficiently complete condyles for standard, knee-based diaphyseal orientation, following Ruff and Hayes (1983a). As discussed in the text, diaphyseal morphological features are employed for orientation of the less complete fossils. The uncertainty in orientations affects only the anatomically oriented second moments of area ($I_x$ and $I_y$) and their section moduli ($Z_x$ and $Z_y$). Those femoral and tibiae that provide sufficiently complete condyles for orientation are indicated by an asterisk.

The earlier samples are strictly chronological. The Late Pleistocene ones, given the presence of both late archaic and early modern humans in the Late Pleistocene, are subdivided into samples of late archaic humans (for which only western Eurasian Neandertals provide data), Middle Paleolithic modern humans (MPMH); and Early/Mid Upper Paleolithic modern humans (EUP/MUP).

## TABLE A1. FEMORAL AND TIBIAL LENGTHS, FEMORAL HEAD DIAMETER, AND ESTIMATED BODY MASS FOR PLEISTOCENE *HOMO*

(estimated values are in parentheses; previously published lengths not included here are considered to be insufficiently reliable for more than the positioning of the cross-sections; additional femoral head diameters are available [Ruff 2010; Trinkaus 2011], but they are not associated with sufficiently complete diaphyses to provide cross-sections and are therefore not included).

| | Femur Maximum Length (mm) | Femur Biomech Length (mm) | Tibia Maximum Length (mm) | Tibia Biomech Length (mm) | Femur Head Diam (mm) | Body Mass Estimate (kg)[1] |
|---|---|---|---|---|---|---|
| **Early Pleistocene** | | | | | | |
| KNM-ER 736[2,3] | (509) | (480) | | | | |
| KNM-ER 737[2,3] | (442) | (415) | | | | |
| KNM-ER 803a,b[2,3,4] | (426) | (400) | (363) | (340) | | |
| KNM-ER 1472 | 404 | 376 | | | 40.0 | 52.1 |
| KNM-ER 1481a | 399 | 370 | | | (44.0) | 61.2 |
| KNM-ER 1808mn[2,3] | (488) | (460) | | | | |
| **Middle Pleistocene** | | | | | | |
| Aïn Maarouf 1[5,6] | (394) | (370) | | | | |
| Boxgrove 1[7] | | | (397) | (373) | | |
| Broken Hill E690[2,3] | (419) | (393) | | | | |
| Broken Hill E691 | | | 416 | 390 | | |
| Gesher-B.-Y. 1[8] | (388) | (364) | | | | |
| Ngandong 14[4] | | | (377) | 354 | | |
| OH 28[2,3] | (452) | (425) | | | (47.8)[9] | 72.4 |
| Zhoukoudian 1[5,10] | (400) | (376) | | | | |

TABLE A1. (continued)

| | Femur Maximum Length (mm) | Femur Biomech Length (mm) | Tibia Maximum Length (mm) | Tibia Biomech Length (mm) | Femur Head Diam (mm) | Body Mass Estimate (kg)[1] |
|---|---|---|---|---|---|---|
| **Neandertals** | | | | | | |
| Amud 1[11] | (484) | (458) | | | (48.1)[9] | 70.9 |
| Chapelle-aux-Saints 1[12] | (440) | (420) | | | 52.4 | 81.1 |
| Feldhofer 1 | 443 | 419 | | | 52.2 | 80.6 |
| Ferrassie 1[13] | (461) | (451) | (370) | (353) | 54.0 | 84.9 |
| Ferrassie 2 | 412 | 386 | 311 | 288 | 45.9 | 66.4 |
| Fond-de-Forêt 1[3,14] | (465) | (438) | | | (48.5)[15] | 72.9 |
| Palomas 92[3,16] | (397) | (372) | | | (44.2)[15] | 61.7 |
| Palomas 96 | 374 | 360 | 304 | 285 | 43.0 | 59.9 |
| Shanidar 2 | | | 338 | 310 | | |
| Shanidar 4[17] | (425) | (404) | | | 49.2 | 73.5 |
| Shanidar 5[17] | (450) | 429 | | | 47.5 | 70.6 |
| Shanidar 6[17] | (388) | (366) | (302) | (282) | | |
| Spy 2 | 425 | 411 | 331 | 307 | 54.0 | 85.5 |
| Tabun 1 | 416 | 391 | 319 | 295 | 44.5 | 63.3 |
| **Middle Paleolithic Modern Humans** | | | | | | |
| Qafzeh 3[11] | | | (365) | (340) | -- | |
| Qafzeh 8[11] | | | (433) | (405) | -- | |
| Qafzeh 9 | 472 | 442 | | | 44.5 | 63.3 |
| Skhul 4 | 494 | 465 | 439 | 411 | 47.3 | 69.0 |
| Skhul 5[18] | (518) | (477) | | | (47.2)[9] | 68.8 |
| Skhul 6 | 477 | 447 | | | 46.5 | 66.9 |
| **Early/Mid Upper Paleolithic** | | | | | | |
| Arene Candide IP | 453 | 427 | 379 | 338 | 49.0 | 73.1 |
| Barma Grande 2 | 516 | 499 | | | 52.4 | 81.1 |
| Cro-Magnon 1[19,20] | (499) | (468) | | | (47.0)[9] | 67.3 |
| Cro-Magnon 4322[3,20] | (493) | (462) | | | | |
| Cro-Magnon 4324[3,20] | (424) | (393) | | | | |
| Cro-Magnon 4330 | | | 384 | 359 | | |
| Cro-Magnon 4332[4,19,20] | | | (398) | (374) | | |
| Dolní Věstonice 3[21] | (427) | (391) | (359) | (338) | 40.5 | 54.3 |
| Dolní Věstonice 13 | 449 | 423 | 382 | 360 | 47.5 | 69.5 |
| Dolní Věstonice 14[21] | (505) | (480) | (420) | (394) | 51.0 | 77.8 |
| Dolní Věstonice 15 | | | 344 | 324 | 46.9 | 67.1 |
| Dolní Věstonice 16[21] | 471 | 443 | (390) | (367) | 50.5 | 76.6 |
| Grotte des Enfants 4 | 514 | 486 | | | 53.0 | 82.5 |
| Minatogawa 1[22] | 398 | 371 | (322) | (300) | 44.0 | 60.4 |
| Minatogawa 2[22] | 360 | 332 | | | 37.0 | 42.9 |
| Minatogawa 3[22] | 382 | 353 | 306 | 287 | 38.5 | 49.9 |
| Minatogawa 4[22] | 360 | 334 | 301 | 285 | (37.0) | 42.9 |

**TABLE A1. (continued)**

| | Femur Maximum Length (mm) | Femur Biomech Length (mm) | Tibia Maximum Length (mm) | Tibia Biomech Length (mm) | Femur Head Diam (mm) | Body Mass Estimate (kg)[1] |
|---|---|---|---|---|---|---|
| **Early/Mid Upper Paleolithic (cont.)** | | | | | | |
| Mladeč 27[23] | (486) | (455) | | | | |
| Nahal 'En-Gev 1[11] | (396) | (365) | | | | |
| Ohalo 2 | 464 | 431 | 384 | 361 | 49.1 | 73.3 |
| Paglicci 25 | 446 | 428 | | | 42.9 | 59.7 |
| Paviland 1 | 478 | 452 | 401 | 379 | 48.7 | 72.4 |
| Pavlov 1[21] | (497) | (450) | | | | |
| Rochette 2 | 412 | 397 | | | 44.8 | 63.1 |
| Sunghir 1 | 499 | 476 | 423 | 399 | 51.1 | 78.0 |
| Tianyuan 1[24] | (463) | (436) | (385) | (363) | (53.8)[15] | 85.1 |
| Veneri 1 | 470 | 453 | 397 | 383 | 50.1 | 75.7 |
| Veneri 2 | 459 | 436 | 382 | 365 | 48.8 | 74.6 |

[1]Body masses estimated from femoral head diameters. For diameters <38mm, the formula of McHenry (1994) (BM=2.239 x FemHdDia – 39.9) was used. For diameters >47mm, the average of the Grine et al. (1995) formula (BM=2.268 x FemHdDia – 36.5) and the appropriate value from Ruff et al. (1991) was employed. Ruff et al. (1991) provided sex specific formulae (males: (2.741 x FemHdDia – 54.9) x 0.90; females: (2.426 x FemHdDia – 35.1) x 0.90), which were used for pelvically sexed Pleistocene remains; for remains without diagnostic pelvic remains, the average of those two estimates was used. For intermediate head diameters (38 to 47mm), the average of the McHenry, Grine et al., and appropriate Ruff et al. estimates was employed.

[2]Biomechanical length estimated from the partial diaphysis using preserved anatomical landmarks.

[3]Maximum femoral length estimated from the biomechanical length using a least squares regression based on a pooled sample of Pleistocene and non-industrial recent humans: FemMaxLen = 1.037 x FemBiomLen + 11.2; $r^2$=0.984, N=72.

[4]Maximum tibial length estimated from the preserved biomechanical length using a least squares regression based on a pooled sample of Pleistocene and non-industrial recent humans: TibMaxLen = 1.027 x TibArtLen + 13.7, $r^2$=0.987, N=126.

[5]The maximum length is from the estimated bicondylar length of Hublin (1992) using a least squares regression of recent humans: FemMaxLen=0.984 x FemBicLen + 9.9, $r^2$=0.992, N=40.

[6]Biomechanical length estimated from maximum length based on a pooled sample of Pleistocene and non-industrial recent humans: FemBiomLen=0.949 x FemMaxLen – 4.0, $r^2$=0.984, N=72.

[7]Length estimates from the largely complete diaphysis, as detailed in Stringer et al. (1998) and Trinkaus et al. (1999b).

[8]Maximum length from the mean estimated bicondylar length of Geraads and Tchernov (1983) using a least squares regression of recent humans: FemMaxLen=0.984 x FemBicLen + 9.9, $r^2$=0.992, N=40.

[9]Femoral head diameter estimated from its associated acetabular height (from the rim adjacent to the anterior inferior iliac spine, using a least squares regression based on a pooled sample of Late Pleistocene and recent humans: FemHdDia=0.917 x AcetHt – 4.6, $r^2$=0.903, N=130.

[10]Maximum length estimate from Weidenreich (1941).

[11]Estimate based on the damaged original with minor reconstruction.

[12]Estimates based on adjustment of Boule's original reconstruction of the right femur using the more complete diaphysis and distal epiphysis of the left femur (cf. Trinkaus 2011). The maximum versus biomechanical length difference derives from the largely complete right proximal femur.

[13]Estimates based on the damaged original with reconstruction, following Heim (1982).

[14]Biomechanical length estimated from the largely complete diaphysis and distal epiphysis (Twiesselmann 1961; Trinkaus and Ruff 1989).

[15]Femoral head diameter estimated from lateral condyle depth (M-22 [Bräuer, 1988]) using a least squares regression based on diverse recent humans and the available Late Pleistocene specimens: FHD=0.641 x LatCondAP + 5.8, $r^2$=0.881, N=45.

[16]Biomechanical length estimated from the damaged original (Walker et al. 2011a).

[17]Shanidar femur lengths estimated from their preserved portions (Trinkaus 1983; Trinkaus and Ruff 1999a). The Shanidar 6 tibia maximum length was estimated from its fibular length (Trinkaus 1983, 2011), and its biomechanical length was estimated from its maximum length using a least squares regression based on a pooled Pleistocene and recent human sample: TibBiomLen=0.961 x TibMaxLen – 8.7, $r^2$=0.987, N=126.

[18]Estimates based on the damaged original with reconstruction, following McCown and Keith (1939).

[19]Cro-Magnon 1 includes elements 4314 (pelvis), 4323B (femur right), and 4325 (femur left). The Cro-Magnon 4332 tibia has been associated with Cro-Magnon 1, but the attribution cannot be verified (Vallois and Billy 1965).

[20]The Cro-Magnon femoral and tibial length biomechanical estimates were done for the largely complete diaphyses and partial epiphyses using the more complete specimens as guides to the dimensions of the missing portions, given their similar sizes.

[21]Length estimates from Sládek et al. (2000) for the largely complete femora and tibiae.

[22]Minatogawa lengths from Baba and Endo (1982), plus Trinkaus (pers. observ.) for femur biomechanical length.

[23]Length estimates for the Mladeč 27 diaphysis from Trinkaus et al. (2006), based on the largely complete diaphysis.

[24]Length estimates for the largely complete femur and tibia from Shang and Trinkaus (2010).

## TABLE A2. DISTAL (20%) FEMORAL DIAPHYSIAL CROSS-SECTIONAL PARAMETERS.

| | | TA | CA | $I_x$ | $I_y$ | $I_{max}$ | $I_{min}$ | J |
|---|---|---|---|---|---|---|---|---|
| **Early Pleistocene** | | | | | | | | |
| KNM-ER 737 | L | 808 | 370 | 28961 | 48254 | 48333 | 27882 | 76215 |
| KNM-ER 1472* | R | 529 | 308 | 15417 | 22226 | 22319 | 15324 | 37643 |
| KNM-ER 1481a* | L | 509 | 260 | 13566 | 18136 | 18196 | 13505 | 31702 |
| KNM-ER 1808mn[1] | R | 711 | 520 | 32276 | 43323 | 43465 | 32134 | 75599 |
| **Middle Pleistocene** | | | | | | | | |
| Aïn Maarouf 1 | L | 662 | 311 | 22542 | 28260 | 28892 | 21909 | 50802 |
| **Neandertals** | | | | | | | | |
| Amud 1 | L | 1000 | 517 | 58991 | 62572 | 63098 | 58465 | 121563 |
| Chapelle-aux-Saints 1 | L | 8367 | 418 | 36092 | 47688 | 48723 | 35057 | 83780 |
| Feldhofer 1* | R | 919 | 274 | 31411 | 36684 | 36686 | 31409 | 68095 |
| Ferrassie 1 | L | 937 | 443 | 46152 | 53432 | 53434 | 46149 | 99584 |
| Fond-de-Forêt 1* | L | 930 | 275 | 30076 | 39441 | 40492 | 29024 | 69517 |
| Spy 2* | R | 947 | 305 | 31861 | 45360 | 45389 | 31832 | 77221 |
| **MPMH** | | | | | | | | |
| Skhul 4* | R | 943 | 426 | 44747 | 54166 | 54794 | 44120 | 98914 |
| | L | 904 | 392 | 41440 | 48006 | 49968 | 39478 | 89446 |
| Skhul 6 | L | 853 | 386 | 35323 | 46685 | 47709 | 34299 | 82008 |
| **EUP/MUP** | | | | | | | | |
| Cro-Magnon 1 | R | 1119 | 488 | 61219 | 81509 | 82822 | 59907 | 142728 |
| Cro-Magnon 4322 | L | 841 | 358 | 30124 | 49905 | 50759 | 29269 | 80029 |
| Dolní Věstonice 3 | R | 673 | 251 | 17702 | 26902 | 26917 | 17687 | 44604 |
| Dolní Věstonice 13* | R | 847 | 321 | 31994 | 39404 | 39554 | 31844 | 71398 |
| | L | 864 | 338 | 31167 | 46048 | 46063 | 31152 | 77215 |
| Dolní Věstonice 14* | L | 904 | 292 | 30552 | 42570 | 43619 | 29503 | 73122 |
| Dolní Věstonice 16 | R | 786 | 301 | 30552 | 31830 | 32157 | 30226 | 62382 |
| | L | 856 | 277 | 28614 | 33754 | 33820 | 28548 | 62368 |
| Minatogawa 1[2]* | R | 840 | 342 | 30080 | 43180 | 43190 | 30070 | 73260 |
| | L | 866 | 297 | 28450 | 40970 | 41410 | 28010 | 69420 |
| Minatogawa 3* | R | 559 | 300 | 17280 | 21670 | 21690 | 17260 | 39950 |
| | L | 569 | 253 | 14800 | 21210 | 21240 | 14770 | 36010 |
| Minatogawa 4* | R | 607 | 203 | 12220 | 22180 | 22320 | 12080 | 34400 |
| Mladeč 27 | R | 880 | 311 | 32414 | 40825 | 41359 | 31880 | 73239 |
| Ohalo 2* | R | 945 | 362 | 44528 | 45095 | 48908 | 40716 | 89624 |
| | L | 892 | 367 | 41285 | 43090 | 45856 | 38519 | 84375 |
| Paviland 1* | L | 938 | 296 | 32225 | 43586 | 43593 | 32218 | 75812 |
| Pavlov 1* | R | 980 | 269 | 26228 | 49395 | 49397 | 26225 | 75622 |
| | L | 934 | 293 | 29448 | 47559 | 47609 | 29398 | 77007 |
| Tianyuan 1[3] | R | 906 | 495 | 67464 | 41012 | 67464 | 41012 | 108476 |

[1]The KNM-ER 1808 long bone diaphyses are covered with a thick layer of pathological new bone that was deposited shortly before death and did not disturb the underlying cortical bone (Walker et al. 1982). The femoral cross-sections (Tables A2 to A6) measured only the non-pathological diaphyseal bone (see Ruff 1995 for details).

[2]All of the Minatogawa femoral and tibial cross-sectional data except the femur 80% section are from T. Kimura (pers. comm.; see also Kimura and Takahashi 1992).

[3]The Tianyuan 1 femora have an abnormal midshaft and mid-distal posterior crest, which does not appear to have affected the more proximal and distal cross-sections (Shang and Trinkaus 2010). Therefore, the 35% and 50% values are not included here, but the other ones are. The midshaft to distal tibial values appear to have been unaffected.

## TABLE A3. MID-DISTAL (35%) FEMORAL DIAPHYSEAL CROSS-SECTIONAL PARAMETERS.

| | | TA | CA | $I_x$ | $I_y$ | $I_{max}$ | $I_{min}$ | J |
|---|---|---|---|---|---|---|---|---|
| **Early Pleistocene** | | | | | | | | |
| KNM-ER 736 | L | 963 | 658 | 67261 | 66338 | 70710 | 62889 | 133599 |
| KNM-ER 737 | L | 662 | 445 | 28850 | 33691 | 33942 | 28599 | 62541 |
| KNM-ER 803a | L | 636 | 505 | 31051 | 32282 | 38414 | 24919 | 63333 |
| KNM-ER 1472* | R | 470 | 359[3] | 16093 | 17127 | 18438 | 14782 | 33220 |
| KNM-ER 1481a* | L | 382 | 310 | 10682 | 12069 | 13276 | 9475 | 22751 |
| KNM-ER1808mn | R | 552 | 469 | 21873 | 26396 | 27162 | 21108 | 48269 |
| **Middle Pleistocene** | | | | | | | | |
| Arago 53[1] | R | 772 | 628 | -- | -- | 48121 | 34238 | 82359 |
| Aïn Maarouf 1 | L | 498 | 396 | 19881 | 18232 | 20250 | 17864 | 38113 |
| Broken Hill E690 | L | 499 | 414 | 22112 | 17148 | 22118 | 17142 | 39260 |
| Gesher-B.-Y. 1 | R | 394 | 262 | 9622 | 12823 | 13071 | 9374 | 22445 |
| Kresna 11[2] | L | 569 | 422 | 23912 | 25593 | 27388 | 22133 | 49505 |
| OH 28 | L | 588 | 399 | 21530 | 28738 | 29509 | 20759 | 50268 |
| **Neandertals** | | | | | | | | |
| Amud 1 | L | 775 | 599 | 51892 | 39696 | 53620 | 37968 | 91588 |
| Chapelle-aux-Saints 1 | L | 657 | 445 | 33859 | 27877 | 34284 | 27453 | 61736 |
| Feldhofer 1* | R | 697 | 459 | 38222 | 30716 | 39370 | 29568 | 68938 |
| Ferrassie 1 | R | 776 | 471 | 42459 | 39197 | 46212 | 35444 | 81656 |
| | L | 760 | 531 | 39724 | 43353 | 46004 | 37074 | 83078 |
| Ferrassie 2* | R | 622 | 424 | 26175 | 29345 | 30678 | 24842 | 55520 |
| | L | 677 | 416 | 32134 | 30356 | 33858 | 28632 | 62490 |
| Fond-de-Forêt 1* | L | 752 | 509 | 45374 | 37252 | 50467 | 32159 | 82626 |
| Spy 2* | R | 668 | 451 | 32087 | 31168 | 32088 | 31167 | 63255 |
| Tabun 1 | R | 535 | 381 | 20279 | 20636 | 21911 | 19003 | 40915 |
| **MPMH** | | | | | | | | |
| Qafzeh 9 | R | 730 | 625 | 48111 | 35572 | 48259 | 35425 | 83683 |
| Skhul 4* | R | 685 | 447 | 37618 | 29555 | 37666 | 29507 | 67173 |
| | L | 629 | 451 | 38928 | 22957 | 38937 | 22948 | 61885 |
| Skhul 5 | R | 804 | 518 | 64322 | 33788 | 65225 | 32884 | 98109 |
| Skhul 6 | L | 684 | 449 | 36754 | 29667 | 37241 | 29180 | 66421 |
| Skhul 7 | R | 502 | 363 | 19351 | 18481 | 22251 | 15581 | 37832 |
| **EUP/MUP** | | | | | | | | |
| Cro-Magnon 1 | R | 878 | 483 | 61147 | 45019 | 61154 | 45012 | 106166 |
| | L | 774 | 492 | 57528 | 33746 | 58193 | 33081 | 91274 |
| Cro-Magnon 4322 | L | 632 | 428 | 34204 | 25472 | 34693 | 24983 | 59676 |
| Cro-Magnon 4328 | R | 611 | 461 | 33403 | 24138 | 33456 | 24085 | 57541 |
| Dolní Věstonice 3 | R | 476 | 262 | 14763 | 14607 | 14936 | 14434 | 29370 |
| | L | 466 | 264 | 14855 | 13504 | 14895 | 13464 | 28359 |
| Dolní Věstonice 13* | R | 638 | 382 | 29950 | 25720 | 30996 | 24674 | 55670 |
| | L | 668 | 405 | 30546 | 29943 | 32416 | 28074 | 60489 |
| Dolní Věstonice 14* | R | 615 | 330 | 25721 | 22483 | 26686 | 21519 | 48204 |
| | L | 618 | 339 | 28176 | 21324 | 28322 | 21179 | 49501 |

## TABLE A3. (continued)

| | | TA | CA | $I_x$ | $I_y$ | $I_{max}$ | $I_{min}$ | J |
|---|---|---|---|---|---|---|---|---|
| **EUP/MUP (cont.)** | | | | | | | | |
| Dolní Věstonice 16 | R | 645 | 356 | 32425 | 22858 | 32766 | 22517 | 55283 |
| | L | 667 | 334 | 31244 | 23461 | 31315 | 23389 | 54704 |
| Dolní Věstonice 40 | R | 495 | 403 | 20801 | 17981 | 22440 | 16342 | 38782 |
| Minatogawa 1* | R | 616 | 334 | 23670 | 24010 | 24060 | 23620 | 47680 |
| | L | 563 | 316 | 19060 | 21850 | 22010 | 18910 | 40920 |
| Minatogawa 3* | R | 420 | 308 | 13630 | 12680 | 13670 | 12640 | 26310 |
| | L | 429 | 373 | 14600 | 14470 | 14930 | 14140 | 29070 |
| Minatogawa 4* | R | 414 | 245 | 9960 | 12990 | 13030 | 9920 | 22950 |
| Mladeč 27 | R | 562 | 310 | 25065 | 15758 | 25077 | 15746 | 40823 |
| Nahal 'En-Gev 1 | L | 465 | 355 | 15825 | 17003 | 17207 | 15621 | 32828 |
| Ohalo 2* | R | 694 | 424 | 44392 | 24925 | 44472 | 24845 | 69317 |
| | L | 703 | 477 | 42782 | 30665 | 42816 | 30630 | 73446 |
| Paviland 1* | L | 678 | 379 | 35154 | 25022 | 35157 | 25019 | 60176 |
| Pavlov 1* | R | 718 | 350 | 31429 | 30539 | 32351 | 29617 | 61968 |
| | L | 709 | 357 | 30264 | 30687 | 31680 | 29271 | 60951 |
| Sunghir 1 | R | 771 | 488 | 47674 | 36827 | 50724 | 33776 | 84500 |
| Sunghir 4 | L | 683 | 457 | 41152 | 27675 | 41255 | 27573 | 68827 |

[1] The Arago femoral cross-sectional data are from Lovejoy (1982).

[2] The Kresna femoral cross-sectional data are from Puymerail (2011). In each case, the polar moment of area (J) is computed as the sum of the sum of the anteroposterior ($I_x$) and mediolateral ($I_y$) second moments of area, following Puymerail (2011: 221–222).

[3] This number was originally shown incorrectly as 159 in the table published in this article in *PaleoAnthropology* on 9 February 2012; note that the correct figure of 359 was, however, used in all analyses and graphs. This corrected table was published in *PaleoAnthropology* on 12 March 2012.

## TABLE A4. MIDSHAFT (50%) FEMORAL DIAPHYSEAL CROSS-SECTIONAL PARAMETERS.

| | | TA | CA | $I_x$ | $I_y$ | $I_{max}$ | $I_{min}$ | J |
|---|---|---|---|---|---|---|---|---|
| **Early Pleistocene** | | | | | | | | |
| KNM-ER 736 | L | 871 | 659 | 56553 | 60075 | 65146 | 51482 | 116628 |
| KNM-ER 737 | L | 586 | 441 | 21538 | 32802 | 33140 | 20200 | 54340 |
| KNM-ER 803a | L | 626 | 504 | 27573 | 34793 | 38942 | 23424 | 62366 |
| KNM-ER 1472* | R | 464 | 400 | 16191 | 17987 | 20429 | 13748 | 34178 |
| KNM-ER 1481a* | L | 391 | 332 | 10167 | 14416 | 14848 | 9734 | 24583 |
| KNM-ER1808mn | R | 551 | 478 | 20813 | 27251 | 27330 | 20735 | 48064 |
| **Middle Pleistocene** | | | | | | | | |
| Aïn Maarouf 1 | L | 506 | 428 | 19718 | 20306 | 22010 | 18015 | 40024 |
| Berg Aukas 1 | R | 800 | 708 | 51599 | 51050 | 61019 | 41631 | 102649 |
| Broken Hill E690 | L | 468 | 420 | 19363 | 15999 | 21229 | 14134 | 35362 |
| Broken Hill E793 | -- | 587 | 428 | 26198 | 25272 | 28746 | 22724 | 51470 |
| Castel del Guido 1 | R | 666 | 582 | 42003 | 29626 | 43024 | 28605 | 71629 |
| La Chaise-BD 5[1] | R | 502 | 410 | 17883 | 21149 | 21561 | 17471 | 39032 |
| Ehringsdorf 5 | R | 814 | 666 | 52616 | 49833 | 57005 | 45444 | 102449 |
| Gesher-B.-Y. 1 | R | 373 | 316 | 8991 | 13418 | 13513 | 8896 | 22408 |
| Kresna 11 | L | 591 | 454 | 23587 | 30202 | 30637 | 23149 | 53789 |
| Mammolo 1 | R | 761 | 609 | 51832 | 37927 | 51847 | 37911 | 89759 |
| OH 28 | L | 576 | 410 | 18731 | 31758 | 32379 | 18110 | 50489 |
| Tabun E1[2] | R | 577 | 544 | 24709 | 28951 | 31218 | 22442 | 53660 |

TABLE A4. (continued)

| | | TA | CA | $I_x$ | $I_y$ | $I_{max}$ | $I_{min}$ | J |
|---|---|---|---|---|---|---|---|---|
| **Middle Pleistocene (cont.)** | | | | | | | | |
| Zhoukoudian 1 | L | 572 | 497 | 22521 | 29366 | 29673 | 22215 | 51887 |
| Zhoukoudian 2 | L | 453 | 413 | 13726 | 19686 | 19702 | 13710 | 33412 |
| Zhoukoudian 4 | R | 515 | 428 | 17804 | 24029 | 24769 | 17064 | 41833 |
| Zhoukoudian 5 | L | 470 | 420 | 14573 | 20717 | 20762 | 14528 | 35290 |
| Zhoukoudian 6 | L | 502 | 440 | 19282 | 21367 | 24295 | 16354 | 40649 |
| **Neandertals** | | | | | | | | |
| Amud 1 | L | 749 | 660 | 44164 | 46307 | 55455 | 35016 | 90471 |
| Chapelle-aux-Saints 1 | L | 725 | 606 | 38088 | 43120 | 43178 | 38030 | 81208 |
| Feldhofer 1* | R | 652 | 504 | 33955 | 30596 | 37384 | 27166 | 64551 |
| Ferrassie 1 | R | 721 | 565 | 38744 | 42513 | 50953 | 30304 | 81257 |
| | L | 728 | 581 | 35191 | 46398 | 46829 | 34761 | 81590 |
| Ferrassie 2* | R | 601 | 461 | 24392 | 30914 | 32334 | 22971 | 55305 |
| | L | 627 | 482 | 27378 | 32515 | 35561 | 24332 | 59893 |
| Fond-de-Forêt 1* | L | 727 | 571 | 40732 | 41154 | 48582 | 33305 | 81886 |
| Palomas 96 | R | 429 | 284 | 14158 | 15017 | 16739 | 12437 | 29175 |
| Quina 5 | R | 618 | 537 | 29356 | 30141 | 30386 | 29111 | 59497 |
| Rochers-de-V. 1 | L | 646 | 545 | 34007 | 30948 | 34057 | 30898 | 64955 |
| Saint-Césaire 1 | R | 740 | 624 | 47905 | 38670 | 52020 | 34555 | 86575 |
| Shanidar 4 | R | 768 | 610 | 46120 | 43883 | 47274 | 42729 | 90003 |
| Shanidar 5 | R | 813 | 620 | 50193 | 49511 | 52327 | 47376 | 99704 |
| Shanidar 6 | R | 548 | 414 | 21399 | 23735 | 23800 | 21333 | 45133 |
| Spy 2* | R | 616 | 493 | 27664 | 30579 | 31873 | 26371 | 58243 |
| Tabun 1 | R | 497 | 427 | 16166 | 23002 | 23105 | 16063 | 39168 |
| Tabun 3 | R | 390 | 328 | 11012 | 12960 | 14070 | 9902 | 23972 |
| **MPMH** | | | | | | | | |
| Qafzeh 3[3] | L | 576 | 438 | 30596 | 21246 | 30621 | 21221 | 51842 |
| Qafzeh 8[3] | R | 775 | 636 | 66853 | 35575 | 67446 | 34981 | 102428 |
| Qafzeh 9[3] | R | 770 | 624 | 53769 | 40845 | 54488 | 40126 | 94614 |
| Skhul 3 | L | 708 | 523 | 42627 | 34322 | 42986 | 33963 | 76949 |
| Skhul 4* | R | 598 | 468 | 33312 | 23360 | 35271 | 21401 | 56672 |
| | L | 563 | 476 | 32067 | 20664 | 32860 | 19871 | 52731 |
| Skhul 5 | R | 760 | 525 | 58890 | 32473 | 60811 | 30552 | 91363 |
| | L | 691 | 528 | 55730 | 25144 | 55776 | 25098 | 80874 |
| Skhul 6 | R | 606 | 481 | 36153 | 22770 | 36963 | 21960 | 58923 |
| Skhul 7 | R | 520 | 403 | 18906 | 22599 | 23880 | 17625 | 41505 |
| **EUP/MUP** | | | | | | | | |
| Arene Candide 1[4]* | R | 569 | 309 | 26000 | 15500 | 26000 | 15500 | 41500 |
| Barma Grande 2[4]* | L | 737 | 603 | 53900 | 33800 | 54500 | 33200 | 87700 |
| Cro-Magnon 1 | R | 790 | 642 | 71055 | 38435 | 71985 | 37505 | 109490 |
| | L | 732 | 581 | 52695 | 37038 | 53069 | 36664 | 89733 |
| Cro-Magnon 4322 | L | 555 | 476 | 33207 | 18635 | 33607 | 18235 | 51842 |
| Cro-Magnon 4324 | L | 541 | 432 | 28345 | 18966 | 28477 | 18834 | 47311 |
| Dolní Věstonice 3 | R | 411 | 307 | 14539 | 11552 | 15495 | 10596 | 26091 |
| | L | 406 | 306 | 14290 | 11054 | 14348 | 10996 | 25343 |

**TABLE A4. (continued)**

| | | TA | CA | $I_x$ | $I_y$ | $I_{max}$ | $I_{min}$ | J |
|---|---|---|---|---|---|---|---|---|
| **EUP/MUP (cont.)** | | | | | | | | |
| Dolní Věstonice 13* | R | 574 | 429 | 27986 | 22501 | 28842 | 21646 | 50487 |
| | L | 557 | 401 | 23190 | 22898 | 23519 | 22568 | 46087 |
| Dolní Věstonice 14* | R | 551 | 389 | 26759 | 19015 | 26790 | 18984 | 45774 |
| | L | 552 | 404 | 29908 | 17673 | 29933 | 17648 | 47581 |
| Dolní Věstonice 16 | R | 614 | 422 | 36190 | 22041 | 36444 | 21787 | 58231 |
| | L | 624 | 422 | 36490 | 22762 | 36704 | 22547 | 59251 |
| Dolní Věstonice 35 | R | 588 | 384 | 33208 | 20320 | 35131 | 18397 | 53528 |
| Grotte-des-Enfants 4[4]* | R | 717 | 545 | 52300 | 31400 | 52300 | 31400 | 83700 |
| Minatogawa 1* | R | 508 | 385 | 19190 | 19900 | 20590 | 18500 | 39090 |
| | L | 499 | 401 | 19620 | 18950 | 20150 | 18420 | 38570 |
| Minatogawa 2 | L | 350 | 257 | 8460 | 9800 | 9800 | 8450 | 18260 |
| Minatogawa 3* | R | 390 | 354 | 13110 | 11500 | 13120 | 11490 | 24610 |
| | L | 391 | 365 | 12320 | 12460 | 12910 | 11870 | 24780 |
| Minatogawa 4* | R | 327 | 236 | 8040 | 7880 | 8530 | 7390 | 15920 |
| Mladeč 27 | R | 498 | 391 | 23588 | 15493 | 24169 | 14912 | 39081 |
| Nahal 'En-Gev 1 | L | 455 | 390 | 18328 | 14981 | 18453 | 14856 | 33308 |
| Ohalo 2* | R | 660 | 506 | 47715 | 25000 | 49490 | 23225 | 72715 |
| | L | 641 | 518 | 43365 | 24777 | 44031 | 24111 | 68142 |
| Paglicci 25[4]* | R | 615 | 482 | 34900 | 24300 | 34900 | 24300 | 59200 |
| Paviland 1* | L | 608 | 466 | 34298 | 22793 | 34466 | 22625 | 57091 |
| Pavlov 1* | R | 611 | 411 | 30665 | 25570 | 32324 | 23912 | 56235 |
| | L | 633 | 423 | 28040 | 30871 | 34266 | 24645 | 58911 |
| Rochette 2[3]* | R | 524 | 443 | 23200 | 20700 | 24400 | 19500 | 43900 |
| Sunghir 1[5] | R | 788 | 591 | 57640 | 40076 | 60680 | 37036 | 97716 |
| | L | 678 | 518 | 40882 | 34264 | 48086 | 27060 | 75146 |
| Sunghir 4[4] | L | 622 | 462 | 34894 | 24437 | 34914 | 24418 | 59331 |
| Veneri 1[4]* | L | 767 | 617 | 61300 | 36000 | 61400 | 35900 | 97300 |
| Veneri 2[4]* | L | 671 | 543 | 44100 | 28700 | 44300 | 28400 | 72800 |
| Willendorf 1 | R | 477 | 375 | 20811 | 15249 | 21036 | 15025 | 36060 |
| Zhoukoudian-UC 67[6] | R | 728 | 577 | 67611 | 26028 | 67917 | 25723 | 93639 |
| Zhoukoudian-UC 68[6] | R | 634 | 512 | 45154 | 21576 | 45156 | 21575 | 66730 |

[1]The La Chaise Bourgois-Delaunay (BD) 5 50% and 80% femoral cross-sectional data was generated from the CT slices (#4 and #7) in Condemi (2001: Photo IX-6). The proximal diaphyseal one is centered on the gluteal buttress and therefore should closely approximate the 80% section. The midshaft diaphyseal one may be located too proximal, but the next two more distal sections differ little from it in shape.

[2]The Tabun E1 femoral midshaft experienced exfoliation of posterior and posterolateral subperiosteal lamellar bone. The missing bone was reconstructed using the thickness of the missing portions along the exfoliation margins to produce the subperiosteal contour.

[3]The Qafzeh 3, 8 and 9 femora are missing sections of the cortical diaphyseal bone, some of which have been filled with plaster. As needed for missing bone, the subperiosteal contours were reconstructed using even circumferential contours, and the cortical thicknesses employed for the endosteal margin were derived in part from proximodistally extending the radiographic internal margins.

[4]The Arene Candide, Barma Grande, Grotte-des-Enfants (Fanciulli), Paglicci, La Rochette, and Veneri (Parabita) data are from Holt (1999).

[5]Midshaft cross-sectional parameters were previously computed from sawed midshaft sections of the femora (Mednikova and Trinkaus 2001). The values here differ in that they use more precise locations of the 50% section, especially on the largely complete Sunghir 1 femora.

[6]The Zhoukoudian-Upper Cave femoral sections are from scaled photographs of the distal breaks, near the original midshafts, of casts of the bones. The originals are lost, and the cross-section drawing in Weidenreich (1941) is inaccurate given available external diameters. It is possible that the very high $I_x/I_y$ ratio of ZKD-UC 67 is from cast distortion.

## TABLE A5. MID-PROXIMAL (65%) FEMORAL DIAPHYSEAL CROSS-SECTIONAL PARAMETERS.

| | | TA | CA | $I_x$ | $I_y$ | $I_{max}$ | $I_{min}$ | J |
|---|---|---|---|---|---|---|---|---|
| **Early Pleistocene** | | | | | | | | |
| KNM-ER 736 | L | 890 | 712 | 56200 | 65999 | 66775 | 55425 | 122199 |
| KNM-ER 737 | L | 654 | 523 | 27809 | 40273 | 41382 | 26701 | 68082 |
| KNM-ER 803a | L | 657 | 550 | 28547 | 39918 | 40372 | 28094 | 68465 |
| KNM-ER 1472* | R | 492 | 427 | 17252 | 20981 | 21344 | 16889 | 38233 |
| KNM-ER 1481a* | L | 450 | 384 | 11803 | 21137 | 21191 | 11749 | 32940 |
| KNM-ER 1808mn | R | 574 | 502 | 18360 | 37183 | 37216 | 18327 | 55543 |
| **Middle Pleistocene** | | | | | | | | |
| Aïn Maarouf 1 | L | 503 | 457 | 19062 | 21129 | 22388 | 17800 | 40188 |
| Arago 48 | R | 634 | 587 | -- | -- | 34420 | 24029 | 58449 |
| Broken Hill E690 | L | 486 | 454 | 15882 | 22250 | 22438 | 15694 | 38132 |
| Gesher-B.-Y. 1 | R | 404 | 336 | 9405 | 16959 | 17014 | 9350 | 26364 |
| Kresna 11 | L | 643 | 496 | 25850 | 39454 | 39864 | 25397 | 65304 |
| OH 28 | L | 622 | 451 | 20122 | 40586 | 40775 | 19932 | 60708 |
| Tabun E1 | R | 575 | 543 | 23317 | 29558 | 29558 | 23317 | 52875 |
| **Neandertals** | | | | | | | | |
| Amud 1 | R | 770 | 701 | 42100 | 52267 | 52697 | 41670 | 94367 |
| Feldhofer 1* | R | 682 | 556 | 33025 | 38528 | 39437 | 32116 | 71553 |
| Ferrassie 1 | R | 749 | 625 | 36695 | 51254 | 52401 | 35548 | 87949 |
| | L | 711 | 576 | 34341 | 43637 | 43859 | 34119 | 77978 |
| Ferrassie 2* | R | 616 | 474 | 25807 | 32332 | 33931 | 24208 | 58139 |
| | L | 613 | 448 | 24972 | 30439 | 30555 | 24857 | 55412 |
| Fond-de-Forêt 1* | L | 748 | 585 | 38637 | 46822 | 48072 | 37387 | 85459 |
| Krapina 257.32 | L | 632 | 565 | 22346 | 44428 | 44502 | 22272 | 66774 |
| Krapina 257.33 | L | 564 | 537 | 20671 | 33537 | 36744 | 17463 | 54208 |
| Palomas 52 | L | 386 | 327 | 11800 | 11423 | 12294 | 10929 | 23223 |
| Palomas 92 | R | 534 | 454 | 25935 | 19222 | 26499 | 18657 | 45157 |
| Palomas 96 | R | 415 | 366 | 12402 | 14771 | 14960 | 12213 | 27173 |
| Quina 38 | L | 591 | 530 | 24229 | 32584 | 33657 | 23155 | 56813 |
| Shanidar 6 | L | 542 | 484 | 20116 | 26606 | 26887 | 19834 | 46722 |
| Spy 2* | R | 608 | 521 | 29654 | 29954 | 37854 | 21754 | 59608 |
| **MPMH** | | | | | | | | |
| Qafzeh 6 | R | 758 | 603 | 47331 | 39477 | 50246 | 36562 | 86808 |
| Qafzeh 8 | R | 768 | 646 | 55184 | 38847 | 55760 | 38271 | 94031 |
| Qafzeh 9 | R | 696 | 664 | 43534 | 34996 | 44032 | 34498 | 78530 |
| Skhul 4* | R | 582 | 525 | 27678 | 26044 | 28621 | 25101 | 53722 |
| | L | 558 | 503 | 25916 | 23483 | 26000 | 23400 | 49400 |
| Skhul 5 | R | 740 | 523 | 45599 | 33883 | 49629 | 30353 | 79481 |
| **EUP/MUP** | | | | | | | | |
| Cro-Magnon 1 | R | 798 | 695 | 61856 | 40435 | 61921 | 40370 | 102291 |
| | L | 797 | 702 | 55864 | 45166 | 58061 | 42968 | 101029 |
| Cro-Magnon 4322 | L | 599 | 510 | 28532 | 28347 | 33127 | 23752 | 56879 |
| Cro-Magnon 4324 | L | 556 | 473 | 26011 | 23069 | 29817 | 19263 | 49080 |

**TABLE A5. (continued)**

| | | TA | CA | $I_x$ | $I_y$ | $I_{max}$ | $I_{min}$ | J |
|---|---|---|---|---|---|---|---|---|
| **EUP/MUP (cont.)** | | | | | | | | |
| Dolní Věstonice 3 | R | 406 | 321 | 11195 | 14236 | 14348 | 11083 | 25431 |
| | L | 383 | 317 | 10560 | 12397 | 12423 | 10533 | 22956 |
| Dolní Věstonice 13* | R | 557 | 437 | 24110 | 23194 | 25518 | 21786 | 47304 |
| | L | 549 | 456 | 21672 | 25492 | 27599 | 19565 | 47164 |
| Dolní Věstonice 14* | R | 584 | 442 | 27946 | 24549 | 32716 | 19778 | 52495 |
| | L | 564 | 444 | 29987 | 19696 | 30527 | 19155 | 49683 |
| Dolní Věstonice 16 | R | 625 | 428 | 31927 | 25075 | 31988 | 25014 | 57002 |
| | L | 626 | 443 | 33880 | 24457 | 34191 | 24146 | 58337 |
| Dolní Věstonice 41 | R | 517 | 439 | 17712 | 24431 | 24483 | 17660 | 42143 |
| Minatogawa 1* | R | 509 | 421 | 18340 | 22340 | 23030 | 17650 | 40680 |
| | L | 517 | 435 | 21100 | 21310 | 24280 | 18130 | 42410 |
| Minatogawa 3* | R | 393 | 359 | 11940 | 13010 | 14970 | 9970 | 24940 |
| | L | 395 | 379 | 11290 | 13950 | 14760 | 10480 | 25240 |
| Minatogawa 4* | R | 354 | 284 | 8430 | 11080 | 11540 | 7970 | 19510 |
| Mladeč 27 | R | 504 | 397 | 20056 | 18636 | 20676 | 18016 | 38692 |
| Mladeč 28 | L | 496 | 409 | 16469 | 21937 | 22443 | 15963 | 38406 |
| Nahal 'En-Gev 1 | L | 463 | 403 | 17615 | 16223 | 18490 | 15348 | 33838 |
| Ohalo 2* | R | 628 | 511 | 36720 | 26594 | 39485 | 23730 | 63215 |
| | L | 633 | 529 | 35627 | 27772 | 37627 | 25772 | 63399 |
| Paviland* | L | 613 | 527 | 31823 | 27646 | 34402 | 25068 | 59470 |
| Pavlov 1* | R | 636 | 497 | 32681 | 28904 | 32706 | 28879 | 61585 |
| | L | 644 | 508 | 29765 | 33473 | 34172 | 29066 | 63238 |
| Sunghir 1 | R | 767 | 612 | 39549 | 51697 | 52000 | 39246 | 91246 |
| | L | 714 | 608 | 38775 | 41271 | 41649 | 38397 | 80046 |
| Sunghir 4 | L | 681 | 497 | 38369 | 30553 | 39815 | 29107 | 68922 |
| Tianyuan 1 | R | 717 | 618 | 48760 | 33651 | 49232 | 33178 | 82410 |
| | L | 676 | 559 | 46314 | 28334 | 47001 | 27648 | 74649 |
| Willendorf 1 | R | 506 | 431 | 20714 | 19938 | 22413 | 18238 | 40652 |

**TABLE A6. PROXIMAL (subtrochanteric; 80%) FEMORAL DIAPHYSEAL CROSS-SECTIONAL PARAMETERS.**

| | | TA | CA | $I_x$ | $I_y$ | $I_{max}$ | $I_{min}$ | J |
|---|---|---|---|---|---|---|---|---|
| **Early Pleistocene** | | | | | | | | |
| KNM-ER 736 | L | 857 | 656 | 41747 | 72382 | 72409 | 41720 | 114129 |
| KNM-ER 737 | L | 738 | 510 | 29110 | 55466 | 58568 | 26008 | 84576 |
| KNM-ER 803a | L | 706 | 542 | 30943 | 47470 | 50706 | 27707 | 78413 |
| KNM-ER 1472* | R | 502 | 424 | 13576 | 28666 | 29174 | 13068 | 42242 |
| KNM-ER 1481a* | L | 529 | 414 | 16151 | 28797 | 30018 | 14930 | 44948 |
| KNM-ER 1808mn | R | 629 | 498 | 24559 | 43721 | 50333 | 17947 | 68280 |
| **Middle Pleistocene** | | | | | | | | |
| Berg Aukas 1 | R | 842 | 744 | -- | -- | 75604 | 42288 | 117892 |
| Broken Hill E689 | L | 620 | 532 | 27573 | 32583 | 33324 | 26832 | 60156 |
| Broken Hill E690 | L | 527 | 467 | 17338 | 30563 | 33602 | 14300 | 47901 |
| Broken Hill E709 | R | 796 | 698 | 43443 | 55320 | 55984 | 42778 | 98763 |
| La Chaise-BD 5 | R | 532 | 411 | 20523 | 23443 | 27320 | 16646 | 43966 |
| Gesher-B.–Y. 1 | R | 471 | 346 | 13136 | 21097 | 22221 | 12012 | 34233 |
| Kresna 11 | L | 454 | 693 | 26536 | 44846 | 45131 | 26311 | 71382 |
| OH 28 | L | 685 | 446 | 22850 | 49292 | 50717 | 21425 | 72142 |
| Tabun E1 | R | 580 | 545 | 24905 | 30665 | 35402 | 20168 | 55570 |
| **Neandertals** | | | | | | | | |
| Amud 1 | R | 803 | 699 | 47325 | 56044 | 62757 | 40612 | 103369 |
| | L | 877 | 679 | 57149 | 63185 | 76194 | 44141 | 120335 |
| Chapelle-aux-Saints 1 | R | 797 | 634 | 46481 | 51455 | 51467 | 46469 | 97936 |
| Feldhofer 1* | R | 758 | 594 | 41631 | 45609 | 48168 | 39072 | 87240 |
| Ferrassie 1 | R | 896 | 664 | 49388 | 73998 | 76960 | 46426 | 123386 |
| | L | 836 | 574 | 46154 | 56283 | 60604 | 41832 | 102436 |
| Ferrassie 2* | L | 719 | 474 | 34570 | 38803 | 43119 | 30254 | 73373 |
| Krapina 213 | L | 763 | 663 | 34880 | 61419 | 63574 | 32725 | 96298 |
| Krapina 214 | L | 489 | 431 | 13614 | 27100 | 27302 | 13412 | 40714 |
| Saint-Césaire 1 | R | 783 | 550 | 40181 | 49949 | 51085 | 39045 | 90129 |
| Spy 2* | R | 970 | 573 | 57762 | 69356 | 69799 | 57319 | 127118 |
| Tabun 1 | R | 557 | 445 | 20145 | 28546 | 29411 | 19281 | 48691 |
| **MPMH** | | | | | | | | |
| Qafzeh 8 | R | 827 | 688 | 40095 | 73059 | 77914 | 35240 | 113154 |
| Qafzeh 9 | R | 672 | 578 | 36644 | 34288 | 40576 | 30356 | 70932 |
| Skhul 4* | R | 662 | 501 | 28225 | 39076 | 39980 | 27321 | 67301 |
| | L | 626 | 477 | 29111 | 32668 | 38922 | 22857 | 61779 |
| Skhul 5 | R | 745 | 493 | 41908 | 36680 | 41910 | 36678 | 78588 |
| Skhul 6 | L | 590 | 457 | 26484 | 26847 | 31272 | 22058 | 53330 |
| Skhul 9 | L | 814 | 552 | 32638 | 68171 | 68756 | 32053 | 100809 |
| **EUP/MUP** | | | | | | | | |
| Arene Candide 1* | R | 595 | 417 | 19500 | 33500 | 33600 | 19400 | 53000 |
| Barma Grande 2* | L | 844 | 685 | 46200 | 75500 | 88700 | 33000 | 121700 |
| Cro-Magnon 1 | R | 842 | 695 | 50228 | 63339 | 70577 | 42989 | 113566 |
| | L | 789 | 593 | 41151 | 57052 | 64488 | 33715 | 98203 |

TABLE A6. (continued)

| | | TA | CA | $I_x$ | $I_y$ | $I_{max}$ | $I_{min}$ | J |
|---|---|---|---|---|---|---|---|---|
| **EUP/MUP (cont.)** | | | | | | | | |
| Cro-Magnon 4322 | L | 660 | 497 | 28093 | 43204 | 48184 | 23113 | 71297 |
| Dolní Věstonice 3 | R | 451 | 329 | 12075 | 20882 | 23231 | 9726 | 32957 |
| | L | 441 | 340 | 10536 | 22260 | 23695 | 9101 | 32796 |
| Dolní Věstonice 13* | R | 635 | 491 | 25173 | 38569 | 40786 | 22956 | 63741 |
| | L | 586 | 477 | 22935 | 36349 | 42611 | 16673 | 59284 |
| Dolní Věstonice 14* | R | 653 | 438 | 22813 | 45364 | 49342 | 18835 | 68176 |
| | L | 662 | 434 | 26275 | 42119 | 48043 | 20352 | 68395 |
| Dolní Věstonice 16 | R | 688 | 456 | 32254 | 37263 | 44033 | 25483 | 69517 |
| | L | 680 | 434 | 34065 | 33121 | 43623 | 23563 | 67186 |
| Dolní Věstonice 35 | R | 585 | 473 | 23306 | 33261 | 37566 | 19001 | 56567 |
| Grotte-des-Enfants 4* | R | 761 | 563 | 34200 | 56600 | 57800 | 33000 | 90800 |
| Minatogawa 1* | R | 520 | 428 | 18891 | 23855 | 25710 | 17036 | 42746 |
| | L | 546 | 454 | 20878 | 26612 | 29305 | 18186 | 47491 |
| Minatogawa 2 | L | 356 | 269 | 7935 | 12162 | 13393 | 6705 | 20097 |
| Minatogawa 3* | R | 376 | 339 | 8851 | 14936 | 15398 | 8039 | 23437 |
| | L | 393 | 348 | 9952 | 15746 | 16838 | 8860 | 25698 |
| Minatogawa 4* | R | 366 | 307 | 8587 | 13349 | 14357 | 7579 | 21936 |
| Mladeč 27 | R | 597 | 390 | 21089 | 29263 | 29325 | 21027 | 50352 |
| Mladeč 28 | L | 574 | 427 | 21049 | 32743 | 37190 | 16602 | 53792 |
| Nahal 'En-Gev 1 | L | 475 | 370 | 13300 | 22439 | 22960 | 12779 | 35739 |
| Ohalo 2* | R | 642 | 461 | 26513 | 35881 | 39119 | 23276 | 62395 |
| | L | 632 | 481 | 26588 | 35402 | 39419 | 22572 | 61991 |
| Paglicci 25* | R | 615 | 548 | 23600 | 39500 | 41800 | 21300 | 63100 |
| Paviland 1* | L | 681 | 482 | 32212 | 41073 | 50430 | 22856 | 73286 |
| Pavlov 1* | R | 706 | 458 | 28507 | 47136 | 52435 | 23209 | 75643 |
| Rochette 2* | R | 651 | 508 | 29500 | 36400 | 40500 | 25400 | 65900 |
| Sunghir 1 | R | 793 | 548 | 42781 | 56920 | 70613 | 29089 | 99702 |
| | L | 810 | 579 | 49008 | 51237 | 64451 | 35795 | 100246 |
| Sunghir 4 | L | 700 | 478 | 33430 | 38699 | 43884 | 28245 | 72129 |
| Tianyuan 1 | R | 752 | 637 | 39607 | 49206 | 49674 | 39139 | 88813 |
| | L | 716 | 589 | 36648 | 43131 | 44526 | 35253 | 79779 |
| Veneri 1* | L | 843 | 648 | 53900 | 55900 | 68300 | 41500 | 109800 |
| Veneri 2* | L | 805 | 623 | 51600 | 50000 | 64500 | 37100 | 101600 |

## TABLE A7. DISTAL (20%) TIBIAL DIAPHYSEAL CROSS-SECTIONAL PARAMETERS.

| | | TA | CA | $I_x$ | $I_y$ | $I_{max}$ | $I_{min}$ | J |
|---|---|---|---|---|---|---|---|---|
| **Early Pleistocene** | | | | | | | | |
| KNM-ER 1481c | L | 286 | 166 | 4942 | 5885 | 5919 | 4909 | 10828 |
| **Middle Pleistocene** | | | | | | | | |
| Broken Hill E691* | L | 513 | 273 | 15847 | 16908 | 16941 | 15814 | 32755 |
| Boxgrove 1 | L | 797 | 333 | 44499 | 45647 | 46131 | 44015 | 90146 |
| **Neandertals** | | | | | | | | |
| Amud 1 | L | 487 | 351 | 14682 | 22763 | 25027 | 12418 | 37445 |
| Ferrassie 1 | R | 576 | 314 | 24373 | 18600 | 25422 | 17552 | 42974 |
| | L | 539 | 291 | 23094 | 14521 | 23171 | 14444 | 37615 |
| Ferrassie 2 | R | 430 | 204 | 9114 | 12689 | 12695 | 9108 | 21803 |
| | L | 462 | 242 | 10812 | 16032 | 16113 | 10730 | 26843 |
| Shanidar 2* | L | 540 | 259 | 17198 | 17674 | 17791 | 17081 | 34872 |
| Spy 2* | L | 590 | 233 | 17212 | 18495 | 18540 | 17167 | 35707 |
| Tabun 1 | R | 388 | 197 | 8745 | 9575 | 9829 | 8491 | 18320 |
| **MPMH** | | | | | | | | |
| Skhul 4* | R | 528 | 299 | 21307 | 15903 | 21368 | 15842 | 37210 |
| | L | 565 | 262 | 21140 | 15645 | 21144 | 15641 | 36785 |
| Skhul 6 | L | 497 | 286 | 17460 | 15493 | 18094 | 14860 | 32954 |
| **EUP/MUP** | | | | | | | | |
| Cro-Magnon 4330* | L | 497 | 245 | 15098 | 15462 | 16982 | 13578 | 30560 |
| Cro-Magnon 4331 | L | 614 | 359 | 25628 | 24405 | 29912 | 20121 | 50033 |
| Cro-Magnon 4332 | R | 624 | 277 | 21667 | 21737 | 23600 | 19803 | 43403 |
| Dolní Věstonice 13* | R | 390 | 240 | 10795 | 10498 | 11837 | 9455 | 21292 |
| | L | 404 | 264 | 11759 | 11936 | 13913 | 9783 | 23696 |
| Dolní Věstonice 14 | R | 403 | 230 | 12767 | 9609 | 14149 | 8228 | 22377 |
| | L | 411 | 217 | 12733 | 9459 | 14257 | 7935 | 22192 |
| Dolní Věstonice 15* | R | 355 | 197 | 8058 | 8165 | 8463 | 7760 | 16223 |
| | L | 382 | 221 | 9416 | 10271 | 11582 | 8105 | 19687 |
| Dolní Věstonice 16 | R | 477 | 207 | 11895 | 12946 | 13117 | 11724 | 24841 |
| | L | 450 | 208 | 10746 | 12544 | 12670 | 10620 | 23290 |
| Minatogawa 3* | R | 328 | 264 | 7755 | 8875 | 9480 | 7150 | 16630 |
| | L | 329 | 215 | 7180 | 8270 | 8360 | 7090 | 15450 |
| Minatogawa 4* | R | 283 | 180 | 5150 | 6000 | 6070 | 5080 | 11150 |
| Ohalo 2* | R | 460 | 252 | 13842 | 14495 | 17731 | 10607 | 28338 |
| | L | 465 | 247 | 13178 | 14485 | 15893 | 11770 | 27663 |
| Tianyuan 1 | R | 518 | 334 | 22914 | 15714 | 24052 | 14577 | 38629 |

## TABLE A8. MID-DISTAL (35%) TIBIAL DIAPHYSEAL CROSS-SECTIONAL PARAMETERS.

| | | TA | CA | $I_x$ | $I_y$ | $I_{max}$ | $I_{min}$ | J |
|---|---|---|---|---|---|---|---|---|
| **Early Pleistocene** | | | | | | | | |
| KNM-ER 803b | L | 360 | 283 | 9462 | 10668 | 11175 | 8955 | 20130 |
| **Middle Pleistocene** | | | | | | | | |
| Broken Hill 691* | L | 537 | 448 | 26275 | 18104 | 29151 | 17228 | 46379 |
| Boxgrove 1 | L | 699 | 482 | 45043 | 32088 | 45222 | 31909 | 77131 |
| **Neandertals** | | | | | | | | |
| Amud 1 | L | 613 | 500 | 34086 | 26821 | 39225 | 21682 | 60907 |
| Chapelle-aux-Saints 1 | L | 501 | 386 | 23841 | 15333 | 24985 | 14189 | 39174 |
| Ferrassie 1 | R | 541 | 387 | 32261 | 14804 | 32328 | 14738 | 47066 |
| | L | 553 | 418 | 35519 | 15042 | 35544 | 15017 | 50561 |
| Ferrassie 2 | R | 397 | 275 | 12063 | 11184 | 14133 | 9114 | 23247 |
| Palomas 96 | L | 365 | 275 | 11460 | 8940 | 11488 | 8912 | 20400 |
| Shanidar 2* | L | 566 | 428 | 30707 | 19701 | 30722 | 19685 | 50408 |
| Spy 2* | L | 493 | 340 | 22055 | 15006 | 23126 | 13935 | 37061 |
| Tabun 1 | R | 368 | 268 | 12286 | 8343 | 12515 | 8114 | 20629 |
| **MPMH** | | | | | | | | |
| Qafzeh 8 | R | 611 | 432 | 31579 | 23453 | 31590 | 23441 | 55032 |
| Skhul 3 | L | 581 | 405 | 32888 | 19018 | 34019 | 17887 | 51906 |
| Skhul 4* | R | 528 | 414 | 26824 | 17496 | 28168 | 16301 | 44469 |
| | L | 524 | 417 | 27304 | 16831 | 27972 | 16164 | 44136 |
| Skhul 5 | L | 633 | 413 | 36904 | 21121 | 37051 | 20974 | 58025 |
| Skhul 6 | L | 531 | 427 | 28812 | 17356 | 30323 | 15845 | 46168 |
| **EUP/MUP** | | | | | | | | |
| Cro-Magnon 4330* | L | 518 | 386 | 26118 | 18217 | 30032 | 14303 | 44335 |
| Cro-Magnon 4331 | L | 537 | 364 | 27647 | 16822 | 30656 | 13812 | 44468 |
| Cro-Magnon 4332 | R | 570 | 413 | 28436 | 21179 | 31111 | 18504 | 49615 |
| Dolní Věstonice 3 | R | 260 | 150 | 5001 | 4414 | 6078 | 3338 | 9416 |
| | L | 267 | 154 | 4909 | 4730 | 5629 | 4010 | 9639 |
| Dolní Věstonice 13* | R | 406 | 318 | 14782 | 12005 | 17402 | 9385 | 26787 |
| | L | 417 | 338 | 16396 | 12567 | 19501 | 9462 | 28963 |
| Dolní Věstonice 14 | R | 395 | 290 | 18352 | 9188 | 21215 | 6324 | 27539 |
| | L | 389 | 278 | 17466 | 8913 | 20280 | 6099 | 26379 |
| Dolní Věstonice 15* | R | 322 | 253 | 10212 | 6608 | 11017 | 5804 | 16821 |
| | L | 369 | 289 | 13433 | 9427 | 16262 | 6598 | 22860 |
| Dolní Věstonice 16 | R | 429 | 319 | 15711 | 12870 | 17875 | 10705 | 28581 |

TABLE A8. (continued)

| | | TA | CA | $I_x$ | $I_y$ | $I_{max}$ | $I_{min}$ | J |
|---|---|---|---|---|---|---|---|---|
| **EUP/MUP (cont.)** | | | | | | | | |
| Minatogawa 3* | R | 293 | 272 | 8640 | 5990 | 9730 | 4900 | 14630 |
| | L | 284 | 240 | 8055 | 5155 | 8540 | 4670 | 13210 |
| Minatogawa 4* | R | 265 | 209 | 6080 | 4960 | 6720 | 4320 | 11040 |
| Nahal 'En-Gev 1 | L | 274 | 213 | 7657 | 4337 | 7659 | 4336 | 11994 |
| Ohalo 2* | R | 451 | 352 | 19573 | 15304 | 25046 | 9831 | 34877 |
| | L | 444 | 329 | 18750 | 14002 | 23134 | 9617 | 32751 |
| Paviland 1* | L | 490 | 343 | 21824 | 15511 | 25878 | 11457 | 37335 |
| Sunghir 1 | R | 432 | 334 | 17883 | 14362 | 22962 | 9284 | 32246 |
| | L | 456 | 359 | 18264 | 16330 | 22866 | 11728 | 34594 |
| Tianyuan 1 | R | 545 | 440 | 33973 | 17495 | 37655 | 13813 | 51468 |

TABLE A9. MIDSHAFT (50%) TIBIAL DIAPHYSEAL CROSS-SECTIONAL PARAMETERS.

| | | TA | CA | $I_x$ | $I_y$ | $I_{max}$ | $I_{min}$ | J |
|---|---|---|---|---|---|---|---|---|
| **Early Pleistocene** | | | | | | | | |
| KNM-ER 803b | L | 427 | 378 | 15957 | 13642 | 17894 | 11705 | 29599 |
| KNM-ER 813b | R | 458 | 366 | 22060 | 11963 | 22596 | 11427 | 34023 |
| **Middle Pleistocene** | | | | | | | | |
| Broken Hill E691* | L | 602 | 521 | 41596 | 20531 | 42758 | 19369 | 62127 |
| Boxgrove 1 | L | 766 | 567 | 65851 | 33887 | 66856 | 32881 | 99737 |
| Hoedjiespunt 1[1] | R | 554 | 452 | 28023 | 20518 | 29495 | 19047 | 48542 |
| Ngandong 13[2] | R | 712 | 538 | 53160 | 28441 | 54888 | 26713 | 81601 |
| Ngandong 14[2] | R | 445 | 358 | 21844 | 11714 | 23032 | 10526 | 33558 |
| Sambungmacan 2[3] | R | 466 | 423 | 28199 | 11493 | 28200 | 11493 | 39693 |
| **Neandertals** | | | | | | | | |
| Amud 1 | L | 603 | 493 | 46438 | 17714 | 47162 | 16990 | 64152 |
| Chapelle-aux-Saints 1 | L | 583 | 446 | 43092 | 15410 | 43777 | 14725 | 58502 |
| Ferrassie 1 | R | 611 | 459 | 49772 | 16172 | 49817 | 16126 | 65943 |
| | L | 585 | 436 | 42657 | 15970 | 42860 | 15767 | 58627 |
| Ferrassie 2 | R | 439 | 307 | 17653 | 11578 | 19296 | 9936 | 29232 |
| | L | 464 | 305 | 20044 | 11988 | 21604 | 10427 | 32031 |
| Krapina 257.15 | R | 462 | 357 | 22431 | 12652 | 23815 | 11268 | 35083 |
| Krapina 257.20 | R | 418 | 339 | 19155 | 9328 | 19173 | 9311 | 28484 |
| Oliveira 4 | L | 476 | 369 | 23726 | 12446 | 23785 | 12387 | 36172 |
| Palomas 96 | L | 420 | 332 | 19260 | 9600 | 19375 | 9485 | 28860 |
| Saint-Césaire 1 | L | 519 | 427 | 30578 | 15197 | 31904 | 13870 | 45774 |
| Shanidar 2* | L | 680 | 523 | 50674 | 24616 | 51305 | 23986 | 75291 |
| Shanidar 6 | R | 466 | 305 | 22217 | 10511 | 22226 | 10502 | 32728 |
| Spy 2* | L | 569 | 452 | 33084 | 19523 | 35106 | 17500 | 52606 |
| Tabun 1 | R | 408 | 345 | 13600 | 10016 | 17686 | 9530 | 27216 |

TABLE A9. (continued)

| | | TA | CA | $I_x$ | $I_y$ | $I_{max}$ | $I_{min}$ | J |
|---|---|---|---|---|---|---|---|---|
| **MPMH** | | | | | | | | |
| Qafzeh 8 | R | 644 | 449 | 41506 | 24196 | 41617 | 24085 | 65702 |
| Qafzeh 9 | R | 631 | 498 | 49285 | 20220 | 49720 | 19785 | 69506 |
| Skhul 4* | R | 604 | 484 | 37045 | 22920 | 38996 | 20968 | 59965 |
| | L | 641 | 486 | 45090 | 22623 | 46108 | 21604 | 67712 |
| Skhul 5 | L | 741 | 515 | 59885 | 26684 | 59914 | 26655 | 86569 |
| Skhul 6 | L | 566 | 438 | 36772 | 17992 | 38464 | 16300 | 54764 |
| EUP/MUP | | | | | | | | |
| Arene Candide 1 | R | 486 | 367 | 26900 | 12400 | 26900 | 12400 | 39300 |
| Cro-Magnon 4330* | L | 609 | 473 | 46031 | 21065 | 47723 | 19373 | 67096 |
| Cro-Magnon 4332 | R | 633 | 507 | 45787 | 24126 | 50394 | 19519 | 69913 |
| Cro-Magnon 4333 | R | 550 | 420 | 36333 | 15608 | 36568 | 15372 | 51940 |
| Dolní Věstonice 3 | R | 277 | 192 | 7052 | 4807 | 7916 | 3943 | 11859 |
| | L | 284 | 204 | 7041 | 5250 | 7638 | 4652 | 12291 |
| Dolní Věstonice 13* | R | 478 | 370 | 24903 | 13415 | 25965 | 12353 | 38318 |
| | L | 491 | 398 | 27357 | 14297 | 29867 | 11787 | 41654 |
| Dolní Věstonice 14 | R | 445 | 296 | 25812 | 9535 | 28064 | 7283 | 35347 |
| | L | 423 | 299 | 22860 | 9188 | 25178 | 6870 | 32048 |
| Dolní Věstonice 15* | R | 377 | 290 | 16266 | 7786 | 16421 | 7631 | 24052 |
| | L | 377 | 303 | 15592 | 8707 | 17126 | 7173 | 24299 |
| Dolní Věstonice 16 | R | 507 | 377 | 27261 | 15739 | 30064 | 12936 | 43000 |
| | L | 497 | 347 | 27797 | 13127 | 29856 | 11068 | 40923 |
| Grotte-des-Enfants 4* | R | 606 | 533 | 44800 | 22800 | 46700 | 20900 | 67600 |
| Minatogawa 1* | R | 397 | 297 | 17160 | 8780 | 17620 | 8320 | 25940 |
| | L | 375 | 303 | 15715 | 7795 | 15900 | 7610 | 23510 |
| Minatogawa 3* | R | 318 | 296 | 12580 | 5800 | 13230 | 5150 | 18380 |
| | L | 322 | 301 | 12320 | 6170 | 12960 | 5530 | 18490 |
| Minatogawa 4* | R | 296 | 217 | 9115 | 4935 | 9890 | 4160 | 14050 |
| Ohalo 2* | R | 503 | 406 | 32054 | 14024 | 34698 | 11381 | 46079 |
| | L | 490 | 387 | 29445 | 13040 | 31768 | 10717 | 42485 |
| Paviland 1* | L | 549 | 427 | 40945 | 14847 | 43735 | 12057 | 55791 |
| Sunghir 1 | R | 497 | 387 | 28834 | 16959 | 35112 | 10681 | 45793 |
| | L | 529 | 402 | 27559 | 22229 | 37474 | 12314 | 49788 |
| Tianyuan 1 | R | 666 | 555 | 65930 | 20110 | 68031 | 18008 | 86039 |
| Veneri 1* | L | 625 | 528 | 58600 | 17900 | 59500 | 17000 | 76500 |
| Veneri 2* | L | 563 | 465 | 35200 | 18400 | 35200 | 18400 | 53600 |

[1]Hoedjiespunt 1 cross-sectional data generated from a photograph of the approximately midshaft fossilization break, provided by S.E. Churchill (cf., Churchill et al. 2000).

[2]The Ngandong tibial midshaft cross-sections were generated using casts for the subperiosteal contours and cortical thicknesses from Nelson (1995, personal communication).

[3]The Sambungmacan 2 cross-sections parameters were digitized from the cross-sectional rendition in Baba and Aziz (1992).

## TABLE A10. MID-PROXIMAL (65%) TIBIAL DIAPHYSEAL CROSS-SECTIONAL PARAMETERS.

| | | TA | CA | $I_x$ | $I_y$ | $I_{max}$ | $I_{min}$ | J |
|---|---|---|---|---|---|---|---|---|
| **Early Pleistocene** | | | | | | | | |
| KNM-ER 803b | L | 500 | 423 | 22785 | 18681 | 27233 | 14233 | 41466 |
| KNM-ER 1481b* | L | 375 | 301 | 15995 | 7775 | 16715 | 7055 | 23770 |
| **Middle Pleistocene** | | | | | | | | |
| Broken Hill E691* | L | 733 | 563 | 58797 | 29690 | 60811 | 27676 | 88487 |
| Boxgrove 1 | L | 910 | 554 | 94176 | 40839 | 96343 | 38672 | 135015 |
| **Neandertals** | | | | | | | | |
| Amud 1 | R | 718 | 620 | 60356 | 30401 | 64831 | 25926 | 90757 |
| Chapelle-aux-Saints 1 | L | 667 | 400 | 48521 | 18168 | 49737 | 16952 | 66689 |
| Ferrassie 1 | R | 706 | 503 | 64689 | 21955 | 65299 | 21345 | 86644 |
| | L | 708 | 508 | 64736 | 21984 | 65027 | 21692 | 86719 |
| Ferrassie 2 | R | 548 | 280 | 21751 | 15925 | 24299 | 13377 | 37676 |
| | L | 529 | 301 | 23381 | 15382 | 26806 | 11957 | 38763 |
| Shanidar 2* | L | 705 | 467 | 54391 | 23280 | 55885 | 21786 | 77671 |
| Spy 2* | L | 704 | 390 | 45963 | 23802 | 49381 | 20385 | 69766 |
| **MPMH** | | | | | | | | |
| Qafzeh 3 | L | 550 | 410 | 41980 | 12874 | 41994 | 12860 | 54854 |
| Skhul 4* | R | 710 | 499 | 55739 | 27721 | 60113 | 23348 | 83460 |
| | L | 717 | 503 | 57127 | 27840 | 60253 | 24714 | 84967 |
| Skhul 5 | L | 844 | 529 | 86874 | 26516 | 87133 | 26258 | 113391 |
| Skhul 6 | L | 683 | 421 | 50522 | 21055 | 51868 | 19708 | 71577 |
| **EUP/MUP** | | | | | | | | |
| Cro-Magnon 4330* | L | 659 | 453 | 60914 | 18388 | 61769 | 17533 | 79302 |
| Cro-Magnon 4332 | R | 724 | 485 | 68626 | 22896 | 71659 | 19862 | 91521 |
| Dolní Věstonice 3 | R | 356 | 202 | 13244 | 5815 | 13611 | 5448 | 19059 |
| | L | 339 | 217 | 12391 | 5489 | 12521 | 5359 | 17879 |
| Dolní Věstonice 13* | R | 553 | 379 | 37706 | 14252 | 39120 | 12838 | 51958 |
| | L | 587 | 394 | 38209 | 18573 | 42096 | 14686 | 56782 |
| Dolní Věstonice 14 | R | 511 | 340 | 33635 | 11556 | 35329 | 9862 | 45191 |
| | L | 526 | 341 | 34613 | 12138 | 36058 | 10694 | 46752 |
| Dolní Věstonice 15* | R | 468 | 288 | 23479 | 10342 | 23727 | 10094 | 33822 |
| | L | 473 | 348 | 26287 | 12263 | 27856 | 10694 | 38550 |
| Dolní Věstonice 16 | R | 589 | 371 | 35097 | 19083 | 38801 | 15380 | 54180 |
| | L | 596 | 369 | 39655 | 16011 | 41244 | 14421 | 55665 |
| Minatogawa 3* | R | 366 | 269 | 16855 | 6235 | 17400 | 5690 | 23090 |
| | L | 362 | 306 | 15900 | 7150 | 16830 | 6210 | 23040 |
| Minatogawa 4* | R | 354 | 192 | 12090 | 5640 | 13030 | 4700 | 17730 |
| Ohalo 2* | R | 588 | 428 | 39871 | 19646 | 45051 | 14465 | 59516 |
| | L | 593 | 401 | 40028 | 17654 | 43767 | 13915 | 57682 |
| Paviland 1* | L | 630 | 429 | 50376 | 17691 | 52139 | 15927 | 68067 |
| Sunghir 1 | L | 648 | 447 | 40289 | 29126 | 50436 | 18979 | 69415 |

## TABLE A11. PROXIMAL (80%) TIBIAL DIAPHYSEAL CROSS-SECTIONAL PARAMETERS.

| | | TA | CA | $I_x$ | $I_y$ | $I_{max}$ | $I_{min}$ | J |
|---|---|---|---|---|---|---|---|---|
| **Early Pleistocene** | | | | | | | | |
| KNM-ER 803b | L | 592 | 372 | 33398 | 20600 | 38458 | 15540 | 53998 |
| KNM-ER 1481b* | L | 487 | 305 | 22060 | 11963 | 25734 | 10539 | 26273 |
| **Middle Pleistocene** | | | | | | | | |
| Broken Hill E691* | L | 962 | 507 | 86664 | 39015 | 88476 | 37203 | 125679 |
| Boxgrove 1 | L | 1134 | 489 | 128727 | 60630 | 135141 | 54215 | 189356 |
| **Neandertals** | | | | | | | | |
| Chapelle-aux-Saints 1 | L | 943 | 418 | 78612 | 35004 | 84837 | 28779 | 113616 |
| Shanidar 2* | L | 929 | 432 | 65274 | 38306 | 69561 | 34019 | 103580 |
| Spy 2* | L | 1098 | 418 | 79006 | 51893 | 90543 | 40355 | 130898 |
| **MPMH** | | | | | | | | |
| Qafzeh 3 | L | 662 | 359 | 51498 | 15702 | 51683 | 15517 | 67200 |
| Skhul 4* | R | 848 | 435 | 63287 | 34206 | 69386 | 28107 | 97493 |
| | L | 897 | 512 | 57903 | 41959 | 78979 | 35213 | 114192 |
| Skhul 5 | L | 1184 | 532 | 138535 | 45265 | 140600 | 43200 | 183799 |
| **EUP/MUP** | | | | | | | | |
| Cro-Magnon 4332 | R | 980 | 491 | 103434 | 36263 | 109863 | 29835 | 139698 |
| Dolní Věstonice 3 | R | 511 | 213 | 19502 | 11317 | 21057 | 9763 | 30819 |
| Dolní Věstonice 13* | R | 769 | 408 | 60005 | 25343 | 62922 | 22427 | 85348 |
| | L | 760 | 359 | 49585 | 27092 | 55426 | 21251 | 76677 |
| Dolní Věstonice 14 | R | 828 | 424 | 61585 | 27352 | 63434 | 25504 | 88937 |
| | L | 803 | 419 | 51102 | 32470 | 53114 | 30458 | 83572 |
| Dolní Věstonice 15* | R | 689 | 345 | 44073 | 19428 | 44577 | 18924 | 63501 |
| | L | 689 | 364 | 43768 | 25017 | 49961 | 18824 | 68785 |
| Minatogawa 3* | R | 528 | 418 | 28690 | 16420 | 29840 | 15270 | 45110 |
| | L | 499 | 361 | 24900 | 13930 | 26050 | 12790 | 38830 |
| Minatogawa 4* | R | 576 | 175 | 18745 | 11595 | 20980 | 9360 | 30340 |
| Ohalo 2* | R | 787 | 402 | 58130 | 27372 | 63587 | 21915 | 85502 |
| | L | 800 | 380 | 53308 | 28713 | 58964 | 23056 | 82020 |
| Paviland 1* | L | 818 | 311 | 62548 | 20073 | 66992 | 15629 | 82621 |

## TABLE A12. FEMORAL AND TIBIAL MIDSHAFT (50%) SECTION MODULI COMPUTED FROM THEIR SECOND MOMENTS OF AREA AND EXTERNAL DIAPHYSEAL DIAMETERS.

| | | Femur 50% | | | Tibia 50% | | |
|---|---|---|---|---|---|---|---|
| | | $Z_x$[1] | $Z_y$[2] | $Z_p$[3] | $Z_x$[4] | $Z_y$[5] | $Z_p$[6] |
| **Early Pleistocene** | | | | | | | |
| KNM-ER 736 | L | 2829 | 3130 | 5496 | | | |
| KNM-ER 737 | L | 1468 | 1917 | 3165 | | | |
| KNM-ER 803ab | L | 1816 | 2061 | 3598 | 1071 | 1199 | 1892 |
| KNM-ER 813b | R | | | | 1430 | 977 | 2067 |
| KNM-ER 1472 | R | 1168 | 1308 | 2303 | | | |
| KNM-ER 1481a | L | 863 | 1106 | 1847 | | | |
| KNM-ER1808mn | R | 1441 | 1793 | 3006 | | | |
| **Middle Pleistocene** | | | | | | | |
| Aïn Maarouf 1 | L | 1408 | 1460 | 2663 | | | |
| Berg Aukas 1 | R | 2648 | 3058 | 5244 | | | |
| Boxgrove 1 | L | | | | 3124 | 2083 | 4552 |
| Broken Hill E690 | L | 1271 | 1255 | 2354 | | | |
| Broken Hill E691 | L | | | | 2248 | 1483 | 3256 |
| Broken Hill E793 | -- | 1642 | 1853 | 3227 | | | |
| Castel del Guido 1 | R | 2219 | 1767 | 3716 | | | |
| La Chaise-BD 5 | R | 1290 | 1502 | 2595 | | | |
| Ehringsdorf 5 | R | 3201 | 2853 | 5575 | | | |
| Gesher-B.-Y. 1 | R | 802 | 1086 | 1774 | | | |
| Hoedjiespunt 1 | R | | | | 1732 | 1477 | 2738 |
| Kresna 11 | L | 1657 | 2010 | 3404 | | | |
| Mammolo 1 | R | 2979 | 2494 | 5087 | | | |
| Ngandong 13 | R | | | | 2598 | 1807 | 4939 |
| Ngandong 14 | R | | | | 1403 | 983 | 2606 |
| OH 28 | L | 1418 | 1851 | 3077 | | | |
| Sambungmacan 2 | | | | | 1658 | 965 | 2306 |
| Tabun E1 | R | 1766 | 1902 | 3401 | | | |
| Zhoukoudian 1 | L | 1550 | 1884 | 3192 | | | |
| Zhoukoudian 2 | L | 1135 | 1432 | 2402 | | | |
| Zhoukoudian 4 | R | 1334 | 1571 | 2710 | | | |
| Zhoukoudian 5 | L | 1158 | 1352 | 2349 | | | |
| Zhoukoudian 6 | L | 1383 | 1407 | 2591 | | | |
| **Neandertals** | | | | | | | |
| Amud 1 | L | 2522 | 2702 | 4825 | 2254 | 1278 | 3144 |
| Chapelle-aux-Saints 1 | L | 2263 | 2800 | 4658 | 2262 | 1189 | 3084 |
| Feldhofer 1 | R | 2035 | 1981 | 3720 | | | |
| Ferrassie 1 | R | 2400 | 2515 | 4543 | 2576 | 1250 | 3453 |
| | L | 2235 | 2828 | 4687 | 2297 | 1235 | 3144 |
| Ferrassie 2 | R | 1718 | 1987 | 3441 | 1199 | 985 | 1854 |
| | L | 1809 | 2159 | 3673 | 1331 | 974 | 1968 |
| Fond-de-Forêt 1 | L | 2281 | 2571 | 4472 | | | |
| Krapina 257.15 | R | | | | 1762 | 1066 | 2413 |
| Krapina 257.20 | R | | | | 1342 | 876 | 1914 |

TABLE A12. (continued)

| | | Femur 50% | | | Tibia 50% | | |
|---|---|---|---|---|---|---|---|
| | | $Z_x$[1] | $Z_y$[2] | $Z_p$[3] | $Z_x$[4] | $Z_y$[5] | $Z_p$[6] |
| **Neandertals (cont.)** | | | | | | | |
| Oliveira 4 | L | | | | 1575 | 1099 | 2310 |
| Palomas 96 | R | 1095 | 1200 | 2137 | | | |
| | L | | | | 1373 | 854 | 1915 |
| Quina 5 | R | 2090 | 1914 | 3693 | | | |
| Rochers-de-V. 1 | L | 2105 | 2108 | 3900 | | | |
| Saint-Césaire 1 | R | 2817 | 2258 | 4685 | | | |
| | L | | | | 1741 | 1154 | 2513 |
| Shanidar 2 | | | | | 2636 | 1679 | 3776 |
| Shanidar 4 | R | 2398 | 2669 | 4667 | | | |
| Shanidar 5 | R | 2536 | 2818 | 4933 | | | |
| Shanidar 6 | R | 1405 | 1622 | 2805 | 1426 | 884 | 1998 |
| Spy 2 | R | 1779 | 1989 | 3488 | | | |
| | L | | | | 1895 | 1484 | 2911 |
| Tabun 1 | R | 1265 | 1607 | 2681 | 973 | 896 | 1801 |
| Tabun 3 | R | 931 | 1046 | 1848 | | | |
| **MPMH** | | | | | | | |
| Qafzeh 3 | L | 1734 | 1565 | 3084 | | | |
| Qafzeh 8 | R | 2977 | 2236 | 4940 | 2308 | 1639 | 3412 |
| Qafzeh 9 | R | 2660 | 2495 | 4784 | 2530 | 1468 | 3541 |
| Skhul 3 | L | 2208 | 2124 | 4018 | | | |
| Skhul 4 | R | 1846 | 1660 | 3275 | 2134 | 1544 | 3166 |
| | L | 1773 | 1571 | 3135 | 2495 | 1584 | 3556 |
| Skhul 5 | R | 2739 | 2233 | 4694 | | | |
| | L | 2708 | 1784 | 4318 | 2927 | 1676 | 4047 |
| Skhul 6 | R | 1948 | 1614 | 3347 | | | |
| | L | | | | 2045 | 1323 | 2935 |
| Skhul 7 | R | 1322 | 1568 | 2685 | | | |
| **EUP/MUP** | | | | | | | |
| Arene Candide 1 | R | 1540 | 1199 | 2589 | 1634 | 1070 | 2358 |
| Barma Grande 2 | L | 2648 | 2158 | 4507 | | | |
| Cro-Magnon 1 | R | 3255 | 2329 | 5280 | | | |
| | L | 2597 | 2341 | 4599 | | | |
| Cro-Magnon 4322 | L | 1924 | 1334 | 3079 | | | |
| Cro-Magnon 4324 | L | 1639 | 1424 | 2872 | | | |
| Cro-Magnon 4330 | L | | | | 2275 | 1398 | 3220 |
| Cro-Magnon 4332 | R | | | | 2229 | 1629 | 3353 |
| Cro-Magnon 4333 | R | | | | 1976 | 1082 | 2672 |
| Dolní Věstonice 3 | R | 1050 | 968 | 1890 | 554 | 518 | 878 |
| | L | 1059 | 960 | 1893 | 591 | 561 | 946 |
| Dolní Věstonice 13 | R | 1707 | 1631 | 3103 | 1517 | 1047 | 2208 |
| | L | 1468 | 1617 | 2857 | 1559 | 1197 | 2378 |
| Dolní Věstonice 14 | R | 1603 | 1395 | 2806 | 1487 | 930 | 2142 |
| | L | 1722 | 1376 | 2926 | 1297 | 932 | 1947 |

TABLE A12. (continued)

| | | Femur 50% | | | Tibia 50% | | |
|---|---|---|---|---|---|---|---|
| | | $Z_x$[1] | $Z_y$[2] | $Z_p$[3] | $Z_x$[4] | $Z_y$[5] | $Z_p$[6] |
| **EUP/MUP (cont.)** | | | | | | | |
| Dolní Věstonice 15 | R | | | | 1113 | 679 | 1534 |
| | L | | | | 1031 | 752 | 1517 |
| Dolní Věstonice 16 | R | 1928 | 1569 | 3294 | 1536 | 1198 | 2347 |
| | L | 1881 | 1637 | 3303 | 1569 | 1048 | 2276 |
| Dolní Věstonice 35 | R | 1768 | 1344 | 2932 | | | |
| Grotte-des-Enfants 4 | R | 2605 | 1992 | 4322 | 2287 | 1374 | 3171 |
| Minatogawa 1 | R | 1356 | 1469 | 2623 | 1212 | 832 | 1755 |
| | L | 1386 | 1376 | 2566 | 1115 | 711 | 1563 |
| Minatogawa 2 | L | 750 | 853 | 1503 | | | |
| Minatogawa 3 | R | 1034 | 956 | 1860 | 937 | 629 | 1343 |
| | L | 974 | 1032 | 1872 | 953 | 666 | 1381 |
| Minatogawa 4 | R | 715 | 667 | 1299 | 778 | 575 | 1139 |
| Mladeč 27 | R | 1554 | 1246 | 2632 | | | |
| Nahal 'En-Gev 1 | L | 1297 | 1247 | 2372 | | | |
| Ohalo 2 | R | 2337 | 1806 | 3936 | 1796 | 1070 | 2508 |
| | L | 2264 | 1752 | 3793 | 1756 | 1050 | 2451 |
| Paglicci 25 | R | 1918 | 1719 | 3397 | | | |
| Paviland 1 | L | 1968 | 1593 | 3336 | 2057 | 1187 | 2900 |
| Pavlov 1 | R | 1748 | 1720 | 3220 | | | |
| | L | 1672 | 1972 | 3368 | | | |
| Rochette 2 | R | 1494 | 1526 | 2803 | | | |
| Sunghir 1 | R | 3063 | 2250 | 4927 | 1621 | 1463 | 2629 |
| | L | 2161 | 2114 | 3961 | 1539 | 1829 | 2797 |
| Sunghir 4 | L | 1931 | 1741 | 3429 | | | |
| Tianyuan 1 | R | | | | 3200 | 1623 | 4415 |
| Veneri 1 | L | 2967 | 2205 | 4864 | 2718 | 1306 | 3665 |
| Veneri 2 | L | 2327 | 1886 | 3946 | 1938 | 1242 | 2751 |
| Willendorf 1 | R | 1376 | 1228 | 2437 | | | |
| Zhoukoudian-UC 67 | R | 3447 | 1914 | 5210 | | | |
| Zhoukoudian-UC 68 | R | 2577 | 1760 | 4150 | | | |

[1]Femur 50% $Z_x=((I_x/(AP/2)) \times 0.906)+44$
[2]Femur 50% $Z_y=((I_y/(ML/2) \times 0.929)+47$
[3] Femur 50% $Z_P=((J/((AP+ML)/4)) \times 0.842)+115$
[4]Tibia 50% $Z_x=((I_x/(AP/2)) \times 0.908)+58$
[5]Tibia 50% $Z_y=((I_y/(ML/2)) \times 0.836)+59$
[6]Tibia 50% $Z_P=((J/((AP+ML)/4) \times 0.756)+50$

## TABLE A13. LINEAR DIAPHYSEAL DIAMETERS FOR PLEISTOCENE *HOMO* FEMORA AND TIBIAE.

**(in millimeters; M-# refers to the equivalent number in the Martin system [Bräuer 1988]; measurements are from personal measurement of the original remains [many of which have been previously published], supplemented by those published in primary paleontological descriptions [see references]; when multiple measurements are available, the most recent ones [or personal ones taken on the originals] are employed; differences are rarely more than 1mm)**

| | | Femur | | | | Tibia | | | |
|---|---|---|---|---|---|---|---|---|---|
| | | Proximal | | Midshaft | | Proximal | | Midshaft | |
| | | A-P | M-L | A-P | M-L | A-P | M-L | A-P | M-L |
| | | M-10 | M-9 | M-6 | M-7 | M-8a | M-9a | M-8 | M-9 |
| **Early Pleistocene** | | | | | | | | | |
| Dmanisi D3901[1] | R | | | | | -- | -- | 27.0 | 18.0 |
| Dmanisi D4167[1] | R | -- | -- | 26.5 | 22.2 | | | | |
| KNM-ER 736[2] | L | 30.0 | 40.0 | 36.8 | 36.2 | | | | |
| KNM-ER 737[2] | L | 27.1 | 39.3 | 27.4 | 32.6 | | | | |
| KNM-ER 803a,b[2] | L | (27.6) | (34.4) | 28.2 | 32.1 | -- | -- | 28.6 | 20.0 |
| KNM-ER 1472[2] | R | 22.0 | 32.0 | (26.1) | (26.5) | | | | |
| KNM-ER 813b | | | | | | -- | -- | 29.2 | 21.8 |
| KNM-ER 1481a[2] | L | 23.0 | 30.8 | 22.5 | 25.3 | | | | |
| **Middle Pleistocene** | | | | | | | | | |
| Aïn Maarouf 1[3] | L | -- | -- | 26.2 | 26.7 | | | | |
| Arago 48[4] | R | 27.1 | 35.2 | -- | -- | | | | |
| Atapuerca-SH 19[5] | R | | | | | -- | -- | 27.6 | 20.0 |
| Atapuerca-SH 85[5] | R | | | | | 36.3 | 24.0 | 29.3 | 22.5 |
| Berg Aukas 1[6] | L | 30.0 | 40.8 | 35.9 | 31.5 | | | | |
| Broken Hill E689 | L | 27.0 | 30.4 | -- | -- | | | | |
| Broken Hill E690 | L | 21.8 | 31.1 | 28.6 | 24.6 | | | | |
| Broken Hill E691 | L | | | | | 38.6 | 25.7 | 34.5 | 24.1 |
| Broken Hill E793[7] | - | -- | -- | 29.7 | 26.0 | | | | |
| Boxgrove 1[8] | L | | | | | 48.5 | 33.2 | 39.0 | 28.0 |
| Castel del Guido 1[9] | R | -- | -- | 35.0 | 32.0 | | | | |
| La Chaise-BD 5[10] | R | 23.0 | 29.0 | 26.0 | 27.0 | | | | |
| Ehringsdorf 5[11] | R | 26.8 | 37.1 | 30.2 | 33.0 | | | | |
| Gesher-B.-Y. 1 | R | 19.6 | 28.2 | 21.5 | 24.0 | | | | |
| Gesher-B.-Y. 2 | R | -- | -- | 27.0 | 28.0 | | | | |
| Hoedjiespunt 1[12] | R | | | | | -- | -- | 30.4 | 24.2 |
| Kresna 11[13] | L | 25.0 | 32.5 | 26.5 | 28.58 | | | | |
| Mammolo 1[14] | R | 29.0 | 35.2 | 32.0 | 28.8 | | | | |
| Ngandong 13[15] | R | | | | | 42.2 | 28.4 | 38.0 | 27.2 |
| Ngandong 14[15] | R | | | | | 35.7 | 24.3 | 29.5 | 21.2 |
| OH 28[16] | L | 23.3 | 37.4 | 24.7 | 32.7 | | | | |
| Sambungmacan 2[17] | R | | | | | -- | -- | 32.0 | 21.2 |
| Sedia-del-Diavolo 1[18] | R | -- | -- | 31.0 | 29.0 | | | | |
| Tabun E1 | R | | | (26.0) | (29.0) | | | | |
| Zhoukoudian 1[11] | L | 23.2 | 34.3 | 27.1 | 29.7 | | | | |
| Zhoukoudian 2[11] | L | -- | -- | 22.8 | 26.4 | | | | |
| Zhoukoudian 4[11] | R | 22.7 | 34.3 | 25.0 | 29.3 | | | | |
| Zhoukoudian 5[11] | L | -- | -- | 23.7 | 29.5 | | | | |
| Zhoukoudian 6[11] | L | -- | -- | 26.1 | 29.2 | | | | |
| Zhoukoudian PA65[19] | L | | | | | -- | -- | 27.0 | 21.0 |

TABLE A13. (continued)

| | | Femur | | | | Tibia | | | |
|---|---|---|---|---|---|---|---|---|---|
| | | Proximal | | Midshaft | | Proximal | | Midshaft | |
| | | A-P | M-L | A-P | M-L | A-P | M-L | A-P | M-L |
| | | M-10 | M-9 | M-6 | M-7 | M-8a | M-9a | M-8 | M-9 |
| **Neandertals** | | | | | | | | | |
| Amud 1 | R | 30.3 | 36.5 | -- | -- | 42.6 | 26.2 | -- | -- |
| | L | 29.4 | 36.9 | 32.3 | 32.4 | -- | -- | 38.4 | 24.3 |
| Chapelle-aux-Saints 1 | R | 29.4 | 33.0 | | | | | 35.5 | 22.8 |
| | L | | | 31.1 | 29.1 | 38.2 | 27.0 | 35.5 | 22.8 |
| Feldhofer 1 | R | 29.0 | 32.8 | 31.3 | 28.2 | | | | |
| | L | 29.3 | 35.5 | 30.5 | 30.6 | | | | |
| Ferrassie 1 | R | 29.9 | 38.0 | 29.8 | 32.0 | 39.7 | 26.6 | 35.9 | 22.7 |
| | L | 29.7 | 36.0 | 29.1 | 31.0 | 38.8 | 29.0 | 34.6 | 22.7 |
| Ferrassie 2 | R | 27.6 | 33.4 | 26.4 | 29.6 | 34.4 | 29.6 | 28.1 | 20.9 |
| | L | 27.9 | 32.0 | 28.1 | 28.6 | 34.7 | 25.5 | 28.6 | 21.9 |
| Fond-de-Forêt 1 | L | -- | -- | 33.0 | 30.3 | | | | |
| Hortus 34 | L | 24.0 | 30.0 | -- | -- | | | | |
| Kiik-Koba 1 | R | | | | | 43.1 | 30.4 | 33.9 | 23.8 |
| Krapina 213 | L | 26.1 | 36.4 | -- | -- | | | | |
| Krapina 214 | L | 22.3 | 29.6 | -- | -- | | | | |
| Krapina 257.15 | R | | | | | 33.3 | 24.1 | 23.9 | 21 |
| Krapina 257.20 | R | | | | | -- | -- | 27.1 | 19.1 |
| Krapina 257.32 | L | 24.6 | 33.6 | -- | -- | | | | |
| Krapina 257.33 | L | 21.9 | 33 | -- | -- | | | | |
| Oliveira 4 | L | | | | | -- | -- | 28.4 | 20.0 |
| Palomas 52 | L | 19.2 | 25.5 | -- | -- | | | | |
| Palomas 96 | R | -- | -- | 24.4 | 24.2 | -- | -- | 26.6 | 20.2 |
| Pofi 1[20] | R | | | | | 38.0 | 23.0 | -- | -- |
| Quina 5[21] | L | 26.0 | 33.5 | 26.0 | 30.0 | | | | |
| Quina 38 | L | 26.8 | 34.5 | -- | -- | | | | |
| Rochers-de-V. 1 | L | -- | -- | 29.9 | 27.9 | | | | |
| Saint-Césaire 1 | R | 29.1 | 35.9 | 31.3 | 32.5 | 38.0 | 26.5 | -- | -- |
| | L | | | | | -- | -- | 33.0 | 23.2 |
| Santa Croce 1[22] | R | 25.5 | 30.8 | 29.5 | 28.8 | | | | |
| Shanidar 1 | R | 28.6 | 35.3 | -- | -- | | | | |
| Shanidar 2 | L | | | | | 42.1 | 28.8 | 35.7 | 25.4 |
| Shanidar 4 | R | -- | -- | 35.5 | 31.1 | | | | |
| | L | 31.0 | 36.5 | -- | -- | | | | |
| Shanidar 5 | R | -- | -- | 36.5 | 33.2 | | | | |
| Shanidar 6 | R | -- | -- | 28.5 | 28.0 | | | | |
| | L | 24.6 | 30.5 | -- | -- | -- | -- | 29.5 | 21.3 |
| Spy 2 | R | 28.4 | 35.0 | 29.3 | 29.1 | | | | |
| | L | 28.2 | 35.8 | 28.5 | 29.4 | 40.0 | 27.9 | 32.7 | 22.9 |
| Stadelhöhle 1[23] | R | 26.6 | 31.0 | 29.0 | 29.6 | | | | |
| Tabun 1 | R | 22.6 | 30.4 | 24.0 | 27.4 | -- | -- | 27.0 | 20.0 |
| | L | | | | | 32.5 | 25.0 | 28.6 | 21.4 |
| Tabun 3 | R | -- | -- | 22.5 | 24.1 | | | | |
| Zafarraya 1[24] | R | 28.0 | 34.0 | -- | -- | | | | |

TABLE A13. (continued)

| | | Femur | | | | Tibia | | | |
|---|---|---|---|---|---|---|---|---|---|
| | | Proximal | | Midshaft | | Proximal | | Midshaft | |
| | | A-P | M-L | A-P | M-L | A-P | M-L | A-P | M-L |
| | | M-10 | M-9 | M-6 | M-7 | M-8a | M-9a | M-8 | M-9 |
| **MPMH** | | | | | | | | | |
| Omo-Kibish 1[25] | L | | | | | -- | -- | 35.5 | 23.5 |
| Omo-Kibish 158-1a[26] | L | | | | | 33.9 | 21.4 | 28.6 | 21.7 |
| Qafzeh 3 | L | -- | -- | 32.8 | 26.0 | 38.2 | 22.1 | 35.1 | 22.2 |
| Qafzeh 8 | R | 29.0 | 39.8 | 41.3 | 30.2 | -- | -- | 33.5 | 25.6 |
| Qafzeh 9[27] | R | 27.3 | 32.4 | 37.8 | 29.1 | -- | -- | 36.2 | 24.0 |
| | L | 27.1 | 32.5 | -- | -- | | | | |
| Skhul 3 | R | -- | -- | 35.7 | 30.7 | -- | -- | 34.7 | 25.0 |
| Skhul 4 | R | 26.5 | 32.0 | 33.5 | 26.9 | 37.4 | 27.3 | 32.4 | 25.8 |
| | L | 26.0 | 33.3 | 33.6 | 25.2 | 37.6 | 27.9 | 33.6 | 24.8 |
| Skhul 5 | R | 32.5 | 28.8 | 39.6 | 27.6 | | | | |
| | L | 29.4 | 30.9 | 37.9 | 26.9 | 50.9 | 29.8 | 37.9 | 27.6 |
| Skhul 6 | L | 26.2 | 30.4 | 34.4 | 27.0 | -- | -- | 33.6 | 23.8 |
| Skhul 7 | R | -- | -- | 26.8 | 27.6 | | | | |
| Skhul 9 | L | 29.3 | 38.3 | -- | -- | | | | |
| Skhul '4'[28] | R | | | | | 35.0 | 25.0 | 29.0 | 22..0 |
| Skhul '7'[28] | L | -- | -- | 32.0 | 27.0 | | | | |
| Skhul '9'[28] | L | -- | -- | 23.5 | 25.0 | | | | |
| | | | | | | | | | |
| **EUP/MUP** | | | | | | | | | |
| Arene Candide 1[29] | R | 26.0 | 32.0 | 31.0 | 24.0 | 37.0 | 25.0 | 31.0 | 21.0 |
| | L | 26.0 | 31.0 | 32.0 | 26.0 | 37.0 | 25.0 | 31.0 | 20.0 |
| Barma Grande 1[30] | R | 29.5 | 42.5 | -- | -- | 48.0 | 28.0 | -- | -- |
| | L | 31.0 | 41.5 | -- | -- | 47.0 | 28.0 | -- | -- |
| Barma Grande 2[31] | R | 31.0 | 40.0 | -- | 29.5 | 48.0 | 29.0 | 41.0 | 27.0 |
| | L | 31.0 | 40.5 | 37.5 | 30.0 | 47.0 | 27.0 | 42.0 | 25.0 |
| Barma Grande 5[31] | R | | | | | 51.0 | 30.0 | 45.0 | 28.0 |
| Barma Grande 6[32] | R | 31.5 | 42.5 | 41.0 | 31.0 | 48.0 | 28.0 | 45.0 | 28.0 |
| | L | | | | | 54.0 | 28.0 | -- | -- |
| Caviglione 1 | R | 28.8 | 37.2 | 36.6 | 28.4 | 43 | 27.2 | 35.1 | 25.8 |
| Cro-Magnon 1 | R | 30.6 | 38.5 | 40.1 | 31.3 | | | | |
| | L | 28.7 | 39.0 | 37.4 | 30.0 | | | | |
| Cro-Magnon 4323A | R | 25.7 | 36.3 | -- | -- | | | | |
| Cro-Magnon 4322 | L | 25.9 | 36.0 | 32.0 | 26.9 | | | | |
| Cro-Magnon 4324 | L | -- | -- | 32.2 | 25.6 | | | | |
| Cro-Magnon 4330 | L | | | | | 41.6 | 26.9 | 37.7 | 26.3 |
| Cro-Magnon 4331 | L | | | | | -- | -- | 36.6 | 24.8 |
| Cro-Magnon 4332 | R | | | | | 46.0 | 27.0 | 38.3 | 25.7 |
| Cro-Magnon 4333 | R | | | | | -- | -- | 34.4 | 25.5 |
| Dolní Věstonice 3 | R | 20.8 | 30.6 | 26.2 | 23.3 | 31.7 | 19.0 | 25.8 | 17.5 |
| | L | 19.8 | 29.8 | 25.5 | 22.5 | 29.8 | 18.0 | 24.0 | 17.5 |
| Dolní Věstonice 13 | R | 25.6 | 34.1 | 30.5 | 26.4 | 38.5 | 23.5 | 31.0 | 22.7 |
| | L | 23.5 | 35.2 | 29.5 | 27.1 | 36.0 | 23.3 | 33.1 | 21.0 |

TABLE A13. (continued)

| | | Femur | | | | Tibia | | | |
|---|---|---|---|---|---|---|---|---|---|
| | | Proximal | | Midshaft | | Proximal | | Midshaft | |
| | | A-P | M-L | A-P | M-L | A-P | M-L | A-P | M-L |
| | | M-10 | M-9 | M-6 | M-7 | M-8a | M-9a | M-8 | M-9 |
| **EUP/MUP (cont.)** | | | | | | | | | |
| Dolní Věstonice 14 | R | 24.3 | 38.3 | 31.1 | 26.2 | 37.9 | 22.0 | 32.8 | 18.3 |
| | L | 25.3 | 37.6 | 32.3 | 24.7 | 37.7 | 25.2 | 33.5 | 17.6 |
| Dolní Věstonice 15 | R | | | | | 30.6 | 22.3 | 28.0 | 21.0 |
| | L | | | | | 34.8 | 20.2 | 29.1 | 21.0 |
| Dolní Věstonice 16 | R | 27.8 | 34.6 | 34.8 | 26.9 | 39.3 | 24.5 | 33.5 | 23.1 |
| | L | 28.1 | 34.8 | 36.0 | 26.6 | -- | -- | 33.4 | 22.2 |
| Dolní Věstonice 35 | R | 24.3 | 35.0 | 34.9 | 29.1 | | | | |
| Grotte-des-Enfants 4[31] | R | 29.5 | 38.0 | 37.0 | 30.0 | 40.0 | 29.5 | 36.0 | 29.0 |
| | L | 30.0 | *38.0* | 37.0 | 30.0 | 43.0 | 30.0 | 37.0 | 29.0 |
| Grotte des Enfants 5[33] | - | 27.0 | 33.0 | -- | -- | 38.0 | 26.0 | -- | -- |
| Minatogawa 1[34] | R | 23.0 | 29.0 | 26.5 | 26.0 | 33.0 | 23.0 | 27.0 | 19.0 |
| | L | 22.0 | 30.0 | 26.5 | 26.5 | 34.0 | 23.0 | 27.0 | 20.0 |
| Minatogawa 2[34] | L | 18.0 | 25.0 | 21.0 | 22.0 | | | | |
| Minatogawa 3[34] | R | 19.0 | 26.5 | 24.0 | 23.5 | 30.0 | 18.0 | 26.0 | 17.0 |
| | L | 19.0 | 26.0 | 24.0 | 23.5 | 28.0 | 19.0 | 25.0 | 17.0 |
| Minatogawa 4[34] | R | 18.5 | 26.0 | 21.0 | 23.0 | 26.0 | 18.0 | 23.0 | 16.0 |
| Mladeč 27 | R | 25.5 | 30.0 | 28.3 | 24.0 | | | | |
| Mladeč 28 | L | 23.5 | 33.8 | -- | -- | | | | |
| Nahal 'En-Gev 1[35] | L | 22.0 | 28.0 | 26.5 | 23.2 | 31.0 | 21.0 | 28.0 | 17.0 |
| Ohalo2 | R | 27.5 | 29.8 | 37.7 | 26.4 | 34.6 | 24.1 | 33.5 | 23.2 |
| | L | 26.7 | 30.8 | 35.4 | 27.0 | 35.0 | 23.2 | 31.5 | 22.0 |
| Paglicci 25[36] | R | 26.0 | 35.0 | 34.0 | 27.0 | 39.5 | 25.0 | 36.0 | 25.0 |
| | L | 26.0 | 33.5 | 33.5 | 27.5 | | | | |
| Paviland 1 | L | 26.8 | 35.9 | 32.3 | 27.4 | 39.6 | 22.0 | 37.2 | 22.0 |
| Pavlov 1 | R | 27.4 | 36.5 | 32.6 | 28.4 | | | | |
| | L | 26.9 | 37.3 | 31.2 | 29.8 | | | | |
| Předmostí 3[37] | R | 24.0 | 38.0 | 30.8 | 30.0 | 41.5 | 20.5 | 37.7 | 20.5 |
| | L | 24.0 | 38.0 | 31.0 | 29.0 | 42.0 | 19.0 | 38.0 | 19.0 |
| Předmostí 4[37] | R | 25.0 | 35.8 | 29.0 | 28.0 | 35.5 | 20.5 | 31.6 | 20.0 |
| | L | 25.0 | 34.0 | 29.0 | 28.0 | 36.0 | 21.0 | 31.0 | 19.0 |
| Předmostí 9[37] | R | 23.0 | 33.0 | 27.0 | 25.0 | 32.0 | 22.5 | 27.0 | 20.0 |
| | L | 23.0 | 33.0 | 27.5 | 26.0 | 32.3 | 23.0 | 28.0 | 20.0 |
| Předmostí 10[37] | R | 22.6 | 35.0 | 25.4 | 27.5 | 31.0 | 21.0 | 29.5 | 20.0 |
| | L | 23.0 | 35.3 | 24.5 | 27.3 | 33.0 | 21.0 | 28.0 | 18.5 |
| Předmostí 14[37] | R | 22.5 | 33.0 | 26.4 | 26.4 | 37.0 | 22.5 | 30.5 | 19.5 |
| | L | 23.4 | 35.0 | 26.0 | 27.5 | 36.0 | 21.0 | 30.5 | 21.0 |
| Rochette 2[38] | R | 26.5 | 33.0 | 29.0 | 26.0 | | | | |
| Sunghir 1 | R | 27.1 | 39.4 | 34.6 | 33.8 | 39.2 | 24.2 | 33.5 | 20.2 |
| | L | 28.0 | 38.0 | 35.0 | 30.8 | 37.0 | 24.4 | 33.8 | 21.0 |
| Sunghir 4 | L | 27.4 | 33.7 | 33.5 | 26.8 | | | | |
| Tianyuan 1[39] | R | 26.2 | 33.6 | -- | -- | -- | -- | 38.1 | 21.5 |
| | L | 26.5 | 31.5 | -- | -- | | | | |

**TABLE A13. (continued)**

| | | Femur | | | | Tibia | | | |
|---|---|---|---|---|---|---|---|---|---|
| | | Proximal | | Midshaft | | Proximal | | Midshaft | |
| | | A-P | M-L | A-P | M-L | A-P | M-L | A-P | M-L |
| | | M-10 | M-9 | M-6 | M-7 | M-8a | M-9a | M-8 | M-9 |
| **EUP/MUP (cont.)** | | | | | | | | | |
| Veneri 1[30] | R | 29.0 | 41.0 | 39.0 | 31.0 | 44.0 | 26.0 | 39.0 | 24.0 |
| | L | 31.0 | 37.0 | 37.0 | 31.0 | 46.0 | 26.0 | 41.0 | 24.0 |
| Veneri 2[30] | R | 30.0 | 34.0 | 35.0 | 29.0 | 41.0 | 26.5 | 32.0 | 26.0 |
| | L | 30.0 | 37.0 | 35.0 | 29.0 | 40.5 | 25.0 | 36.0 | 26.0 |
| Willendorf 1 | R | -- | -- | 28.3 | 24.0 | | | | |
| Zhoukoudian UC 67[40] | R | 26.5 | 32.7 | 36.0 | 25.9 | | | | |
| Zhoukoudian UC 68[40] | R | 24.7 | 29.0 | 32.3 | 23.4 | | | | |

[1]Data from Lordkipanidze et al. (2007).
[2]Data from Leakey et al. (1978). KNM-ER 736, 813 and 1472 midshaft diameters and KNM-ER 803 subtrochanteric diameters from personal measurement.
[3]Data from Hublin (1992).
[4]Data from Sigmon (1982).
[5]Data from Arsuaga et al. (1991).
[6]Data from Grine et al. (1995).
[7]Data from Clark et al. (1968).
[8]Data from Stringer et al. (1998).
[9]Data from Mallegni et al. (1983).
[10]Data from Condemi (2001).
[11]Data from Weidenreich (1941).
[12]Data from Churchill et al. (2000).
[13]Data from Grimaud-Hervé et al. (1994).
[14]Data from Biddittu et al. (1987).
[15]Data from Santa Luca (1980).
[16]Data from Day (1971).
[17]Data from Baba and Aziz (1993).
[18]Data from Mallegni (1986).
[19]Data from Wu and Poirier (1995).
[20]Data from Passarello and Palmieri (1968).
[21]Data from Martin (1923).
[22]Data from Cardini (1955).
[23]Data from Kunter and Wahl (1992).
[24]Data from García Sánchez (1986).
[25]Data from Pearson et al. (2008a).
[26]Data from Pearson et al. (2008b).
[27]Data from Vandermeersch (1981).
[28]Data from McCown and Keith (1939).
[29]Data from Sergi et al. (1974).
[30]Data from Mallegni et al. (2000)
[31]Data from Formicola (1990).
[32]Data from Massari (1958).
[33]Data from Verneau (1906).
[34]Data from Baba and Endo (1982).
[35]Data from Arensburg (1977).
[36]Data from Mallegni et al. (1999)
[37]Data from Matiegka (1938).
[38]Data from Klaatsch and Lustig (1914).
[39]The Tianyuan 1 femoral midshafts are pathological, and measurements are not included for them. The proximal femoral and midshaft tibial ones appear to be normal (Shang and Trinkaus 2010).
[40]Personal measurement on cast (originals are lost).

## TABLE A14. RESIDUAL (reduced major axis – RMA) FORMULAE AND P-VALUES (ANOVA and Kruskal-Wallis) FOR THE COMPARISONS.

**(All residual equations were derived from the earlier Upper Paleolithic (EUP/MUP) sample, and then applied across the five comparative samples. P<0.05 (*) and <0.01 (**) after a sequentially reductive multiple comparison correction within sets of comparisons. The ANOVA P-values that do not meet all of the criteria of normality are in parentheses.)**

| Dependent | Independ. | Slope | Intercept | N | r | ANOVA P | K-W P |
|---|---|---|---|---|---|---|---|
| ***Areas*** | | | | | | | |
| ***Femur*** | | | | | | | |
| 35% CA | 35% TA | 0.990 | -0.406 | 18 | 0.716 | **0.003 | **0.006 |
| 50% CA | 50% TA | 1.082 | -0.788 | 29 | 0.913 | (*0.009) | *0.014 |
| 65% CA | 65% TA | 0.983 | -0.088 | 21 | 0.952 | 0.493 | 0.486 |
| 80% CA | 80% TA | 0.959 | -0.045 | 27 | 0.928 | 0.371 | 0.387 |
| ***Tibia*** | | | | | | | |
| 50% CA | 50% TA | 0.115 | -0.954 | 19 | 0.970 | 0.086 | 0.126 |
| 65% CA | 65% TA | 1.155 | -1.380 | 12 | 0.957 | 0.059 | 0.162 |
| ***Second Moments of Area*** | | | | | | | |
| ***Femur*** | | | | | | | |
| 35% $I_x$ | 35% $I_y$ | 1.427 | -4.080 | 18 | 0.924 | **0.001 | **0.005 |
| 50% $I_x$ | 50% $I_y$ | 1.344 | -3.070 | 29 | 0.896 | **<0.0001 | **<0.0001 |
| 65% $I_x$ | 65% $I_y$ | 1.380 | -3.793 | 21 | 0.917 | **0.0001 | **0.0001 |
| 80% $I_x$ | 80% $I_y$ | 1.182 | -2.259 | 27 | 0.948 | (0.054) | 0.057 |
| 80% $I_{min}$ | 80% $I_{max}$ | 1.034 | -0.999 | 27 | 0.935 | **0.004 | *0.011 |
| ***Tibia*** | | | | | | | |
| 35% $I_{max}$ | 35% $I_{min}$ | 1.186 | -0.949 | 15 | 0.946 | (**0.0003) | **0.001 |
| 50% $I_{max}$ | 50% $I_{min}$ | 1.173 | -0.658 | 19 | 0.930 | **0.0004 | **0.001 |
| 65% $I_{max}$ | 65% $I_{min}$ | 1.158 | -0.390 | 12 | 0.979 | (**0.001) | *0.012 |
| ***Diameters*** | | | | | | | |
| ***Femur*** | | | | | | | |
| Mid AP | Mid ML | 1.888 | -19.24 | 36 | 0.731 | (**<0.0001) | **<0.0001 |
| Prox AP | Prox ML | 0.797 | -1.574 | 39 | 0.797 | **0.002 | **0.005 |
| ***Tibia*** | | | | | | | |
| Mid AP | Mid ML | 1.534 | -0.486 | 31 | 0.809 | *0.023 | *0.022 |
| Prox AP | Prox ML | 1.835 | -5.541 | 28 | 0.825 | (**0.001) | **0.002 |
| ***Section Moduli*** | | | | | | | |
| ***Femur*** | | | | | | | |
| 50% $Z_x$ | BMxL | 0.088 | -687 | 19 | 0.837 | 0.406 | 0.459 |
| 50% $Z_y$ | BMxL | 0.060 | -169 | 19 | 0.802 | *0.016 | 0.042 |
| 50% $Z_p$ | BMxL | 0.138 | -781 | 19 | 0.830 | 0.307 | 0.514 |

## TABLE A15. FEMUR NECK-SHAFT ANGLES FOR PLEISTOCENE *HOMO* SPECIMENS.

**(Values in parentheses are estimated. From personal measurement on original specimens unless otherwise indicated.)**

| | | |
|---|---|---|
| **Early Pleistocene** | | |
| KNM-ER 1472[1] | R | 125° |
| KNM-ER 1481[1] | L | 123° |
| KNM-WT 15000 (adol)[2] | L | 110° |
| **Middle Pleistocene** | | |
| Berg Aukas 1[3] | R | 106° |
| Broken Hill E689 | L | 121° |
| Broken Hill E907 | R | 122° |
| Zhoukoudian femur 1[4] | L | (119°) |
| Zhoukoudian femur 4[4] | R | (127°) |
| **Neandertals** | | |
| Amud 1 | R | (113°) |
| La Chapelle-aux-Saints 1 | R | 121° |
| Feldhofer 1 | R | 122° |
| | L | 119° |
| La Ferrassie 1 | R | 120° |
| | L | 122° |
| La Ferrassie 2 | L | 127° |
| Krapina 213 | L | 121° |
| Krapina 214 | L | 122° |
| Shanidar 1 | R | (120°) |
| Spy 2 | L | 116° |
| Tabun 1 | R | 124° |
| **MPMH** | | |
| Qafzeh 9 | R | 131 |
| Skhul 4 | R | 125 |
| | L | 136 |
| Skhul 5 | R | (132°) |
| Skhul 6 | L | 136° |
| Skhul 9 | L | 136° |

| | | |
|---|---|---|
| **EUP/MUP** | | |
| Arene Candide IP (adol)[5] | R | 140° |
| | L | 133° |
| Cro-Magnon 4322 | L | 125° |
| Dolní Věstonice 3[6] | L | (130°) |
| Dolní Věstonice 13[6] | R | 121° |
| | L | 120° |
| Dolní Věstonice 14 (adol)[6] | R | 118° |
| | L | 120° |
| Dolní Věstonice 16[6] | R | 124° |
| | L | (125°) |
| Minatogawa 1[7] | R | 126 |
| | L | 122 |
| Minatogawa 2[7] | L | 133 |
| Minatogawa 3[7] | R | 132 |
| | L | 140 |
| Minatogawa 4[7] | R | 132 |
| Mladeč 28 | L | (124°) |
| Nahal 'En Gev 1 | R | 132° |
| Ohalo 2 | R | 132° |
| | L | 131° |
| Paglicci 25[8] | R | 117° |
| | L | 114° |
| Paviland 1 | L | 121° |
| Předmostí 3[9] | R | 115° |
| | L | 111° |
| Předmostí 4[9] | R | 112° |
| | L | 109° |
| Předmostí 9[9] | R | 117° |
| | L | 117° |
| Předmostí 10[9] | R | 111° |
| | L | 116° |
| Předmostí 14[9] | R | 112° |
| | L | 112° |
| La Rochette 1[10] | R | 116° |
| Sunghir 1 | R | 123° |
| Sunghir 2 (adol) | R | 118° |
| | L | 120° |
| Tianyuan 1 | R | (118°) |
| Zhoukoudian-UC 105[4] | L | (126°) |
| Zhoukoudian-UC 117[4] | L | (127°) |

[1]Data from Leakey et al. (1978).
[2]Measurement from Walker and Leakey (1993).
[3]Angle from Grine et al. (1995).
[4]Data from Weidenreich (1941). The Locality 1 values were estimated by Weidenreich; the values for the lost Upper Cave femora are from a photograph and a radiograph published by Weidenreich.
[5]Data from Sergi et al. (1974).
[6]Data from Sládek et al. (2000).
[7]Data from Baba and Endo (1982).
[8]Data from Mallegni et al. (1999).
[9]Data from Matiegka (1938).
[10]Angle from Klaatsch and Lustig (1914).